UNIVERSITY OF MANITOBA

The Predicted Behaviour of Two Dimensional Flow Over A Slotted Flap

by

Srinath Heragu S.

A Thesis

Submitted to the Faculty of Graduate Studies

in Partial Fulfillment of the Requirements for the

Degree of Master of Science

Department of Mechanical Engineering

Winnipeg, Manitoba

January, 1984

THE PREDICTED BEHAVIOUR OF TWO DIMENSIONAL FLOW OVER A SLOTTED FLAP

by

Srinath Heragu S.

A thesis submitted to the Faculty of Graduate Studies of the University of Manitoba in partial fulfillment of the requirements of the degree of

MASTER OF SCIENCE

SUMMARY

The slotted flap is a high lift device used to reduce the take-off and landing distances of aircraft. The flow around the slotted flap, which determines the pressure distribution and effectiveness of the aerofoil system, is affected by the interaction of the wake of the main aerofoil element and the boundary layer on the flap's upper surface.

The present project has been undertaken to develop a viable calculation method which can predict the above interaction. The principle of momentum flux balance has been effectively used along with Coles profile to represent the turbulent boundary layer and the Gaussian profile to represent the wake. In addition the present method has been improved by taking into account the transverse pressure gradient.

This method has been tested by comparing the predicted results with the experimental data of four cases of flow over an aerofoil system involving the boundary layer and wake interaction. It is seen that the predicted development of the displacement and momentum thicknesses of the shear layers and the skin-friction coefficient is a good estimate of the real one. The predicted development of the velocity profiles is also consistent with physical evidence.

ACKNOWLEDGEMENTS

I express my gratitude and indebtedness to my supervisor, Dr. J. Tinkler, for his invaluable help, guidance and encouragement without which this work would not have been possible. I am also thankful to him for his special efforts in putting me into the groove of a research scholar.

I wish to express my gratitude to my sister and brother-in-law, Vijaya Sitaram and Dr. K.P. Sitaram, for their kind care and support during this programme and to my parents for their encouragement.

I also wish to express my thanks and appreciation to Mrs. Valerie Ring and Miss Carol Plumridge for their typing of the manuscripts and to Fred Kapitoler for his preparation of the drawings.

TABLE OF CONTENTS

NOTATION AND SUBSCRIPTS

VARIABLE	COMPUTER NOTATION	PHYSICAL MEANING
A	A	Constant appearing in the equation (2.4), equal to 5.616
A_i, i = 1 to 8	AI	Numerical integrals defined in Appendix - A
B	B	Constant appearing in the equation (2.4), equal to 4.8
B_i, i = 1 to 4	BI	Numerical integrals defined in Appendix -A
c	C	Unextended chord of the aerofoil system
C_f	CF	Skin friction coefficient based on the local maximum velocity, $C_f = 2\left(\frac{U_\tau}{U_i}\right)^2$ or $C_f = 2\left(\frac{U_\tau}{U_3}\right)^2$
$C_{f\infty}$	CFIF	Skin friction coefficient based on the free stream velocity, $C_{f\infty} = 2U_\tau^2$
C_i, i = 1 to 19	CI	Numerical integrals defined in Appendix - A
C_p		Static pressure coefficient defined by equation (3.7) and formulated as $C_p = f(x)y + g(x)$

VARIABLE	COMPUTER NOTATION	PHYSICAL MEANING
D_i, i = 1 to 8	DI	Coefficients occurring in the functions f (x) and g (x)
E_i, i = 1 to 4	EI	Coefficients defined in Appendix - A
f (x)		Polynomial function occurring in the expression for C_p
F	F	Rate of change of mass flow of the incompressible fluid below the wake centre, $F = \frac{d}{dx} \int_{L_3}^{\delta_2} U \, dy$
g (x)		Polynomial function occurring in the expression for C_p
G_1	G1	Constant used to terminate the inner wake
G_0	GO	Constant used to terminate the outer wake
H_B	HB	Shape parameter of the boundary layer
H_i, i = 1 to 5	HI	Pressure integrals defined in Appendix - A
H_{IW}	HIW	Shape parameter of the inner wake
k	K	Constant equal to ln 2
L	L	Constant equal to ln 10

VARIABLE	COMPUTER NOTATION	PHYSICAL MEANING
L_1	L1	Non-dimensional form of length scale for the inner wake
L_2	L2	The thickness of the potential core region, $L_2 = (\delta_2 - G_1 L_1 - \delta)$
L_3	LMT1	Lower limit of the integrals, $L_3 = \left(\frac{2U_\tau}{\nu}\right)$
L_0	LO	Non-dimensional form of length scale for outer wake
L_s		Non-dimensional form of general length scale.
M_i, i = 1 to 35	MI	Coefficients defined in Appendix - A
n		Exponent appearing in the equation (2.1)
N_i, i = 1 to 7	NI	Coefficients defined in Appendix - A
p_d		Local static pressure
P	P	Profile parameter of the boundary layer
R_i, i = 1 to 42	RI	Coefficients defined in Appendix - A
R_{TW}	RTW	Constant appearing in the equation (3.22)
T_i, i = 1 to 6	TI	Coefficients defined in Appendix - A

VARIABLE	COMPUTER NOTATION	PHYSICAL MEANING
u		Non-dimensional form of turbulent component of velocity in the x-direction
U		Non-dimensional form of mean velocity in the x-direction
U_1	U1	Value of U at the centre of the wake
U_3	U3	Value of U at the outer edge of the boundary layer in the merged case
U_∞	UIF	Free stream velocity
U_e	UE	Value of U at the outer edge of the outer wake
U_i	UI	Value of U at the outer edge of the boundary layer in the unmerged case
U_m		Non-dimensional form of main stream velocity
U_0	U0	Value of U at the outer edge of the inner wake in the unmerged case
U_s		Non-dimensional form of velocity scale
$U_{\delta/2}$	US2	Value of U at $y = (\delta/2)$

VARIABLE	COMPUTER NOTATION	PHYSICAL MEANING
U_τ	UT	Non-dimensional form of friction velocity
v		Non-dimensional form of turbulent component of velocity in the y - direction
V		Non-dimensional form of mean velocity in the y - direction
x	X	Coordinate along the flap surface divided by c
y	Y	Coordinate perpendicular to the flap surface divided by c
α		Angle of attack
γ		Intermittency factor
Δx	DX	Step size of the computation process
δ	S	Value of y at the outer edge of the boundary layer in unmerged case
δ_2	S2	Value of y at the centre of wake
δ_3	S3	Value of y at the outer edge of the boundary layer in merged case

VARIABLE	COMPUTER NOTATION	PHYSICAL MEANING
δ^*		Non-dimensional form of displacement thickness defined in Appendix - B for the three shear layers
δ^*_B	S1B	Value of δ^* for the boundary layer
δ^*_{IW}	S1IW	Value of δ^* for the inner wake
δ^*_{OW}	S1OW	Value of δ^* for the outer wake
θ		Non-dimensional form of momentum thickness defined in Appendix - B for the three shear layers
θ_B	THETB	Value of θ for the boundary layer
θ_{IW}	THETIW	Value of θ for the inner wake
θ_{OW}	THETOW	Value of θ for the outer wake
ν	NUND	Non-dimensional form of kinematic viscosity
ν_T		Non-dimensional form of kinematic eddy viscosity

VARIABLE	COMPUTER NOTATION	PHYSICAL MEANING
ρ		Fluid density
τ		Non-dimensional form of shear stress
$\tau_{(\delta_2 + G_0 L_0)}$	TOUGLO	Value of τ at $y = (\delta_2 + G_0 L_0)$
$\tau_{(\delta_2 + L_0)}$	TOULO	Value of τ at $y = (\delta_2 + L_0)$
τ_{δ_2}	TOUS2	Value of τ at $y = \delta_2$
$\tau_{(\delta_2 - G_1 L_1)}$	TOUGL1	Value of τ at $y = (\delta_2 - G_1 L_1)$
τ_{δ}	TOUS	Value of τ at $y = \delta$
τ_{δ_3}	TOUS3	Value of τ at $y = \delta_3$
$\tau_{\delta/2}$	TOU2	Value of τ at $y = (\delta/2)$
τ_W	TOUW	Value of τ at the aerofoil surface
ω		Wake function appearing in the boundary layer profile
ϕ		Refer to the equation (3.47)

SUBSCRIPTS:

∞	Values in, or referred to, undisturbed stream
d	Dimensional quantity
T	Values, referring to or derived from total values

LIST OF FIGURES

CHAPTER - 1

INTRODUCTION

High values of lift coefficients are required during take-off and landing of aircraft with suitable lift-to-drag ratios so as to allow the desired rates of climb and descent. This is achieved by changing the effective shape of the aerofoil temporarily using devices known as flaps. Flaps fall into two categories which are (a) Powered flaps and (b) Unpowered flaps. Powered flaps provide higher values of lift coefficient than unpowered flaps because of the positive addition of energy in the former case.

Powered flaps or jet flaps use jets of air of sufficient energy to deflect the main flow past the aerofoil and, in effect, increase camber. Jets are also used to prevent boundary layer separation on a flap. These effects of the jet serve to increase the lift. Unpowered flaps or mechanical flaps are those that change the physical shape of the aerofoil to create a flow pattern to give the desired lift. There are many types of mechanical flaps like plain flaps, split flaps, slotted flaps etc. Plain flaps serve to increase the lift, but, because of the early separation that occurs on the upper surface, not only is the increment in maximum lift coefficient limited, but it cannot be used to provide high lift-to-drag ratios over a large range of angles of deflection of the flap. These disadvantages of the plain flaps are overcome by the slotted flaps, which allow air to flow from the high pressure under surface, through the slot, to form

a jet over the flap upper surface to keep the boundary layer attached. Typical total head profiles involving the wake shed by the main aerofoil and the boundary layer on the flap, are shown in Fig. 1.

Many different flow models have been used to predict the lift of multi-component aerofoils. Jacob and Steinbach (1) developed a method for evaluating the lift of a slotted flap aerofoil. The method used potentital flow techniques to take into account the boundary layer displacement effect and also the separation of flow on the flap. The flow separation was simulated by a source distribution on that part of the flap where there was separation. This method was not able to take into account the separation on the wing nor the wake shed by the wing. Very soon it was realised that in some cases the wake shed by the wing influenced the flap boundary layer, to an extent, which would result in early separation of the boundary layer. The total head profiles shown in Fig. 1 provide a good idea of the effect the viscous layers have on each other. Hence it became necessary to develop a mathematical model to predict the interaction of the wake shed by the main aerofoil and the boundary layer on the slotted flap.

Irwin (2) developed an integral method for predicting the above interaction. In this method the boundary layer was represented by the power law profile and the wake by the Gaussian profile. This method also took into account the transverse pressure gradient. It was quite reliable in evaluating the integral parameters of the wake and boundary layer. Also there was good agreement with the measured values of skin-friction, over most of the flap. But this method

could not predict the separation of the boundary layer in the presence of the wake. Also it predicted the merging of the wake and boundary layer to occur, too far downstream of the station at which it actually occurred. The limitations of this method may be because of the following reasons.

(1) The power law which was developed from observations of turbulent flow in pipes and channels is not a very good representation of the velocity profile in a turbulent boundary layer when the streamwise pressure gradient is significant, and, more so, when there is a transverse pressure gradient.

(2) The relation used for predicting the skin-friction coefficient had been developed by Ludwieg and Tillmann, from measurements in thin boundary layers and it may not be valid for thick boundary layers with transverse pressure gradients.

(3) In applying the momentum integral equation, the growth of the boundary layer and wake was neglected in some of the terms.

Kibria (3) made a modification to Irwin's method by using Coles profile to represent the turbulent boundary layer instead of the power law. Coles profile is a good representation of the velocity profile for boundary layers developing in adverse pressure gradients. But the analysis of the problem was simplified by neglecting the transverse pressure gradient. Kibria's method was not as successful as Irwin's method in predicting the integral properties of the wake and boundary layer. It broke down at large streamwise distances, in that, it could not predict the proper qualitative variation of the wake length

scales. Also it could neither predict the possibility of separation nor the flow behaviour in the region of separation. But it could predict the merging point better than Irwin's method. The shortcomings of this method may be because of the following reasons.

(1) The transverse pressure gradient was not taken into account.

(2) The momentum integral equation was used with the same defects as in Irwin's method.

The present work has been undertaken to improve Kibria's method. It is believed that this improved method can be used to provide a reasonably good estimate of the displacing effect of the viscous layer which, in turn, can be used in conjunction with potential flow models to predict the pressure distribution around a slotted flap aerofoil.

The principle of operation of the slotted flap can be understood with reference to Fig. 2. A potential core is entrained by the boundary layer developing on the flap and the wake shed by the wing. With the development of the flow over the flap, the potential core disappears and the wake and boundary layer merge. This merging may cause the boundary layer to separate. It may also happen that the wake and the boundary layer may not merge before the flap trailing edge, in which case the boundary layer would develop without being affected by the presence of the wake. It has been confirmed experimentally by Foster, Irwin and Williams (4) and Ljungstrom (5) that the maximum lift is obtained when the viscous layers just interact at the trailing edge of the flap. Hence an optimum flow development for take-off is one for which the merging occurs at the trailing edge to give a high

lift-to-drag ratio. The high lift coefficient and high drag required during landing can be achieved by using larger flap deflections and hence earlier merging of the wake and boundary layer, with possible earlier boundary layer separation. The merging of the wake and boundary layer and hence their interaction is influenced by many factors like the slot shape, flap shape and the angle of deflection of the flap which determine the pressure field to a large extent, the slot height which determines the thickness of the potential core and the relative lateral position of the flap and the main aerofoil which determines the merging point of the wake and the boundary layer.

In the present analysis it has been decided to develop the equations in such a way that the transverse pressure gradient can be taken into account. The results given by the present calculation method will be compared with four cases of flow over an aerofoil system, involving the interaction of the wake and boundary layer. Two of these cases are reported by Foster, Irwin and Williams (4) and the other two cases are reported by Bario et al (6) and Ljungstrom (5).

Presumably, the local Mach numbers in these test cases are low that the incompressibility assumption made in the present analysis is valid.

CHAPTER 2

THEORY

(i) Introduction: The typical forms of the velocity profiles that occur with the development of a wake and a boundary layer in conjunction with each other are shown in Fig. 3. Initially, the wake shed by an aerofoil element and the boundary layer developing on the adjacent aerofoil element are separated by a layer of potential flow (the potential core). With the development of the flow, the potential core is entrained by the boundary layer on one side and the wake on the other, allowing the merging of the wake and the boundary layer; where the wake and boundary layer are separated by the potential core is known as the unmerged region; downstream of the merging point is known as the merged region. The boundary layer and wake velocity profile representations, their interaction and the simplified flow model will be considered in the following sections of this Chapter.

(ii) Boundary Layer: The boundary layer concept was introduced by Prandtl in 1904. For fluids with low viscosity, it is the region where the shearing action predominates. This region can be either laminar or turbulent. The present analysis involves turbulent boundary layers. The prediction of the velocity profile in a turbulent boundary layer and its associated characteristics is difficult, especially, if the boundary layer is tending towards separa-

tion. The power law velocity profile suggested by Prandtl states that

$$\left(\frac{U_d}{U_{id}}\right) = \left(\frac{y_d}{\delta_d}\right)^{1/n} \qquad \text{(2.1)}$$

where U_{id} is the velocity at the edge of the boundary layer and δ_d is the boundary layer thickness. The subscript 'd' denotes the dimensional form of the variables. Its simplicity was spoilt by the dependency of the exponent on the Reynolds number. Also it is valid only for boundary layer flows with small pressure gradient.

It is known that the boundary layer region can be divided into three regions. The innermost region is known as the sub-layer where the motion is determined by viscosity. The middle layer is a turbulent region where both the viscosity and turbulence have significant effects. The outer region is the fully turbulent region where the motion is similar to the wake flow and is dominated by the eddy viscosity. On this basis a better representation of the velocity profile has been given by Coles (7), in the form

$$\left(\frac{U_d}{U_{\tau d}}\right) = F\left(\frac{y_d\, U_{\tau d}}{\nu_d}\right) + G(x_d, y_d) \qquad \text{(2.2)}$$

where $U_{\tau d}$ is the friction velocity and ν_d is the kinematic viscosity. Coles profile consists of two universal functions, the law of the wall and the law of the wake. The law of the wall is a representation

of the velocity in the inner part of the layer. It consists of two regions, a linear region corresponding to the sub layer region and a logarithmic region corresponding to the middle region. In the linear region, the law of the wall is of the form

$$F\left(\frac{y_d\ U_{\tau d}}{\nu_d}\right) = \left(\frac{y_d\ U_{\tau d}}{\nu_d}\right) \qquad \text{(2.3)}$$

This expression satisfies the no slip condition that the velocity is zero at $y_d = 0$. It is valid for values of $\left(\frac{y_d\ U_{\tau d}}{\nu_d}\right)$ up to about 10. The logarithmic region is valid for values of $\left(\frac{y_d\ U_{\tau d}}{\nu_d}\right)$ greater than about 50. It is of the form

$$F\left(\frac{y_d\ U_{\tau d}}{\nu_d}\right) = \frac{A}{L} \ln\left(\frac{y_d\ U_{\tau d}}{\nu_d}\right) + B \qquad \text{(2.4)}$$

in which A and B are empirical constants and L = ln 10.
The law of the wall is dependent on the type of surface but is independent of outside conditions like the pressure gradient, mainstream turbulence etc. The law of the wake is the representation of the velocity in the outer part of the layer which is constrained more by inertia than by viscosity. It is of the form

$$G(x_d, y_d) = P\omega\left(\frac{y_d}{\delta_d}\right) \qquad \text{(2.5)}$$

where P is known as the profile parameter and $\omega\left(\frac{y_d}{\delta_d}\right)$ is known as the wake function. Since the sublayer is thin and the fluid within it is of low velocity, it has little effect on the boundary layer as a whole. Hence it is usually neglected in the representation of the boundary layer profile. So equation (2.2) reduces to

$$\left(\frac{U_d}{U_{\tau d}}\right) = \frac{A}{L} \ln\left(\frac{y_d\, U_{\tau d}}{\nu_d}\right) + B + P\omega\left(\frac{y_d}{\delta_d}\right) \qquad (2.6)$$

Coles (7) imposed the following normalising condition on the wake function.

$$\int_0^{\omega_1} \left(\frac{y_d}{\delta_d}\right) d\omega = 1 \qquad (2.7)$$

$$\omega_{max} = \omega_1 = 2 \qquad (2.8)$$

Subject to the above conditions, Coles (7) arrived at a series of values for ω for different values of $\left(\frac{y_d}{\delta_d}\right)$ from an investigation of several boundary layer flows. Houghton and Boswell (8) have reported that from a consideration of the above values, the wake function has been approximated by a sine function as

$$\omega\left(\frac{y_d}{\delta_d}\right) = 2 \sin^2\left(\frac{\pi y_d}{2\delta_d}\right) \qquad (2.9)$$

and have given the following form of the Coles profile.

$$\left(\frac{U_d}{U_{\tau d}}\right) = \frac{A}{L} \ln\left(\frac{y_d\, U_{\tau d}}{\nu_d}\right) + B + 2P \sin^2\left(\frac{\pi y_d}{2\delta_d}\right) \qquad (2.10)$$

Using the free-stream velocity and the chord length to non-dimensionalise the velocities and the distances respectively, equation (2.10) leads to

$$\left(\frac{U}{U_\tau}\right) = \frac{A}{L} \ln\left(\frac{yU_\tau}{\nu}\right) + B + 2P \sin^2\left(\frac{\pi y}{2\delta}\right) \qquad (2.11)$$

The absence of the subscript 'd' indicates the corresponding variables are in non-dimensional form.

Coles (7) tested the profile given by equation (2.11), not only for several boundary layers developing in adverse pressure gradients, but also for some boundary layers developing on aerofoils. The results compared well with the experimental ones. Also it is easy to visualize the concept of equilibrium boundary layer flows proposed by Clauser (9), by considering the Coles profile. It has been known for a long time, that all constant pressure turbulent boundary layers at all streamwise stations are identical, when plotted as $\left(\frac{U_i - U}{U_\tau}\right)$ versus $\left(\frac{y}{\delta}\right)$. This fact was recognized by Clauser (9), who presumed that it would be possible to form boundary layers developing in positive pressure gradients, in such a way, that a certain balance exists between the mixing processes. This would result in the profiles at different streamwise stations, collapsing on a single curve, when plotted in the coordinates of $\left(\frac{U_i - U}{U_\tau}\right)$ versus $\left(\frac{y}{\delta}\right)$. In fact Clauser (9) managed to create

experimentally, two such equilibrium flows developing in adverse pressure gradients. The value of U_i is given by

$$\left(\frac{U_i}{U_\tau}\right) = \frac{A}{L} \ln\left(\frac{\delta U_\tau}{\nu}\right) + B + 2P \qquad \text{(2.12)}$$

Equations (2.11) and (2.12) can be used to yield the following equation

$$\left(\frac{U_i - U}{U_\tau}\right) = -\frac{A}{L} \ln\left(\frac{y}{\delta}\right) + 2P \cos^2\left(\frac{\pi y}{2\delta}\right) \qquad \text{(2.13)}$$

If P is constant, it is seen that the profiles are independent of streamwise stations and the condition for equilibrium flows is satisfied. If the pressure gradient causes a non-equilibrium boundary layer, its effect can be accommodated in the profile parameter P which is, in general, a function of x.

From the preceding discussions, it can be seen that the Coles profile is very suitable and reliable for representing the velocity profile in a turbulent boundary layer. Hence it has been used in the present analysis.

(iii) Wakes: Wakes fall into the category of free turbulence where there is no direct effect of any fixed boundary. Wakes are formed in all cases of viscous flow past bodies. It is a region deficient in momentum, caused by viscosity in the flow field over the body

which sheds the wake. The drag experienced by a body increases with the size of the wake it sheds. High values of drag are associated with thick wakes resulting from the separation of the boundary layers on the body. Bodies that experience lift create asymmetric wakes. If the wakes are symmetric and the turbulence structure is uniform, there would be no mass or momentum transfer across the line of minimum velocity in the wake. In the case of asymmetric wakes, there is bound to be mass transfer across the centre of the wake. Also the position of the wake centre changes in a transverse direction with the development of the flow downstream.

Near the body the flow is dependent on viscosity and this region is known as the near wake. This is the region of adjustment from the boundary layer like flow to the self preserving form of the flow which occurs later. The length of the near wake region, after which the wake collapses to a self preserving type of flow, is a function of the boundary layer characteristics at the trailing edge of the body. As noted by Townsend (10), for self-preservation to occur, the following condition should be satisfied.

$$U_d = U_{md} + U_{sd}\, h\left(\frac{y_d}{L_{sd}}\right) \qquad \text{(2.14)}$$

where U_{md} is the mainstream velocity,

U_{sd} is the velocity scale and

L_{sd} is the length scale.

From the motion of the large eddies Townsend (10) arrived at the following form for the mean velocity variation.

$$U_d = U_{md} - (U_{md} - U_{1d}) \, Exp\left(\frac{-y_d^2}{2L_{sd}^2}\right) \qquad \text{(2.15)}$$

In this equation,

U_{1d} = the velocity at the centre of the wake and

L_{sd} = the length scale defined as distance from the centre of the wake to the point where the velocity is

$$U_{md}\,[1 - Exp(-0.5)] + U_{1d}\,[Exp(-0.5)]$$

Following Gartshore (11), Irwin (2) adopted a similar but more suitable form for the wake. The outer half of the wake and the inner half of the wake, known as the outer and inner wake respectively, were defined by two different self preserving profiles, as given below, in non-dimensional form.

Outer Wake:

$$U = U_e - (U_e - U_1) \, Exp\left[-k\left(\frac{y - \delta_2}{L_0}\right)^2\right] \qquad \text{(2.16)}$$

where $k = \ln 2$,

U_e = velocity in the potential region at the edge of the outer wake,

δ_2 = the distance from the aerofoil surface to the centre of the wake and

L_0 = the length scale defined as the distance from the centre of the wake to the point where the velocity is

$$\left(\frac{U_e + U_1}{2}\right)$$

Inner Wake:

$$U = U_0 - (U_0 - U_1)\ \mathrm{Exp}\left[-k\left(\frac{y - \delta_2}{L_1}\right)^2\right] \qquad \text{(2.17)}$$

in the unmerged case where

U_0 = the velocity in the potential core at the edge of the inner wake and

L_1 = the length scale defined as the distance from the centre of the wake to the point where the velocity is $\left(\frac{U_0 + U_1}{2}\right)$

In the merged case,

$$U = U_3 - (U_3 - U_1)\mathrm{Exp}\left[-k\left(\frac{y - \delta_2}{L_1}\right)^2\right] \qquad \text{(2.18)}$$

where U_3 = the velocity at the edge of the inner wake.

The same forms have been adopted in the present analysis.

Because of the exponential terms occurring in the profile representations for the outer and inner wake, these profiles would extend to infinity. Hence the outer wake has been terminated at $y = \delta_2 + G_0 L_0$ and the inner wake at $y = \delta_2 - G_1 L_1$ where the choice of the empirical constants G_0 and G_1 is discussed in the next section.

(iv) Interaction of the Wake and The Boundary Layer: In the unmerged region the thickness of the potential core region decreases with the development of the flow. The inner wake length L_1 and the boundary

layer thickness, δ, increase because of the entrainment of the fluid from the potential core. As a result of the displacing effect of the boundary layer on the potential core the length δ_2 increases. The outer wake length, L_0, increases at a rate to accommodate the net entrainment of the fluid from the mainstream and from across the wake centre. Thus the development of the wake and the boundary layer is almost identical to that of the respective free layers. The merging point of the inner wake and the boundary layer is dependent on the entrainment rates of the shear layers. These entrainment rates are dependent on the intensity of turbulence in the flow field between these shear layers, the intermittency of the flow at the edges of these shear layers, the pressure field and the relative thicknesses of the shear layers.

In the merged region the boundary layer thickness continues to increase because of the entrainment of the fluid from above it. The inner wake length L_1 varies, depending on the pressure field and the mass flow across the wake centre. The length δ_2 still continues to increase because of the displacing effect of the boundary layer. The outer wake length L_0 increases, subject to the same constraints mentioned earlier.

From the above discussions, it is seen that there are not many constraints in the selection of the constant G_0 for terminating the outer wake. Irwin (2) chose a value of G_0 such that at $y = \delta_2 + G_0 L_0$, the velocity defect is 0.5% of the maximum velocity defect. This condition gives a value of $G_0 = 2.77$ on using the

equation (2.16). The same value of G_0 has been adopted in the present analysis.

On the other hand, there are many constraints in the selection of the constant G_1 for terminating the inner wake. It plays a part in the disappearance of the potential region and is influenced by the entrainment rates of the boundary layer and the inner wake. Irwin (2) carried out calculations for different values of G_1 and found that a value of $G_1 = 2.5$ gave the best results when compared with the experimental variation of the momentum thickness. This value of G_1 will be used in the present analysis.

(v) Simplified Flow Model: The interaction of the wake and the boundary layer is so complex that it is necessary to use a simplified model to get an idea of the type of results that would be obtained by varying different parameters, before more exact and complex models can be used. The simplified model is illustrated in Fig. 4. The following assumptions have been made to arrive at the simplified form of the real flow model.

(1) The flap will be represented by a flat plate so that a cartesian coordinate system can be used.

(2) The flow is treated as incompressible and two-dimensional.

(3) The boundary layer is assumed to have developed into a fully turbulent flow right from the start of the calculation process.

(4) Each half of the wake is assumed to have a self preserving profile with the minimum velocity layer having no shear stress

and no mass transported across it.

(5) Only the mean velocity field has been considered in the derivation of the system of equations required to solve the flow model, the turbulent velocity components having been taken into account only in the representation of the shear stresses. Also the intermittency of the flow has been neglected everywhere except in the use of the eddy-viscosity concept in the boundary layer.

(6) The turbulence level in the potential core and main stream is taken as being negligible.

CHAPTER 3

CALCULATIONS

(i) Introduction: In order to predict the interaction of the wake and the boundary layer, a relevant and physically consistent system of equations needs to be developed. These equations should involve all the variables occurring in the expressions for the velocity profiles of the wake and the boundary layer. To achieve this, the momentum integral equation has been used as a valuable tool.

(ii) Momentum Integral Equation: The simplified Prandtl's momentum equations for a boundary layer along a flat surface, placed in line with the free stream and the continuity equation are

$$U_d \frac{\partial U_d}{\partial x_d} + V_d \frac{\partial U_d}{\partial y_d} = \frac{-1}{\rho} \frac{\partial p_d}{\partial x_d} + \frac{1}{\rho} \frac{\partial \tau_d}{\partial y_d} \tag{3.1}$$

$$\left(\frac{1}{\rho}\right) \frac{\partial p_d}{\partial y_d} = 0 \tag{3.2}$$

$$\frac{\partial U_d}{\partial x_d} + \frac{\partial V_d}{\partial y_d} = 0 \tag{3.3}$$

where p_d is the static pressure and

τ_d is the shear stress given by

$$\tau_d = \rho\left(\nu_d \frac{\partial U_d}{\partial y_d} - \overline{u_d v_d}\right)$$

These equations can be expressed in non-dimensional form as,

$$U \frac{\partial U}{\partial x} + V \frac{\partial U}{\partial y} = -\frac{1}{2} \frac{\partial C_p}{\partial x} + \frac{\partial \tau}{\partial y} \tag{3.4}$$

$$\frac{\partial C_p}{\partial y} = 0 \tag{3.5}$$

$$\frac{\partial U}{\partial x} + \frac{\partial V}{\partial y} = 0 \tag{3.6}$$

where $$C_p = \frac{(p_d - p_{\infty d})}{(1/2\ \rho U_\infty^2)} \tag{3.7}$$

Goldstein (12) has shown that the same approximations for the flow along a curved surface of small curvature lead to the following set of boundary layer equations in non-dimensional form.

$$U \frac{\partial U}{\partial x} + V \frac{\partial U}{\partial y} = (-\frac{1}{2}) \frac{\partial C_p}{\partial x} + \frac{\partial \tau}{\partial y} \tag{3.8}$$

$$\frac{\partial C_p}{\partial y} = -\kappa U^2 \tag{3.9}$$

and $$\frac{\partial U}{\partial x} + \frac{\partial V}{\partial y} = 0 \tag{3.10}$$

where κ is the radius of curvature of the surface and x, y are the coordinates measured along the wall and at right angles to it. The above set of equations was adopted by Irwin (2) in order to take into account the transverse pressure gradient. The same set of equations will be used in the present analysis with x, y being cartesian coordinates.

The transverse static pressure gradient is manifested in the term $(\frac{\partial C_p}{\partial x})$ in the equation (3.8). Hence equation (3.9) can be disregarded. So the set of equations (3.8) and (3.10) will be used in the present analysis. By substituting for V from the equation (3.10) into the equation (3.8), the following equation is obtained.

$$\frac{\partial U^2}{\partial x} + \frac{\partial UV}{\partial y} = -\frac{1}{2} \frac{\partial C_p}{\partial x} + \frac{\partial \tau}{\partial y} \tag{3.11}$$

Integrating between arbitrary limits y_1 and y_2, the general momentum integral equation is obtained

$$\int_{y_1}^{y_2} \left(\frac{\partial U^2}{\partial x}\right) dy - U_{y_2} \int_0^{y_2} \left(\frac{\partial U}{\partial x}\right) dy + U_{y_1} \int_0^{y_1} \left(\frac{\partial U}{\partial x}\right) dy + \int_{y_1}^{y_2} \left(\frac{1}{2}\right)\left(\frac{\partial C_p}{\partial x}\right) dy - \left(\tau_{y_2} - \tau_{y_1}\right) = 0 \qquad (3.12)$$

with the boundary condition that $V_{y=0} = 0$

When the Navier-Stokes equation are applied to the wake region and similar simplifying assumptions are made, the set of equations (3.8) to (3.10) are obtained. Hence the general momentum integral equation (3.12) turns out to be the same for both the boundary layer and the wake region. In order to use the momentum integral equation effectively, the shear stresses in the equation will have to be evaluated. This problem is considered in the next section.

(iii) Shear Stresses: Boussinesq introduced the eddy viscosity concept to account for the transverse turbulent momentum exchange which, in effect, acts as a shear stress. It is given by

$$\tau_t = \nu_T \left(\frac{\partial U}{\partial y}\right) \qquad (3.13)$$

where τ_t = the turbulent shear stress

and

ν_T = the kinematic eddy viscosity

The laminar shear stress is given by

$$\tau_l = \nu\left(\frac{\partial U}{\partial y}\right) \qquad (3.14)$$

where τ_l = the laminar shear stress

and

ν = the kinematic viscosity

Typically in a turbulent region the total shear stress τ is given by

$$\tau = \tau_l + \tau_t$$
$$= (\nu + \nu_T) \frac{\partial U}{\partial y} \tag{3.15}$$

But, at large distances from the wall, the turbulence is well established and the contribution of the laminar shear stress to the total shear stress is small. Hence it is neglected. So, except near the wall, the shear stress at a point is given by

$$\tau = \nu_T \left(\frac{\partial U}{\partial y}\right) \tag{3.16}$$

The expression for the eddy viscosity is a complicated and an important one. In a boundary layer where the flow is affected by viscosity this expression is different from that in a wake where the flow is determined only by inertia effects. Within a boundary layer itself the expression is determined by the extent to which the viscosity affects the region. In the sub-layer region it is defined by a modified form of Prandtl's mixing length theory. In the outer region it is dependent on the boundary layer thickness. The constraint used in defining the extent of these regions is the continuity of the eddy viscosity. Smith and Cebeci (13) have used the following

expression suggested by Clauser

$$\nu_T = (0.0168)(\delta_B^*)(U_i) \tag{3.17}$$

This has been further modified by the intermittency factor. An approximate form of the intermittency factor has been reported to be given by Klebanoff as

$$\gamma = [1 + 5.5(\frac{y}{\delta})^{6.}]^{-1} \tag{3.18}$$

so that

$$\nu_T = (0.0168)(\gamma)(\delta_B^*)(U_i) \tag{3.19}$$

Though as stated by Clauser this expression is valid only for equilibrium flows, it has been tested in several non-equilibrium boundary layer flows and has yielded good results. So it has been used to compute the eddy viscosity in the outer part of the boundary layer region with the result that

$$\nu_T = (0.0168)(\gamma)(\delta_B^*)(U_i) \tag{3.20}$$

in the unmerged region and

$$\nu_T = (0.0168)(\gamma)(\delta_B^*)(U_3) \tag{3.21}$$

in the merged region.

For the wake region, the approach of Townsend (10) has been adopted. The large eddies present in each half of a wake flow deter-

mine the self-preservation of the flow. The self-preserving type of flow is established when the two sets of eddies in each half of the flow are in a state of equilibrium with respect to their energy. Townsend (10) has suggested the following expression for the eddy viscosity assuming that it is constant across the flow region

$$\nu_T = \left(\frac{U_s L_s}{R_{TW}}\right) \tag{3.22}$$

This approximation is in error only near the edges of the flow where the flow is intermittent. Based on the equilibrium condition of the eddies, Townsend (10) arrived at a value of R_{TW} lying in the range 14 to 21. Since in the present case the wakes are asymmetric and not self-preserving, a value of $R_{TW} = 40$ suggested by Irwin (2) has been used.

Thus the expression for the eddy viscosity is given by

$$\nu_T = (U_e - U_1)\left(\frac{L_0}{R_{TW}}\right) \tag{3.23}$$

for the outer wake region.

The shear stresses are determined by using the appropriate expressions for the eddy viscosity and the velocity gradient in equation (3.16).

(iv) Pressure Field: As has been reported in Appendix -A, in the general case where the pressure field is two-dimensional, C_p has been represented by the equation

$$C_p = f(x)y + g(x) \tag{3.24}$$

where f (x) and g (x) are third order polynomials of x. In the test cases where the transverse pressure gradient is absent, the function g (x) has been assumed to be a linear function so that, in effect, C_p has been represented by a straight line. Thus the integral involving the pressure gradient $(\frac{\partial C_p}{\partial x})$ is determined in equation (3.12). Further discussion about the comparison of the formulated pressure distributions with the experimental ones will be found in Chapter 4.

(v) System of Equations:

(a) Unmerged Case: In this case the eight variables involved are U_τ, δ and P occurring in equation (2.11), U_1 δ_2 and L_0 occurring in equation (2.16) L_1 occurring in equation (2.17) and L_2 the thickness of the potential core region. Hence a system consisting of eight equations has to be developed. These are the equations obtained by applying the momentum integral equation to five different layers of the entire shear region, the expression for the rate of mass flow across the wake centre, the relation for $(\frac{dU_i}{dx})$ and the geometrical relation $L_2 = (\delta_2 - G_1 L_1)$.

The details involved in these equations and the coefficients of these equations are given in Appendix -A and the equations themselves are given below.

Outer Wake Region: The relations obtained by applying the momentum integral equation (3.12) to this region are

$$M_1\left(\frac{d\delta_2}{dx}\right) + M_2\left(\frac{dU_1}{dx}\right) + M_3\left(\frac{dL_0}{dx}\right) + M_4\left(\frac{dL_1}{dx}\right)$$

$$+ M_5\left(\frac{dU_\tau}{dx}\right) + M_6\left(\frac{dP}{dx}\right) + M_7\left(\frac{d\delta}{dx}\right) = N_1 \qquad (3.25)$$

for $y_1 = \delta_2$ and $y_2 = \delta_2 + G_0L_0$

$$M_8\left(\frac{d\delta_2}{dx}\right) + M_9\left(\frac{dU_1}{dx}\right) + M_{10}\left(\frac{dL_0}{dx}\right) + M_{11}\left(\frac{dL_1}{dx}\right)$$

$$+ M_{12}\left(\frac{dU_\tau}{dx}\right) + M_{13}\left(\frac{dP}{dx}\right) + M_{14}\left(\frac{d\delta}{dx}\right) = N_2 \qquad (3.26)$$

for $y_1 = \delta_2$ and $y_2 = (\delta_2 + L_0)$.

Amongst the shear stresses $\tau_{(\delta_2 + G_0L_0)}$, $\tau_{(\delta_2+L_0)}$ and τ_{δ_2} which occur in the coefficients N_1 and N_2, $\tau_{(\delta_2 + G_0L_0)}$ and τ_{δ_2} are assumed to be zero. The shear stress $\tau_{(\delta_2 + L_0)}$ evaluated using the viscosity expression, equation (3.23), is given by

$$\tau_{(\delta_2 + L_0)} = \left(\frac{k}{R_{TW}}\right)(U_e - U_1)^2 \qquad (3.27)$$

Inner Wake Region: The relation obtained by applying the momentum integral equation to this region is

$$M_{15}\left(\frac{d\delta_2}{dx}\right) + M_{16}\left(\frac{dU_1}{dx}\right) + M_{17}\left(\frac{dL_1}{dx}\right) + M_{18}\left(\frac{dU_\tau}{dx}\right)$$

$$+ M_{19}\left(\frac{dP}{dx}\right) + M_{20}\left(\frac{d\delta}{dx}\right) = N_3 \qquad (3.28)$$

for $y_1 = (\delta_2 - G_1L_1)$ and $y_2 = \delta_2$

The shear stress $\tau_{(\delta_2 - G_1L_1)}$ occurring in the coefficient N_3 is taken

as zero.

Boundary Layer Region: The relations obtained by using equation (3.12) for this region are

$$M_{21}\left(\frac{dU_\tau}{dx}\right) + M_{22}\left(\frac{dP}{dx}\right) + M_{23}\left(\frac{d\delta}{dx}\right) = N_4 \tag{3.29}$$

for $y_1 = L_3$ and $y_2 = \delta$ and

$$M_{24}\left(\frac{dU_\tau}{dx}\right) + M_{25}\left(\frac{dP}{dx}\right) + M_{26}\left(\frac{d\delta}{dx}\right) = N_5 \tag{3.30}$$

for $y_1 = (\delta/2)$ and $y_2 = \delta$

In evaluating the coefficients of $\left(\frac{dU_\tau}{dx}\right)$, $\left(\frac{dP}{dx}\right)$ and $\left(\frac{d\delta}{dx}\right)$ in the equations (3.25), 3.26), (3.28), (3.29) and (3.30) the contribution of a small region near the surface has been neglected; the boundary layer profile has been integrated from $y = L_3$. The reasons for this, are given in Appendix -A. The shear stress τ_δ is taken as zero and the shear stress at $\tau_{(\delta/2)}$ is evaluated using equation (3.20) and is given by

$$\tau_{(\delta/2)} = (0.01547)\,(U_\tau^2)\left(\frac{A}{L} + P\right)\left(\frac{2A}{L} + \pi P\right) \tag{3.31}$$

The shear stress at $y = L_3$ is given by

$$\tau_{L_3} = \tau_W = U_\tau^2 \tag{3.32}$$

These shear stresses occur in the coefficients N_4 and N_5.

Change of Mass Flow Across the Wake Centre: The rate of change of flow across the wake centre, F, given by the equation

$$F = \frac{d}{dx}\int_{L_3}^{\delta_2} U\, dy \tag{3.33}$$

is taken as zero. Hence the following equation is obtained.

$$M_{27}\left(\frac{d\delta_2}{dx}\right) + M_{28}\left(\frac{dU_1}{dx}\right) + M_{29}\left(\frac{dL_1}{dx}\right) + M_{30}\left(\frac{dU_\tau}{dx}\right) + M_{31}\left(\frac{dP}{dx}\right) + M_{32}\left(\frac{d\delta}{dx}\right) = N_6 \tag{3.34}$$

Relation For $\left(\frac{dU_i}{dx}\right)$: By differentiating the relation for U_i, equation (2.12) with respect to x, the following equation is obtained.

$$M_{33}\left(\frac{dU_\tau}{dx}\right) + M_{34}\left(\frac{dP}{dx}\right) + M_{35}\left(\frac{d\delta}{dx}\right) = N_7 \tag{3.35}$$

Referring to Fig. 3(a) it is seen that the thickness of the potential core is given by

$$L_2 = (\delta_2 - G_1 L_1 - \delta) \tag{3.36}$$

which gives the final equation.

Thus the set of equations (3.25) (3.26), (3.28), (3.29), (3.30), (3.34), (3.35) and (3.36) form the system of equations required to solve the flow problem in the unmerged case. It is seen that the derivatives of all the unknowns, except L_2 which appears only in the last equation, are coupled. Thus all the equations except the last

one are solved simultaneously for the x-derivatives of the variables. The step-by-step computation technique is described in the following section. The thickness of the potential core is evaluated using equation (3.36).

The choice of the five layers, in applying the momentum integral equation (3.12), requires discussion. The presence of the shear stresses in the equation requires the use of empirical relations for the eddy viscosity. This introduces further approximations into the equation. Hence, the layers have been chosen whenever possible, such that the shear stresses at their boundaries are already known (zero or τ_w). In this analysis, these layers are the whole regions of the outer wake, inner wake and the boundary layer. The other two equations have been obtained by applying equation (3.12) to parts of two out of the three shear layers.

In the merged case, the development of the outer wake is subject to the same constraints as in the unmerged case, but the intermittency component of the inner wake turbulence structure changes and could have a large effect on the inner wake shear stresses. This would involve the use of a different eddy viscosity expression. Hence in the system of equations for the merged case, equation (3.12) has been applied to part regions of the outer wake and the boundary layer. These part regions are the half velocity and half thickness layers of the outer wake and boundary layer respectively which are sufficiently thick. The outer half of the boundary layer has been

chosen instead of the inner half as it requires only the knowledge of the shear stress at $y = \delta/2$ unlike the inner half which requires the shear stress at $y = 0$, namely U_τ^2, and which may introduce some errors in the system of equations.

In the unmerged case, the development of the outer wake, inner wake and the boundary layer is similar to that of the respective free layers as indicated in section (iv) of Chapter 2. Hence the eddy viscosity expressions suggested earlier would be more or less consistent with the turbulence structure present in the three layers and any pair would serve equally well. So the same two regions were used for the unmerged case.

(b) Merged Case: In this case the variables involved are the same as in the unmerged case but for L_2 which disappears. A new unknown variable U_3, the velocity at the edge of the boundary layer, is introduced because of the disappearance of the potential core; it can no longer be calculated from the pressure field. Hence a slightly different system of equations needs to be developed. The details involved in these equations and the coefficients are given in Appendix -A and the equations are listed below.

Outer Wake Region The equations obtained by applying the momentum integral equation (3.12) to this region are

$$R_1\left(\frac{d\delta_2}{dx}\right) + R_2\left(\frac{dU_1}{dx}\right) + R_3\left(\frac{dL_0}{dx}\right) + R_4\left(\frac{dL_1}{dx}\right) + R_5\left(\frac{dU_\tau}{dx}\right) + R_6\left(\frac{dP}{dx}\right) + R_7\left(\frac{d\delta_3}{dx}\right) + R_8\left(\frac{dU_3}{dx}\right) = T_1 \qquad (3.37)$$

for $y_1 = \delta_2$ and $y_2 = \delta_2 + G_0 L_0$ and

$$R_9\left(\frac{d\delta_2}{dx}\right) + R_{10}\left(\frac{dU_1}{dx}\right) + R_{11}\left(\frac{dL_0}{dx}\right) + R_{12}\left(\frac{dL_1}{dx}\right)$$

$$+ R_{13}\left(\frac{dU_\tau}{dx}\right) + R_{14}\left(\frac{dP}{dx}\right) + R_{15}\left(\frac{d\delta_3}{dx}\right) + R_{16}\left(\frac{dU_3}{dx}\right) = T_2 \qquad (3.38)$$

for $y_1 = \delta_2$ and $y_2 = (\delta_2 + L_0)$

Amongst the shear stresses $\tau_{(\delta_2 + G_0 L_0)}$, $\tau_{(\delta_2 + L_0)}$ and τ_{δ_2} involved in the coefficients T_1 and T_2, $\tau_{(\delta_2 + G_0 L_0)}$ and τ_{δ_2} are taken as zero and the shear stress $\tau_{(\delta_2 + L_0)}$ is evaluated as in the unmerged case.

Inner Wake Region: The equation obtained by applying the momentum integral equation (3.12) to the inner wake region is

$$R_{17}\left(\frac{d\delta_2}{dx}\right) + R_{18}\left(\frac{dU_1}{dx}\right) + R_{19}\left(\frac{dL_1}{dx}\right) + R_{20}\left(\frac{dU_\tau}{dx}\right)$$

$$+ R_{21}\left(\frac{dP}{dx}\right) + R_{22}\left(\frac{d\delta_3}{dx}\right) + R_{23}\left(\frac{dU_3}{dx}\right) = T_3 \qquad (3.39)$$

for $y_1 = (\delta_2 - G_1 L_1)$ and $y_2 = \delta_2$

The shear stress $\tau_{(\delta_2 - G_1 L_1)}$ occurring in T_3 is again taken as zero.

Boundary Layer Region: The equations obtained by applying the equation (3.12) to this region are

$$R_{24}\left(\frac{dU_\tau}{dx}\right) + R_{25}\left(\frac{dP}{dx}\right) + R_{26}\left(\frac{d\delta_3}{dx}\right) = T_4 \qquad (3.40)$$

for $y_1 = L_3$ and $y_2 = \delta_3$ and

$$R_{27}\left(\frac{dU_\tau}{dx}\right) + R_{28}\left(\frac{dP}{dx}\right) + R_{29}\left(\frac{d\delta_3}{dx}\right) = T_5 \qquad (3.41)$$

for $y_1 = \left(\frac{\delta_3}{2}\right)$ and $y_2 = \delta_3$

The contribution of a thin region near the boundary is neglected as before. The shear stresses τ_{δ_3} and τ_{L_3} appearing in the coefficients T_4 and T_5 are taken as zero and U_τ^2 respectively. The shear stress $\tau_{(\delta_{3/2})}$ is obtained by using the eddy viscosity expression, equation (3.21).

Change of Mass Flow Across The Wake Centre: The relation obtained by assuming a zero mass flow across the wake centre is

$$R_{30}\left(\frac{dU_1}{dx}\right) + R_{31}\left(\frac{dL_1}{dx}\right) + R_{32}\left(\frac{dU_\tau}{dx}\right) + R_{33}\left(\frac{dP}{dx}\right) + R_{34}\left(\frac{d\delta_3}{dx}\right) + R_{35}\left(\frac{dU_3}{dx}\right) = T_6 \qquad (3.42)$$

where $T_6 = F = 0$.

Relation For $\left(\frac{dU_3}{dx}\right)$: The expression for the velocity at the edge of the boundary layer is given by

$$U_3 = \left(\frac{AU_\tau}{L}\right) \ln\left(\frac{\delta_3 U_\tau}{\nu}\right) + BU_\tau + 2PU_\tau \qquad (3.43)$$

Differentiating the above equation with respect to x, the following equation is obtained:

$$R_{36}\left(\frac{dU_\tau}{dx}\right) + R_{37}\left(\frac{dP}{dx}\right) + R_{38}\left(\frac{d\delta_3}{dx}\right) + R_{39}\left(\frac{dU_3}{dx}\right) = 0 \qquad (3.44)$$

Referring to Fig. 3 (b) it is seen that

$$\delta_2 = G_1 L_1 + \delta_3 \qquad (3.45)$$

and on differentiation, the following equation is obtained.

$$R_{40}\left(\frac{d\delta_2}{dx}\right) + R_{41}\left(\frac{dL_1}{dx}\right) + R_{42}\left(\frac{d\delta_3}{dx}\right) = 0 \qquad (3.46)$$

The set of equations (3.37), (3.38), (3.39), (3.40), (3.41), (3.42), (3.44) and (3.46) forms the system of equations for the

merged case. Unlike the unmerged case, the x-derivatives of all the variables are coupled by all the equations in this case. Hence it is necessary to solve the system of equations simultaneously.

(vi) Computation Technique: A computer program has been developed to perform the calculations. The flow chart for the program is given in Appendix -C for easy understanding of the program. The program itself is given in Appendix -D. Function subprograms have been used to evaluate the numerical integrals C_7, C_8, C_{15} and C_{16}, the pressure integrals and the potential flow velocities. The Simpson's method with 400 intervals has been used in the subprograms to evaluate the numerical integrals. The numerical technique used in the step by step computation process is the finite difference method and the computer language used is the FORTRAN (WATFIV) language. Double precision is used in the computations to improve the accuracy of the calculations. The system of equations in both cases is solved in matrix form, $QX = S$, where Q, X and S are matrices of the appropriate order. X is the column matrix containing the unknowns, namely the x-derivatives of the variables. It is given by $X = Q^{-1}S$, where Q^{-1} is the inverse of the matrix Q. The subroutine used to evaluate this is the IMSL subroutine LEQT2F. This is a powerful subroutine used in solving systems of linear equations. It can be set to provide warnings as to whether the matrix is singular or the system of equations is ill-conditioned.

In each of the test cases, the most upstream station at which

accurate data is available is used as the initial station. The program is fed with the values at the initial station. The system of equations for the unmerged case is solved. The variables are calculated using the finite difference formula

$$\phi_{i+1} = \phi_i + \frac{d\phi}{dx} \Delta x \qquad (3.47)$$

where ϕ stands for a variable,

$\frac{d\phi}{dx}$ for the x-derivative of the variable,

ϕ_i for the value of the variable at a station and

ϕ_{i+1} for the value of the variable at the next station.

The value of the variable L_2 is calculated at the end of each step. When once it becomes zero or negative, the program proceeds with the prediction of the flow in the merged case.

The program is set to perform as long as the following conditions are satisfied.

(i) $x \leq$ aerofoil length and

(ii) $c_{f\infty} > 0$ (indicating attached flow)

The flow is considered as the development of a wake and a boundary layer as long as the value of $(U_3 - U_1)$ is greater than 0.0025. The results of the program downstream of the station at which this condition is not satisfied are disregarded. Then the flow is treated as the development of an equivalent boundary layer, which is

discussed in the last section of this Chapter.

The step distance Δx in equation (3.47) has been chosen to be equal to 0.001. This resulted in a program requiring a time of about 114 seconds for a flap distance of $x = 0.286$.

(vii) Integral Parameters: The usual integral parameters used for testing the reliability of a calculation method are the displacement thickness δ^* and the momentum thickness θ and the shape parameter H, given by $H = (\delta^*/\theta)$. The calculation method can be judged from a comparison of the predicted values of these parameters with the experimental ones. They are also representative of the quantitative effect of the shear flows on the hypothetical potential flow so that these parameters can be used to simulate the effect of the shear flows. Thus they can be used with potential flow models to predict the behaviour of the real flow model.

The usual definitions of the displacement and momentum thicknesses do not take into account the transverse pressure gradient. Myring (14) has arrived at the definitions of the displacement thickness taking into account the transverse pressure gradient and the momentum thickness compatible with the displacement surface. It has been shown that by neglecting the fact that $(\frac{\partial C_p}{\partial y}) \neq 0$ these thicknesses are those automatically defined along isobars. But in the present analysis no attempt has been made to use the corrected definitions, as it was necessary to compare the predicted values of the integral parameters with the experimental results obtained from the usual definitions. These definitions are given in Appendix -B.

(viii) Far Downstream Solution: As the boundary layer and the wake develop adjacent to each other in the merged region, a particular situation may arise when the inner wake loses its identity. The velocity gradients and hence the shear stresses in the wake become negligibly small and a profile similar to the one shown in Fig. 4 is attained. This region is termed as the far region. A technique similar to the one employed by Kibria (3) has been used in analysing the far region. When the velocity defect (U_3-U_1) becomes less than (0.0025) the whole shear region has been replaced by an equivalent boundary layer having

(i) the same total displacement thickness and momentum thickness,

(ii) the same main stream velocity U_e and

(iii) the same friction velocity U_τ

Treating the whole shear region as one single layer, the total displacement and momentum thicknesses denoted by δ^*_T and θ_T are given by the following equations.

$$\delta^*_T = \int_0^{(\delta_2 + G_0 L_0)} (1 - \frac{U}{U_e})dy \qquad (3.48)$$

$$\theta_T = \int_0^{(\delta_2 + G_0 L_0)} (\frac{U}{U_e})(1 - \frac{U}{U_e})dy \qquad (3.49)$$

The equations for δ^*_T and θ_T are given in Appendix -B. The displacement thickness and momentum thickness of the equivalent boundary layer are also given by the relations

$$\left(\frac{\delta_T}{\delta_T}\right) = \left(\frac{U_\tau}{U_e}\right)\left(\frac{A}{L} + P_T\right) \tag{3.50}$$

$$\left(\frac{\theta_T}{\delta_T}\right) = \left(\frac{\delta^*_T}{\delta_T}\right) - \left(\frac{U_\tau}{U_e}\right)^2 \left[1.5P^2 + 3.18\,\frac{AP}{L} + 2\,\frac{A^2}{L^2}\right] \tag{3.51}$$

where δ_T and P_T are the boundary layer thickness and the profile parameter of the equivalent boundary layer respectively. Thus the parameters δ_T and P_T are calculated. These equations have been obtained from the usual definitions of the displacement and momentum thicknesses for the boundary layer and are identical to equations (B-6) and (B-11) with δ^*_B, θ_B, P, δ and U_i replaced by δ^*_T, θ_T, P_T, δ_T and U_e respectively. Once the parameters of the equivalent boundary layer at the start of the far region have been evaluated, the rest of the flow is treated as the growth of the equivalent boundary layer and calculated using the equations and techniques for the boundary layer region.

CHAPTER 4

RESULTS AND DISCUSSIONS

The results obtained by using the present calculation method are compared with the experimental results of four cases of flow over multi-element aerofoil systems. The geometries of the aerofoil configurations used in the test cases are shown in Fig. 5. Two of these cases are the experimental investigations of flow around a slotted flap reported by Foster, Irwin and Williams (4) and, for which a theoretical analysis has been developed by Irwin (2). Kibria (3) developed an alternative theoretical model for one of these cases, the results of which are also available for comparison. In these cases, the full two-dimensional pressure field over the flap has been measured. The other two cases are the experimental measurements of Bario et al (6) and Ljungstrom (5) where only the surface pressure has been measured.

Test Case 1: The geometry of the two-element system used in this case is shown in Fig. 5. The flap deflection was 30°, the slot height was 0.025c and the angle of attack was 8°. The experiment was conducted in a low speed wind tunnel at a free stream velocity of 61 m/sec. The aerofoil system had an unextended chord of 0.915 m. The chord of the flap was 40% of the unextended chord. It has been reported by Foster, Irwin and Williams (4) that the above flap deflec-

tion corresponds approximately to the landing configuration. The pressure data for this case has been given by Irwin (2) and are reproduced in Fig. 6. For reasons given in section (i) of Appendix - A the static pressure coefficient C_p has been represented as $C_p = f(x)\ y + g(x)$. While evaluating the coefficients occurring in the functions, the function g (x) has been fitted at y=o; the function f(x) has been fitted at suitable y values. In fitting the function g (x), the value of C_p at y =o has been taken as being equal to that measured by the surface pressure tap and not as being equal to that determined from the measurements of the static pressure probe. This has been done because it is known that as a result of the sharp obstruction of the flow when the static pressure probe is used near the surface, the measurements are not as accurate as that of the static pressure tap.

The present method predicts merging at about x = 0.25. The variations of U_1, U_3 and (U_3-U_1) are shown in Fig. 7. It is seen that U_1 decreases with distance, unlike in an ordinary wake where one would expect that it would increase. This is because of the presence of an adverse pressure gradient. Kibria's calculation method also predicts similar results except for increasing values in the vicinity of the flap trailing edge which may be because of the use of the momentum integral equation in its inexact form. The trend in the variation of U_3 is similar in both methods. It is seen that (U_3-U_1) decreases with distance, reaches a minimum in the vicinity

of the flap trailing edge and then increases.

The variations of L_1, L_0 and P are shown in Fig. 8 in comparison with that obtained by Irwin's and Kibria's methods. It is seen that the trend in the qualitative variations of L_1 and L_0 as obtained by this method and Irwin's method is the same all along the flow development and different from Kibria's method which predicts decreasing values near the trailing edge. Again, this is because of using the momentum integral equation in its inexact form. The values of L_1 and L_0 predicted by this method are lower than that predicted by Kibria's method. This may because of the fact that the transverse pressure gradient has been taken into account. The length scale L_0 of the outer wake as predicted by the present method continues to increase until the trailing edge which is consistent with physical evidence. The same observations are noted in the case of L_1. The trend in the variations of the profile parameter P is seen to be similar in the present method as in Kibria's method, the difference being in the maximum value of P attained. The reason for this is partly related to the fact that the initial value of P deduced from the data given by Irwin (2) is different in both methods.

The curves of H_B, θ_B, H_{IW} and θ_{IW} are shown in Fig. 9 in comparison with the experimental values and with the calculated values of Irwin (2) and Kibria (3). The values of H_B and θ_B predicted by the present method are closer to the experimental values than the other two methods. The reason for the improvement over the Irwin's

method may be because Coles profile has been used, instead of the power law. Coles profile is a better representation for boundary layers developing in adverse pressure gradients. In the case of H_{IW} and θ_{IW}, the present calculations are significantly closer to the experimental values than Kibria's calculations. Since the same boundary layer and wake profiles have been used in both cases, the reason for this may be the exact form of the momentum integral equation used. The present method does not predict decreasing values of θ_B and θ_{IW} near the trailing edge like Kibria's method. The reasons for this are the same as that quoted in connection with L_1 and L_0. The values of H_{IW} and θ_{IW} as predicted by the present method also show a slight improvement over that predicted by Irwin's method. The curves of H_{OW}, θ_{OW} and $C_{f\infty}$ are shown in Fig. 10. Improvements are noted in the prediction of H_{OW} and θ_{OW} over the two methods. In the case of $C_{f\infty}$, the curve reaches a minimum at about $x = 0.36$ and then increases. This is related to the fact that a short distance upstream of this point, the value of P starts decreasing. The initial value of $C_{f\infty}$ used in the present method has been obtained from the data given by Irwin (2). In the case of Kibria's method it has been evaluated using the well-known Ludwieg and Tillmann's empirical relation. Thus the initial values are different in the two methods. Hence it is not surprising that the values of $C_{f\infty}$ as predicted by Kibria's method are closer to the experimental values than those predicted by the present method. It

has been reported in (2) that flow separation occurs at about x=0.3.

The velocity profiles are compared in Fig. 11. The profiles at the two downstream stations after the initial station as predicted by the pesent method are closer to the experimental ones than the other two methods only in some regions of the wake and the boundary layer. But as seen earlier there is better agreement of the integral parameters H_B, θ_B, H_{IW}, θ_{IW}, H_{OW} and θ_{OW} with the experimental ones. Hence the complete velocity profiles are a good representation of the experimental ones. At the last station the flow has undergone separation and none of the predicted profiles are close to the experimental ones. The positions of the maximum and minimum in the velocity profiles at all the downstream stations except the last one are quite close to the experimental ones. This implies that the growths of the wake and the boundary layer discussed earlier in terms of L_1, L_0 and P have been predicted well over most of the flap. In particular there has been a significant improvement over Kibria's prediction of the velocity profiles. The reason for this may again be the presence of the transverse pressure gradient and the exact form of the momentum integral equation.

Test Case 2: In this case, the two-element aerofoil configuration is almost the same as that reported in Case 1, except that a smaller slot height of 0.020c has been used. The experimental pressure distribution has been compared with the formulated distribution in Fig. 12. Again there are noticeable differences in the values of

C_p at y = o, the reasons for which are the same as that reported in Case 1.

The present method predicts merging at about x = 0.2. Since there has been early merging, the interaction between the wake and the boundary layer has been strong which affects the relative growths of the boundary layer and the wake. The curves of U_1, U_3 and (U_3-U_1) are shown in Fig. 13. The values of U_1 and U_3 decrease with x as noted in Case 1. The value of (U_3-U_1) increases with x up to the merging point and then decreases up to the flap trailing edge. The variations of L_1 and L_0 are shown in Fig. 14. The length scales L_1 and L_0 increase with distance as noted in Case 1. The curves of H_B, θ_B, H_{IW} and θ_{IW} are shown in Fig. 15. There has been an improvement over Irwin's prediction of these values as seen from the experimental points. The values of θ_{IW} as predicted by Irwin's method approach a constant value near the trailing edge. This is consistent with the behaviour of L_1 near the trailing edge as predicted by the same method, which is shown in Fig. 14. The curves of H_{OW}, θ_{OW} and $C_{f\infty}$ are presented in Fig. 16. There appears to be noticeable improvements in the predictions of H_{OW} and θ_{OW}. The present method predicts low values of $C_{f\infty}$ near the trailing edge indicating imminent separation of the flow. The initial value of $C_{f\infty}$ used in Irwin's method, probably obtained from the empirical relation of Ludwieg and Tillmann, is lower than that used in the present method. This is the reason that the values of $C_{f\infty}$ as predicted by Irwin's method are

closer to the experimental values than that predicted by the present method. The velocity profiles as predicted by the two methods are shown in Fig. 17 in comparison with the experimental ones. Because of the better prediction of H_B, θ_B, H_{IW}, θ_{IW}, H_{OW}, and θ_{OW}, it can be inferred that the velocity profiles are a good representation of the experimental profiles.

Test Case 3: This is the case for which experimental measurements have been reported by Bario et al (6). As shown in Fig. 5, in this case two symmetrical aerofoils were used. The tests were conducted in a low speed variable pressure gradient wind tunnel to create the flow pattern involving a wake and a boundary layer. The chord of the second aerofoil was 0.6m. The tests were conducted at a free stream velocity of about 18 m/sec. The formulated pressure distribution is compared with the experimental distribution in Fig. 18. The pressures were presented on a small scale in (6). This could be a source of error in the formulated distribution which has been represented by two straight lines upstream and downstream of $x = 0.4$.

The present method predicts merging at $x = 0.65$. The actual merging has been stated to occur at about $x = 0.5$. It is possible that merging might have occurred as early as this because it was reported that the boundary layer was not fully turbulent in character and was undergoing transition in the region of the initial development of the flow. Since the boundary layer was not fully

turbulent it implies that the values of $C_{f\infty}$ would be low. The prediction of skin friction coefficient C_f has been compared with the experimental results in Fig. 19. It is seen that there is good agreement up to the merging point after which the measured values of C_f decrease rapidly with separation occurring at x = 0.88. The present method predicts imminent separation near x = 0.98. It is understandable that separation cannot be predicted by Coles profile because of the presence of the logarithmic term. The predicted velocity profiles are compared with the experimental ones in Fig. 20. It is seen from the velocity profile at the initial station that the value of $(\frac{U_1}{U_e})$ is different from the experimental value. This indicates that some errors have been introduced in deducing the initial values from the figures given in (6) which were plotted to a small scale. There is good agreement of the velocity profiles with the experimental ones at all stations except the last one. The reason for this might be the fact that the real flow was close to separation.

Test Case 4: The last case is the experimental work undertaken by Ljungstrom (5) in order to study the effect of different viscous layers on the optimization of a multi-element aerofoil system. The geometry of the three-element system used is shown in Fig. 5. The tests were conducted in a low speed wind tunnel. It has been deduced from the data and the figures given in (5) that the unextended chord of the system was c = 1.1 m. Since sufficient information was not

available to infer the free stream velocity U_∞ at which the tests were conducted, it has been assumed that the test was conducted at a free stream Reynolds number of about $R_\infty = 1.8 \times 10^6$. This yields a free-stream velocity of U_∞ = 25m/sec. These values of c and U_∞ have been used in nondimensionalising the length and velocity variables as in the other test cases. The formulated pressure distribution has been compared with the experimental distrubution in Fig. 21. Again, in this case, the experimental pressure distribution C_p was presented to a small scale in (5). This could be a source of error in the formulated pressure distrubution which has been represented by three straight lines as shown in Fig. 21.

In this case the pressure field was given as a function of the distance on the main aerofoil surface. Hence in the calculations for this case x is equal to the distance measured along the aerofoil upper surface. The total displacement thickness of the flow as predicted by the present method is compared with the experimental results in Fig. 22. It is seen that there is good agreement beyond the merging point up to a distance as far downstream as x = 0.73. After x =0.73, the value of (U_3-U_1) as calculated by the present method became less than 0.0025. This indicated that within a short distance downstream the inner wake would disappear. Hence as suggested in section (viii) of Chapter 3, the whole shear layer has been represented by an equivalent turbulent boundary layer having the same characteristics. When the above concept is used, it is seen that there is not good agreement with the experimental results.

This may be because the equivalent boundary layer thickness increases rapidly with imminent separation being predicted at x=0.88 whereas the actual shear layer does not exhibit separation even at the trailing edge of the main aerofoil.

The predicted velocity profiles are compared in Fig. 23. There is fair agreement at all stations except the last one where the shear layer has been represented by an equivalent turbulent boundary layer. Ljungstrom defines the merging as the station at which the inner wake disappears. This is said to occur between x=0.41 and x=0.59 as compared with the currently predicted value of x=0.73. But from the illustration given in (5) it is seen that the disappearance of the inner wake must have occurred later than x=0.59.

CHAPTER 5

CONCLUSIONS

The integral calculation method developed by Irwin (2) and modified by Kibria (3) has been improved by taking into account the transverse pressure gradient and using the momentum integral equation without making any approximations. The results indicate the features which are given below:

(i) The development of the integral parameters, the displacement and momentum thicknesses and the velocity profiles, predicted by this method, are quite satisfactory when compared with the experimental ones except near separation.

(ii) The prediction of skin friction coefficient is also satisfactory with quite low values obtained in the separation region.

(iii) The predicted growth of the wake and the boundary layer is consistent with physical evidence unlike Kibria's method.

The present method can be improved if the following factors are taken into account

(i) The boundary layer profile should be able to predict separation.

(ii) The flap should be represented by a curved surface.

(iii) The wake mean velocity profiles should be represented by more accurate asymmetric profiles than Townsend's universal law.

(iv) The eddy viscosity expressions should be more compatible with the flow model.

REFERENCES

(1) K. Jacob and D. Steinbach: A Method For Prediction Of Lift For Multi-Element Aerofoil Systems, AGARD Conference Proceedings No. 143, October 1974.

(2) H.P.A.H. Irwin: A Calculation Method For Two-Dimensional Turbulent Flow Over A Slotted Flap, ARC C.P. No. 1267, June 1972.

(3) Md. Golam Kibria: The Predicted Interaction Of A Wake With An Adjacent Turbulent Boundary Layer, M. Sc. Thesis, University of Manitoba, 1980.

(4) D.N. Foster, H.P.A.H. Irwin and B.R. Williams: The Two-Dimensional Turbulent Flow Over A Slotted Flap, A.R.C. R. & M. No. 3681, September 1980.

(5) B.L.G. Ljungstrom Experimental Study OF Viscous Flow On Multi-Element Airfoils, ICAS, 74-46, August 1974.

(6) F. Bario, G. Charnay and K.D. Papailiou An Experiment Concerning The Confluence Of A Wake And A Boundary Layer, J.F.E. Vol. 104, March 1982.

(7) Donald Coles: The Law Of The Wake In The Turbulent Boundary Layer, J.F.M., Vol. 1, Part 2, pp. 191-226, 1956.

(8) E.L.Houghton and R.P. Boswell: Further Aerodynamics For Engineering Students, Edward Arnold Ltd., 1969.

(9) F. Clauser: Turbulent Boundary Layers In Adverse Pressure Gradients, JAS. 21, pp.91-108, February 1954.

(10) A.A. Townsend: The Structure Of Turbulent Shear Flow, Cambridge University Press, 1956.

(11) I.S. Gartshore: Two-Dimensional Turbulent Wakes, J.F.M., Vol. 30, Part 3, pp. 547-560, 1967.

(12) S. Goldstein: Modern Developments In Fluid Dynamics, Clarendon Press, 1938.

(13) A.M.O. Smith and T. Cebeci: Numerical Solution Of The Turbulent-Boundary-Layer Equations, Report No. DAC 33735, May 39, 1967.

(14) D.F. Myring: The Effect Of Normal Pressure Gradients On The Boundary Layer Momentum Integral Equation, RAE Technical Report 68214, August 1968.

APPENDIX - A

(i) Typical Relations Occurring In The Systems of Equations of Chapter 3:

Unmerged Case:

Momentum Integral Equations:

The exact form of the simplified momentum integral equation obtained by using the notion of the order of magnitudes is

$$\int_{y_1}^{y_2} \left(\frac{\partial U^2}{\partial x}\right) dy - U_{y_2} \int_{0}^{y_2} \left(\frac{\partial U}{\partial x}\right) dy + U_{y_1} \int_{0}^{y_1} \frac{\partial U}{\partial x}\, dy + \int_{y_1}^{y_2} \left(\frac{1}{2}\right)\left(\frac{\partial C_p}{\partial x}\right) dy - (\tau_{y_2} - \tau_{y_1}) = 0 \qquad \text{(A-1)}$$

As an example, the application of the momentum integral equation is given in detail for the pair of limits $y_1 = \delta_2$ and $y_2 = (\delta_2 + G_0 L_0)$.

Since $U_{(\delta_2 + G_0 L_0)} = U_e$ and $U_{\delta_2} = U_1$, the momentum integral equation (A-1) becomes

$$\int_{\delta_2}^{(\delta_2 + G_0 L_0)} \left(\frac{\partial U^2}{\partial x}\right) dy - U_e \int_{0}^{(\delta_2 + G_0 L_0)} \left(\frac{\partial U}{\partial x}\right) dy + U_1 \int_{0}^{\delta_2} \left(\frac{\partial U}{\partial x}\right) dy + \int_{\delta_2}^{(\delta_2 + G_0 L_0)} \left(\frac{1}{2}\right)\left(\frac{\partial C_p}{\partial x}\right) dy - \tau_{(\delta_2 + G_0 L_0)} + \tau_{\delta_2} = 0 \qquad \text{(A-2)}$$

The first term in the equation (A-2) has to be integrated only over the outer wake region. The other terms in equation (A-2) require the velocity profiles and their x-derivatives over more limited ranges of the layer. These relations are given below. In the outer wake region U is given by

$$U = U_e - (U_e - U_1)\, \mathrm{Exp}\left[-k\left(\frac{y - \delta_2}{L_0}\right)^2\right] \qquad \text{(A-3)}$$

Since U_e is, in effect, a function of x only, its partial derivative $\left(\frac{\partial U_e}{\partial x}\right)$ and the total derivative $\left(\frac{dU_e}{dx}\right)$ are the same.

Hence $(\frac{\partial U}{\partial x})$ is given by,

$$(\frac{\partial U}{\partial x}) = (\frac{dU_e}{dx}) - \text{Exp}[-k(\frac{y-\delta_2}{L_0})^2](\frac{dU_e}{dx})$$

$$- 2k(\frac{U_e - U_1}{L_0})(\frac{y-\delta_2}{L_0})\ \text{Exp}[-k(\frac{y-\delta_2}{L_0})^2](\frac{d\delta_2}{dx})$$

$$- 2k(\frac{U_e - U_1}{L_0})(\frac{y-\delta_2}{L_0})^2\ \text{Exp}[-k(\frac{y-\delta_2}{L_0})^2](\frac{dL_0}{dx})$$

$$+ \text{Exp}[-k(\frac{y-\delta_2}{L_0})^2](\frac{dU_1}{dx}) \qquad \text{(A-4)}$$

Squaring (A-3) leads to,

$$U^2 = U_e^2 + (U_e - U_1)^2\ \text{Exp}[-2k(\frac{y-\delta_2}{L_0})^2]$$

$$- 2U_e(U_e - U_1)\ \text{Exp}[-k(\frac{y-\delta_2}{L_0})^2] \qquad \text{(A-5)}$$

Differentiating (A-5) with respect to x, the following equation is obtained.

$$\frac{\partial U^2}{\partial x} = \left[2U_e + 2(U_e - U_1)\ \mathrm{Exp}\left\{-2k\left(\frac{y-\delta_2}{L_0}\right)^2\right\}\right.$$

$$\left. - 2U_e\ \mathrm{Exp}\left\{-k\left(\frac{y-\delta_2}{L_0}\right)^2\right\} - 2(U_e - U_1)\ \mathrm{Exp}\left\{-k\left(\frac{y-\delta_2}{L_0}\right)^2\right\}\right]\left(\frac{dU_e}{dx}\right)$$

$$+ \left[4k\frac{(U_e - U_1)^2}{L_0}\left(\frac{y-\delta_2}{L_0}\right)\mathrm{Exp}\left\{-2k\left(\frac{y-\delta_2}{L_0}\right)^2\right\}\right.$$

$$\left. - 4kU_e\left(\frac{U_e - U_1}{L_0}\right)\left(\frac{y-\delta_2}{L_0}\right)\mathrm{Exp}\left\{-k\left(\frac{y-\delta_2}{L_0}\right)^2\right\}\right]\left(\frac{d\delta_2}{dx}\right)$$

$$+ \left[4k\frac{(U_e - U_1)^2}{L_0}\left(\frac{y-\delta_2}{L_0}\right)^2\mathrm{Exp}\left\{-2k\left(\frac{y-\delta_2}{L_0}\right)^2\right\}\right.$$

$$\left. - 4kU_e\left(\frac{U_e - U_1}{L_0}\right)\left(\frac{y-\delta_2}{L_0}\right)^2\mathrm{Exp}\left\{-k\left(\frac{y-\delta_2}{L_0}\right)^2\right\}\right]\left(\frac{dL_0}{dx}\right)$$

$$+ \left[2U_e\mathrm{Exp}\left\{-k\left(\frac{y-\delta_2}{L_0}\right)^2\right\} - 2(U_e - U_1)\ \mathrm{Exp}\left\{-2k\left(\frac{y-\delta_2}{L_0}\right)^2\right\}\right]\left(\frac{dU_1}{dx}\right) \qquad \text{(A-6)}$$

In the inner wake region U is given by

$$U = U_0 - (U_0 - U_1)\ \mathrm{Exp}\left[-k\left(\frac{y-\delta_2}{L_1}\right)^2\right] \qquad \text{(A-7)}$$

and $\left(\frac{\partial U}{\partial x}\right)$ is given by

$$\frac{\partial U}{\partial x} = \frac{dU_0}{dx} - \left\{\mathrm{Exp}\left[-k\left(\frac{y-\delta_2}{L_1}\right)^2\right]\right\}\left(\frac{dU_0}{dx}\right)$$

$$- 2k\left(\frac{U_0 - U_1}{L_1}\right)\left(\frac{y-\delta_2}{L_1}\right)\mathrm{Exp}\left[-k\left(\frac{y-\delta_2}{L_1}\right)^2\right]\left(\frac{d\delta_2}{dx}\right)$$

$$- 2k\frac{(U_0 - U_1)}{L_1}\left(\frac{y-\delta_2}{L_1}\right)^2\mathrm{Exp}\left[-k\left(\frac{y-\delta_2}{L_1}\right)^2\right]\left(\frac{dL_1}{dx}\right)$$

$$+ \mathrm{Exp}\left[-k\left(\frac{y-\delta_2}{L_1}\right)^2\right]\left(\frac{dU_1}{dx}\right) \qquad \text{(A-8)}$$

In the boundary layer region U is given by

$$U = \left(\frac{AU_\tau}{L}\right) \ln\left(\frac{yU_\tau}{\nu}\right) + BU_\tau + 2PU_\tau \sin^2\left(\frac{\pi y}{2\delta}\right) \qquad \text{(A-9)}$$

and $\frac{\partial U}{\partial x}$ is given by

$$\frac{\partial U}{\partial x} = \left[\frac{A}{L} + \frac{A}{L} \ln\left(\frac{yU_\tau}{\nu}\right) + B + 2P \sin^2\left(\frac{\pi y}{2\delta}\right)\right]\left(\frac{dU_\tau}{dx}\right)$$

$$+ \left[2U_\tau \sin^2\left(\frac{\pi y}{2\delta}\right)\right]\left(\frac{dP}{dx}\right)$$

$$- \left[\frac{2PU_\tau \pi}{\delta^2} y \sin\left(\frac{\pi y}{2\delta}\right) \cos\left(\frac{\pi y}{2\delta}\right)\right]\left(\frac{d\delta}{dx}\right) \qquad \text{(A-10)}$$

For clarity, each of the terms in equation (A-2) are derived separately. The coefficients A_i , B_i , C_i , D_i , E_i , H_i , M_i , N_i , R_i and T_i that appear in the equations to follow are given in section (ii) of this appendix.

Using equation (A-6) to evaluate the first term in equation (A-2) leads to

$$\int_{\delta_2}^{(\delta_2 + G_0 L_0)} \left(\frac{\partial U^2}{\partial x}\right) dy = \left[2U_e G_0 L_0 + 2(U_e - U_1) L_0 A_3 \right.$$

$$\left. - 2U_e L_0 A_4 - 2(U_e - U_1) L_0 A_4\right]\left(\frac{dU_e}{dx}\right)$$

$$+ (2U_e)(U_e - U_1)\left[\mathrm{Exp}(-kG_0^2) - 1\right]\left(\frac{d\delta_2}{dx}\right)$$

$$- (U_e - U_1)^2\left[\mathrm{Exp}(-2kG_0^2) - 1\right]\left(\frac{d\delta_2}{dx}\right)$$

$$+ \left[2U_e L_0 A_4 - 2(U_e - U_1) L_0 A_3\right]\left(\frac{dU_1}{dx}\right)$$

$$+ \left[4k(U_e - U_1)^2 A_1 - 4kU_e(U_e - U_1) A_2\right]\left(\frac{dL_0}{dx}\right) \qquad \text{(A-11)}$$

The second term in the equation (A-2) has to be integrated over the whole shear region. It can be written as

$$U_e \int_0^{(\delta_2 + G_0 L_0)} \left(\frac{\partial U}{\partial x}\right) dy = U_e \int_0^{\delta} \left(\frac{\partial U}{\partial x}\right) dy + U_e \int_{\delta}^{(\delta_2 - G_1 L_1)} \left(\frac{\partial U}{\partial x}\right) dy$$

$$+ U_e \int_{(\delta_2 - G_1 L_1)}^{\delta_2} \left(\frac{\partial U}{\partial x}\right) dy + U_e \int_{\delta_2}^{(\delta_2 + G_0 L_0)} \left(\frac{\partial U}{\partial x}\right) dy \qquad \text{(A-12)}$$

The conventional Coles profile used does not properly represent the velocity profile in the sub-layer. It gives values of $U \to -\infty$ as $y \to 0$. A fuller representation of the velocity profile should be made in two parts, $0 < y \leq \delta_s$, $\delta_s < y \leq \delta$ where δ_s is the sub-layer thickness. This complicates the profile representation because δ_s varies with the development of the flow. Since the sub-layer is thin, the low-velocity fluid in the sub-layer contributes a very small amount to the mass flux and momentum flux. Hence a very small error is introduced by assuming $U = 0$ for $0 < y < L_3$, where L_3 is chosen such that it is close to the surface but would not yield a negative value for the velocity. Negative values occur when $(yU_\tau/\nu) < 1$ so a suitable value of L_3 , well within the sublayer, is taken such that $\left(\frac{L_3 U_\tau}{\nu}\right) = 2$. So equation (A-12) can be written as,

$$U_e \int_0^{(\delta_2 + G_0 L_0)} \left(\frac{\partial U}{\partial x}\right) dy \simeq U_e \int_{L_3}^{\delta} \left(\frac{\partial U}{\partial x}\right) dy + U_e \int_{\delta}^{(\delta_2 - G_1 L_1)} \left(\frac{\partial U}{\partial x}\right) dy$$

$$+ U_e \int_{(\delta_2 - G_1 L_1)}^{\delta_2} \left(\frac{\partial U}{\partial x}\right) dy + U_e \int_{\delta_2}^{(\delta_2 + G_0 L_0)} \left(\frac{\partial U}{\partial x}\right) dy \qquad \text{(A-13)}$$

In the potential region between $\delta < y \leq (\delta_2 - G_1 L_1)$, the continuity equation is used to eliminate $(\frac{\partial U}{\partial x})$ so the second term in equation (A-13) is transformed as

$$U_e \int_{\delta}^{(\delta_2 - G_1 L_1)} (\frac{\partial U}{\partial x})\, dy = U_e (V_i - V_0) \qquad \text{(A-14)}$$

Hence equation (A-13) can be written as

$$U_e \int_0^{(\delta_2 + G_0 L_0)} (\frac{\partial U}{\partial x})\, dy \simeq U_e \int_{L_3}^{\delta} (\frac{\partial U}{\partial x})\, dy + U_e (V_i - V_0) + U_e \int_{(\delta_2 - G_1 L_1)}^{\delta_2} (\frac{\partial U}{\partial x})\, dy + U_e \int_{\delta_2}^{(\delta_2 + G_0 L_0)} (\frac{\partial U}{\partial x})\, dy \qquad \text{(A-15)}$$

It will be seen shortly that the normal component of velocity, V, in the potential region is neglected, because it is small. $(V_i - V_0)$ being the difference of two small positive quantities is still smaller. Hence it is also neglected.

Using equations (A-4), (A-8) and (A-10) to substitute for $(\frac{\partial U}{\partial X})$ in the boundary layer, inner wake and the outer wake regions, equation (A-15) reduces to

$$
\begin{aligned}
U_e \int_0^{(\delta_2 + G_0 L_0)} (\tfrac{\partial U}{\partial x})\, dy \simeq\ & (U_e)(G_0 L_0 - L_0 A_4)(\tfrac{dU_e}{dx}) \\
& + (U_e)(G_1 L_1 - B_4 L_1)(\tfrac{dU_0}{dx}) \\
& + (U_e)(U_e - U_1)[\mathrm{Exp}(-kG_0^2) - 1](\tfrac{d\delta_2}{dx}) \\
& + (U_e)(U_0 - U_1)[1 - \mathrm{Exp}(-kG_1^2)](\tfrac{d\delta_2}{dx}) \\
& + (U_e)(L_0 A_4 + L_1 B_4)(\tfrac{dU_1}{dx}) \\
& - (U_e)[2k(U_e - U_1)A_2](\tfrac{dL_0}{dx}) \\
& - (U_e)[2k(U_0 - U_1)B_2](\tfrac{dL_1}{dx}) \\
& + U_e[(\tfrac{A}{L})(\delta - L_3) + \frac{AC_1}{L} + B(\delta - L_3) + 2PC_6](\tfrac{dU_\tau}{dx}) \\
& + (U_e)(2U_\tau C_6)(\tfrac{dP}{dx}) - (U_e)[\frac{2PU_\tau \pi C_5}{\delta^2}](\tfrac{d\delta}{dx}) \qquad \text{(A-16)}
\end{aligned}
$$

The third term in equation (A-2) is given by

$$
\begin{aligned}
U_1 \int_0^{\delta_2} (\tfrac{\partial U}{\partial x})\, dy =\ & U_1 \int_0^{\delta} (\tfrac{\partial U}{\partial x})\, dy + U_1 \int_{\delta}^{(\delta_2 - G_1 L_1)} (\tfrac{\partial U}{\partial x})\, dy \\
& + U_1 \int_{(\delta_2 - G_1 L_1)}^{\delta_2} (\tfrac{\partial U}{\partial x})\, dy \qquad \text{(A-17)}
\end{aligned}
$$

Neglecting the sub-layer and the change in the normal component of velocity in the potential region as before, the above equation reduces to

$$U_1 \int_0^{\delta_2} \left(\frac{\partial U}{\partial x}\right) dy \simeq (U_1)(G_1L_1 - B_4L_1)\left(\frac{dU_0}{dx}\right)$$

$$+ U_1(U_0 - U_1)[1 - \text{Exp}(-kG_1^2)]\left(\frac{d\delta_2}{dx}\right)$$

$$+ (U_1B_4L_1)\left(\frac{dU_1}{dx}\right) - [2kU_1(U_0 - U_1)B_2]\left(\frac{dL_1}{dx}\right)$$

$$+ U_1\left[\frac{A}{L}(\delta - L_3) + \frac{AC_1}{L} + B(\delta - L_3) + 2PC_6\right]\left(\frac{dU_\tau}{dx}\right)$$

$$+ (2U_1U_\tau C_6)\left(\frac{dP}{dx}\right) - \left(\frac{2U_1PU_\tau\pi C_5}{\delta^2}\right)\left(\frac{d\delta}{dx}\right) \qquad \text{(A-18)}$$

By substituting the equations (A-11), (A-16) and (A-18) for the corresponding terms in (A-2) the momentum integral equation becomes

$$[U_e(U_e - U_1)\{\text{Exp}(-kG_0^2) - 1\} - (U_e - U_1)^2\{\text{Exp}(-2kG_0^2) - 1\}$$

$$- U_e(U_0 - U_1)\{1 - \text{Exp}(-kG_1^2)\} + U_1(U_0 - U_1)\{1 - \text{Exp}(-kG_1^2)\}]\left(\frac{d\delta_2}{dx}\right)$$

$$+ [U_eL_0A_4 - 2(U_e - U_1)L_0A_3 - U_eL_1B_4 + U_1L_1B_4]\left(\frac{dU_1}{dx}\right)$$

$$+ [4K(U_e - U_1)^2 A_1 - 2kU_e(U_e - U_1)A_2]\left(\frac{dL_0}{dx}\right)$$

$$+ [2kU_e(U_0 - U_1)B_2 - 2kU_1(U_0 - U_1)B_2]\left(\frac{dL_1}{dx}\right)$$

$$+ [(U_1 - U_e)\{\frac{A}{L}(\delta - L_3) + \frac{AC_1}{L} + B(\delta - L_3) + 2PC_6\}]\left(\frac{dU_\tau}{dx}\right)$$

$$+ [(U_1 - U_e)2U_\tau C_6]\left(\frac{dP}{dx}\right) + [(U_e - U_1)\left(\frac{2PU_\tau\pi C_5}{\delta^2}\right)]\left(\frac{d\delta}{dx}\right)$$

$$+ [U_eG_0L_0 + 2(U_e - U_1)L_0A_3 - U_eL_0A_4 - 2(U_e - U_1)L_0A_4]\left(\frac{dU_e}{dx}\right)$$

$$+ [U_eL_1B_4 - U_eG_1L_1 + U_1G_1L_1 - U_1L_1B_4]\left(\frac{dU_0}{dx}\right)$$

$$= \tau(\delta_2 + G_0L_0) - \tau\delta_2 - H_1 \qquad \text{(A-19)}$$

The derivatives $(\frac{dU_e}{dx})$, $(\frac{dU_0}{dx})$ and $(\frac{dU_i}{dx})$ are evaluated from the knowledge of the static pressure coefficient C_p in the potential regions. Outside the shear layers, the ratio of the normal velocity to the longitudinal velocity is equal to the slope of the streamlines. The streamlines are determined by the displacement thicknesses which grow slowly except near separation. Therefore it is fair to assume that $V << U$ in the potential flow region. Hence the velocity U in the potential region has been approximated by the equation

$$U = \sqrt{1 - C_p} \tag{A-20}$$

In the general case, the pressure field contains a transverse pressure gradient. The experimental investigations conducted by Foster, Irwin and Williams (4) and reported by Irwin (2) which are used as test cases have constant transverse pressure gradients. Hence it was decided to formulate C_p by the following equation.

$$C_p = f(x)y + g(x) \tag{A-21}$$

In order to be accurate in the representation of the experimental pressure distribution the functions $f(x)$ and $g(x)$ were assumed to be third order polynomials so that

$$f(x) = D_1x^3 + D_2x^2 + D_3x + D_4 \tag{A-22}$$

$$g(x) = D_5x^3 + D_6x^2 + D_7x + D_8 \tag{A-23}$$

The coefficients D_i were evaluated from the data given by Irwin (2). A comparison of the formulated pressure distribution with the experimental ones are given in Figures 6 and 12 for the two test cases. Hence U_e , U_0

and U_i have been approximated by the following equations.

$$U_e = \sqrt{1 - E_1(\delta_2 + G_0 L_0) - E_3} \qquad \text{(A-24)}$$

$$U_0 = \sqrt{1 - E_1(\delta_2 - G_1 L_1) - E_3} \qquad \text{(A-25)}$$

$$U_i = \sqrt{1 - E_1\delta - E_3} \qquad \text{(A-26)}$$

where the coefficients E_1 and E_3 are the values of the functions $f(x)$ and $g(x)$ respectively at specific values of x.

Differentiating the above equations with respect to x, the following equations for $\frac{dU_e}{dx}$, $\frac{dU_0}{dx}$ and $\frac{dU_i}{dx}$ are obtained.

$$\frac{dU_e}{dx} = \left(\frac{-1}{2U_e}\right)\left[E_1\left(\frac{d\delta_2}{dx} + G_0\frac{dL_0}{dx}\right) + (\delta_2 + G_0L_0)E_2 + E_4\right] \qquad \text{(A-27)}$$

$$\frac{dU_0}{dx} = \left(\frac{-1}{2U_0}\right)\left[E_1\left(\frac{d\delta_2}{dx} - G_1\frac{dL_1}{dx}\right) + (\delta_2 - G_1L_1)E_2 + E_4\right] \qquad \text{(A-28)}$$

$$\frac{dU_i}{dx} = \left(\frac{-1}{2U_i}\right)\left[E_1\frac{d\delta}{dx} + \delta E_2 + E_4\right] \qquad \text{(A-29)}$$

Substituting the equations (A-27), (A-28) and (A-29) for $\frac{dU_e}{dx}$, $\frac{dU_0}{dx}$, and $\frac{dU_i}{dx}$ respectively in equation (A-19) the equation obtained by using the momentum integral equation for the pair of limits $y_1 = \delta_2$ and $y_2 = \delta_2 + G_0L_0$ is

$$M_1\left(\frac{d\delta_2}{dx}\right) + M_2\left(\frac{dU_1}{dx}\right) + M_3\left(\frac{dL_0}{dx}\right) + M_4\left(\frac{dL_1}{dx}\right)$$

$$+ M_5\left(\frac{dU_\tau}{dx}\right) + M_6\left(\frac{dP}{dx}\right) + M_7\frac{d\delta}{dx} = N_1 \qquad \text{(A-30)}$$

Rate of Mass Flow Across the Wake Centre:

The equation for the rate of change of the mass flow below the minimum velocity in the wake is given by

$$\frac{d}{dx}\left[\int_0^{\delta_2} U\,dy\right] = F \qquad \text{(A-31)}$$

Again, as before, the sub-layer region has been neglected and the above equation has been integrated from $y = L_3$ and equation (A-31) can be written as

$$\frac{d}{dx}\left[\int_{L_3}^{\delta} Udy + \frac{d}{dx}\left[\int_{\delta}^{(\delta_2 - G_1L_1)} U\,dy\right] + \frac{d}{dx}\left[\int_{(\delta_2 - G_1L_1)}^{\delta_2} Udy\right] \simeq F \qquad \text{(A-32)}\right.$$

Again each of the terms are derived separately for clarity.

$$\frac{d}{dx}\left[\int_{L_3}^{\delta} Udy\right] = \frac{d}{dx}\left[\int_{L_3}^{\delta}\left(\frac{AU_\tau}{L}\right)\left\{\ln\left(\frac{yU_\tau}{\nu}\right)\right\}dy\right] + \frac{d}{dx}\left[\int_{L_3}^{\delta}(BU_\tau)dy\right]$$

$$+ \frac{d}{dx}\left[\int_{L_3}^{\delta}(2PU_\tau)\left\{\sin^2\left(\frac{\pi y}{2\delta}\right)\right\}dy\right]$$

$$= \left[-\frac{AU_\tau}{L}\ln\left(\frac{\delta U_\tau}{\nu}\right) + BU_\tau + PU_\tau\right.$$

$$+ \left\{\frac{\sin\left(\frac{\pi L_3}{\delta}\right)}{\pi}\right\}(PU_\tau) - \left\{\cos\left(\frac{\pi L_3}{\delta}\right)\right\}\left(\frac{PU_\tau L_3}{\delta}\right)\left](\frac{d\delta}{dx}\right)$$

$$+ \left[\frac{A\delta}{L}\ln\left(\frac{\delta U_\tau}{\nu}\right) + B\delta + P\delta - \frac{AL_3}{L}\left\{\ln\left(\frac{L_3U_\tau}{\nu}\right)\right\}\right.$$

$$- BL_3 - PL_3 + \left\{\frac{\sin\left(\frac{\pi L_3}{\delta}\right)}{\pi}\right\}(P\delta)\left](\frac{dU_\tau}{dx}\right)$$

$$+ \left[U_\tau\delta - L_3U_\tau + \left\{\frac{\sin\left(\frac{\pi L_3}{\delta}\right)}{\pi}\right\}(U_\tau\delta)\right](\frac{dP}{dx}) \qquad \text{(A-33)}$$

$$\frac{d}{dx}\left[\int_{\delta}^{(\delta_2 - G_1L_1)} U\,dy\right] = \frac{d}{dx}\left[\int_{\delta}^{(\delta_2 - G_1L_1)} (1 - E_1y - E_3)^{1/2}\,dy\right]$$

$$= \frac{d}{dx}\left[\left(\frac{-2}{3E_1}\right)\{1 - E_1(\delta_2 - G_1L_1) - E_3\}^{3/2} + \left(\frac{2}{3E_1}\right)\{1 - E_1\delta - E_3\}^{3/2}\right]$$

$$= \left[\left(\frac{U_0}{E_1}\right)\{E_2(\delta_2 - G_1L_1) + E_4\} - \left(\frac{U_i}{E_1}\right)(E_2\delta + E_4)\right.$$

$$+ \left(\frac{2E_2}{3E_1^2}\right)\{U_0^3 - U_i^3\} + U_0\left(\frac{d\delta_2}{dx}\right)$$

$$\left. - G_1U_0\left(\frac{dL_1}{dx}\right) - U_i\left(\frac{d\delta}{dx}\right)\right] \qquad \text{(A-34)}$$

$$\frac{d}{dx}\left[\int_{(\delta_2 - G_1L_1)}^{\delta_2} U\,dy\right] = \frac{d}{dx}\left[\int_{(\delta_2 - G_1L_1}^{\delta_2} U_0\,dy\right] - \frac{d}{dx}\left[\int_{(\delta_2 - G_1L_1)}^{\delta_2} (U_0 - U_1)\mathrm{Exp}\{-k\left(\frac{y-\delta_2}{L_1}\right)^2\}dy\right]$$

$$= \frac{d}{dx}(U_0G_1L_1) - \frac{d}{dx}\left[U_0 - U_1)L_1B_4\right]$$

$$= \left[G_1L_1\left(\frac{dU_0}{dx}\right) + G_1U_0\left(\frac{dL_1}{dx}\right) - B_4(U_0 - U_1)\left(\frac{dL_1}{dx}\right)\right.$$

$$\left. - B_4L_1\left(\frac{dU_0}{dx}\right) + B_4L_1\left(\frac{dU_1}{dx}\right)\right] \qquad \text{(A-35)}$$

By substituting the equations (A-33), (A-34) and (A-35) for the corresponding terms in equation (A-32) the following equation is obtained.

$$U_0\left(\frac{d\delta_2}{dx}\right) + B_4L_1\left(\frac{dU_1}{dx}\right) - \left[B_4(U_0 - U_1)\right]\left(\frac{dL_1}{dx}\right)$$

$$+ \left[\frac{A\delta}{L}\ln\left(\frac{\delta U_\tau}{\nu}\right) + B\delta + P\delta - \frac{AL_3}{L}\ln\left(\frac{L_3U_\tau}{\nu}\right)\right.$$

$$\left. - BL_3 - PL_3 + \left\{\frac{\sin\left(\frac{\pi L_3}{\delta}\right)}{\pi}\right\}(P\delta)\right]\left(\frac{dU_\tau}{dx}\right)$$

$$+ \left[U_\tau\delta - U_\tau L_3 + \left\{\frac{\sin\left(\frac{\pi L_3}{\delta}\right)}{\pi}\right\}(U_\tau\delta)\right]\left(\frac{dP}{dx}\right)$$

$$+ \left[\frac{AU_\tau}{L}\ln\left(\frac{\delta U_\tau}{\nu}\right) + BU_\tau + PU_\tau - U_i\right.$$

$$\left. + \left\{\frac{\sin\left(\frac{\pi L_3}{\delta}\right)}{\pi}\right\}(PU_\tau) - \left\{\cos\left(\frac{\pi L_3}{\delta}\right)\right\}\left(\frac{PU_\tau L_3}{\delta}\right)\right]\left(\frac{d\delta}{dx}\right)$$

$$+ (G_1L_1 - B_4L_1)\left(\frac{dU_0}{dx}\right) = F + \left(\frac{2E_2}{3E_1^2}\right)(U_i^3 - U_0^3)$$

$$+ \left(\frac{U_i}{E_1}\right)(E_2\delta + E_4) - \left(\frac{U_0}{E_1}\right)\left[E_2(\delta_2 - G_1L_1) + E_4\right] \qquad \text{(A-36)}$$

Equation (A-28) is used to eliminate $\left(\frac{dU_0}{dx}\right)$ in equation (A-36) to give

$$M_{27}\left(\frac{d\delta_2}{dx}\right) + M_{28}\left(\frac{dU_1}{dx}\right) + M_{29}\left(\frac{dL_1}{dx}\right) + M_{30}\left(\frac{dU_\tau}{dx}\right) + M_{31}\left(\frac{dP}{dx}\right) + M_{32}\left(\frac{d\delta}{dx}\right) = N_6 \qquad \text{(A-37)}$$

Relation For $\frac{dU_i}{dx}$:

The velocity U_i at the edge of the boundary layer is given by

$$U_i = \frac{AU_\tau}{L}\ln\left(\frac{\delta U_\tau}{\nu}\right) + BU_\tau + 2PU_\tau \qquad \text{(A-38)}$$

Differentiating (A-38) with respect to x, the following equation is obtained.

$$\frac{dU_i}{dx} = \left(\frac{A}{L} + \frac{U_i}{U_\tau}\right)\frac{dU_\tau}{dx} + (2U_\tau)\left(\frac{dP}{dx}\right) + \left(\frac{AU_\tau}{L\delta}\right)\left(\frac{d\delta}{dx}\right) \qquad \text{(A-39)}$$

By eliminating $\left(\frac{dU_i}{dx}\right)$ between equations (A-29) and (A-39), the following equation is obtained.

$$M_{33}\left(\frac{dU_\tau}{dx}\right) + M_{34}\left(\frac{dP}{dx}\right) + M_{35}\left(\frac{d\delta}{dx}\right) = N_7 \qquad \text{(A-40)}$$

Merged Case:

The equations obtained by using the momentum integral equation between specific pairs of limits are similar to those obtained for the corresponding pairs of limits in the unmerged case. Hence only the equation for the rate of change of mass flow across the minimum velocity in the wake and the equation for $\left(\frac{dU_3}{dx}\right)$, which differ from the unmerged case, are given here in detail.

Rate of Change of Mass Flow Across the Wake Centre:

The equation for the rate of change of flow below the minimum velocity in the wake is

$$\frac{d}{dx}\left[\int_0^{\delta_3} U\,dy\right] + \frac{d}{dx}\left[\int_{\delta_3}^{\delta_2} U\,dy\right] = F \qquad \text{(A-41)}$$

$$\frac{d}{dx}\left[\int_0^{\delta_3} U\,dy\right] \simeq \frac{d}{dx}\left[\int_{L_3}^{\delta_2} U\,dy\right]$$

$$= \frac{d}{dx}\left[\int_{L_3}^{\delta_3} \frac{AU_\tau}{L}\ln\left(\frac{yU_\tau}{\nu}\right)dy\right]$$

$$+ \frac{d}{dx}\left[\int_{L_3}^{\delta_3} BU_\tau\,dy\right] + \frac{d}{dx}\left[\int_{L_3}^{\delta_3} 2PU_\tau\left\{\sin^2\left(\frac{\pi y}{2\delta_3}\right)\right\}dy\right]$$

$$\frac{d}{dx}\left[\int_{L_3}^{\delta_3} U\,dy\right] = \left[\frac{A\delta_3}{L}\ln\left(\frac{\delta_3 U_\tau}{\nu}\right) + B\delta_3 + P\delta_3\right.$$

$$- \frac{AL_3}{L}\ln\left(\frac{L_3 U_\tau}{\nu}\right) - BL_3 - PL_3$$

$$\left. + \left\{\frac{\sin\left(\frac{\pi L_3}{\delta_3}\right)}{\pi}\right\}(P\delta_3)\right]\left(\frac{dU_\tau}{dx}\right)$$

$$+ \left[U_\tau\delta_3 - L_3U_\tau + \left\{\frac{\sin\left(\frac{\pi L_3}{\delta_3}\right)}{\pi}\right\}(U_\tau\delta_3)\right]\left(\frac{dP}{dx}\right)$$

$$+ \left[\frac{AU_\tau}{L}\ln\left(\frac{\delta_3 U_\tau}{\nu}\right) + BU_\tau + PU_\tau\right.$$

$$\left. + \left\{\frac{\sin\left(\frac{\pi L_3}{\delta_3}\right)}{\pi}\right\}(PU_\tau) - \left\{\cos\left(\frac{\pi L_3}{\delta_3}\right)\right\}\left(\frac{PU_\tau L_3}{\delta_3}\right)\right]\left(\frac{d\delta_3}{dx}\right) \qquad \text{(A-42)}$$

$$\frac{d}{dx}\left[\int_{\delta_3}^{\delta_2} U\,dy\right] = \frac{d}{dx}\left[\int_{(\delta_2 - G_1L_1)}^{\delta_2} U\,dy\right]$$

$$= \frac{d}{dx}\left[\int_{(\delta_2 - G_1L_1)}^{\delta_2} U_3\,dy\right] - \frac{d}{dx}\left[\int_{(\delta_2 - G_1L_1)}^{\delta_2} (U_3 - U_1)\ \mathrm{Exp}\left\{-k\left(\frac{y - \delta_2}{L_1}\right)^2\right\}dy\right]$$

$$= \frac{d}{dx}\left(U_3G_1L_1\right) - \frac{d}{dx}\left[(U_3 - U_1)\,L_1B_4\right]$$

$$= G_1U_3\left(\frac{dL_1}{dx}\right) + G_1L_1\left(\frac{dU_3}{dx}\right)$$

$$- B_4(U_3 - U_1)\left(\frac{dL_1}{dx}\right) - B_4L_1\left(\frac{dU_3}{dx}\right) + B_4L_1\left(\frac{dU_1}{dx}\right) \qquad \text{(A-43)}$$

Hence by substituting equations (A-42) and (A-43) for the corresponding terms

in equation (A-41) the equation for the rate of change of mass flow is obtained.

$$R_{30}\left(\frac{dU_1}{dx}\right) + R_{31}\left(\frac{dL_1}{dx}\right) + R_{32}\left(\frac{dU_\tau}{dx}\right) + R_{33}\left(\frac{dP}{dx}\right) + R_{34}\left(\frac{d\delta_3}{dx}\right) + R_{35}\left(\frac{dU_3}{dx}\right) = T_6$$

Relation For $\left(\frac{dU_3}{dx}\right)$:

The velocity at $y = \delta_3$ is given by

$$U_3 = \frac{AU_\tau}{L} \ln\left(\frac{\delta_3 U_\tau}{\nu}\right) + BU_\tau + 2PU_\tau \qquad \text{(A-44)}$$

Differentiating (A-44) with respect to x the following equation is obtained

$$R_{36}\left(\frac{dU_\tau}{dx}\right) + R_{37}\left(\frac{dP}{dx}\right) + R_{38}\left(\frac{d\delta_3}{dx}\right) + R_{39}\left(\frac{dU_3}{dx}\right) = 0 \qquad \text{(A-45)}$$

(ii) Integrals and Coefficients Appearing in Section (i)

The integrals A_i, B_i, C_i and H_i the coefficients D_i, E_i, M_i, N_i, R_i and T_i are given below.

$$A_1 = \int_0^{G_0} (\eta^2)[\text{Exp}\ (-2k\eta^2)]d\eta$$

$$A_2 = \int_0^{G_0} (\eta^2)[\text{Exp}\ (-k\eta^2)]d\eta$$

$$A_3 = \int_0^{G_0} [\text{Exp}\ (-2k\eta^2)]d\eta = 0.7527$$

$$A_4 = \int_0^{G_0} [\text{Exp}\ (-k\eta^2)]d\eta = 1.0633$$

$$A_5 = \int_0^{1} (\eta^2)[\text{Exp}\ (-2k\eta^2)]d\eta$$

$$A_6 = \int_0^{1} (\eta^2)[\text{Exp}\ (-k\eta^2)]d\eta$$

$$A_7 = \int_0^{1} [\text{Exp}\ (-2k\eta^2)]d\eta = 0.6805$$

$$A_8 = \int_0^{1} [\text{Exp}\ (-k\eta^2)]d\eta = 0.8101$$

$$B_1 = \int_{-G_1}^{0} (\eta^2)[\text{Exp}\ (-2k\eta^2)]d\eta$$

$$B_2 = \int_{-G_1}^{0} (n^2)[\text{Exp}\ (-kn^2)]dn$$

$$B_3 = \int_{-G_1}^{0} [\text{Exp}\ (-2kn^2)]dn = 0.7526$$

$$B_4 = \int_{-G_1}^{0} [\text{Exp}(-kn^2)]\,dn = 1.061$$

$$C_1 = \int_{L_3}^{\delta} [\ln\ (\frac{yU_\tau}{\nu})]\ dy$$

$$C_2 = \int_{L_3}^{\delta} [\ln\ (\frac{yU_\tau}{\nu})]^2\ dy$$

$$C_3 = \int_{L_3}^{\delta} (y)\ [\sin^3\ (\frac{\pi y}{2\delta})\ \cos\ (\frac{\pi y}{2\delta})]\ dy$$

$$C_4 = \int_{L_3}^{\delta} [\sin^4\ (\frac{\pi y}{2\delta})]dy$$

$$C_5 = \int_{L_3}^{\delta} (y)\ [\sin\ (\frac{\pi y}{2\delta})\ \cos\ (\frac{\pi y}{2\delta})]dy$$

$$C_6 = \int_{L_3}^{\delta} [\sin^2\ (\frac{\pi y}{2\delta})]\ dy$$

$$C_7 = \int_{L_3}^{\delta} [\ln\ (\frac{yU_\tau}{\nu})\ \sin^2\ (\frac{\pi y}{2\delta})]\ dy$$

$$C_8 = \int_{L_3}^{\delta} (y) \left[\sin \left(\frac{\pi y}{2\delta}\right) \cos \left(\frac{\pi y}{2\delta}\right) \ln \left(\frac{yU_\tau}{\nu}\right)\right] dy$$

$$C_9 = \int_{\delta/2}^{\delta} \left[\ln \left(\frac{yU_\tau}{\nu}\right)\right] dy$$

$$C_{10} = \int_{\delta/2}^{\delta} \left[\ln \left(\frac{yU_\tau}{\nu}\right)^2\right] dy$$

$$C_{11} = \int_{\delta/2}^{\delta} (y) \left[\sin^3 \left(\frac{\pi y}{2\delta}\right) \cos \left(\frac{\pi y}{2\delta}\right)\right] dy$$

$$C_{12} = \int_{\delta/2}^{\delta} \left[\sin^4 \left(\frac{\pi y}{2\delta}\right)\right] dy$$

$$C_{13} = \int_{\delta/2}^{\delta} (y) \left[\sin \left(\frac{\pi y}{2\delta}\right) \cos \left(\frac{\pi y}{2\delta}\right)\right] dy$$

$$C_{14} = \int_{\delta/2}^{\delta} \left[\sin^2 \left(\frac{\pi y}{2\delta}\right)\right] dy$$

$$C_{15} = \int_{\delta/2}^{\delta} \left[\ln \left(\frac{yU_\tau}{\nu}\right) \sin^2 \left(\frac{\pi y}{2\delta}\right)\right] dy$$

$$C_{16} = \int_{\delta/2}^{\delta} (y) \left[\sin \left(\frac{\pi y}{2\delta}\right) \cos \left(\frac{\pi y}{2\delta}\right) \ln \left(\frac{yU_\tau}{\nu}\right)\right] dy$$

$$C_{17} = \int_{L_3}^{\delta/2} \left[\ln \left(\frac{yU_\tau}{\nu}\right)\right] dy$$

$$C_{18} = \int_{L_3}^{\delta/2} (y)[\sin(\frac{\pi y}{2\delta}) \cos(\frac{\pi y}{2\delta})]\, dy$$

$$C_{19} = \int_{L_3}^{\delta/2} [\sin^2(\frac{\pi y}{2\delta})]\, dy$$

(For the merged case, δ is replaced by δ_3 in the integrals C_1 to C_{19})

$$H_1 = \int_{\delta_2}^{(\delta_2 + G_0 L_0)} (\frac{1}{2})(\frac{\partial C_p}{\partial x})\, dy$$

$$H_2 = \int_{\delta_2}^{(\delta_2 + L_0)} (\frac{1}{2})(\frac{\partial C_p}{\partial x})\, dy$$

$$H_3 = \int_{(\delta_2 - G_1 L_1)}^{\delta_2} (\frac{1}{2})(\frac{\partial C_p}{\partial x})\, dy$$

$$H_4 = \int_{L_3}^{\delta} (\frac{1}{2})(\frac{\partial C_p}{\partial x})\, dy$$

$$H_5 = \int_{\delta/2}^{\delta} (\frac{1}{2})(\frac{\partial C_p}{\partial x})\, dy$$

(For the merged case δ is replaced by δ_3 in the integrals H_4 and H_5)

D_1, D_2, D_3 and D_4 - coefficients that appear in the function f(x) that occurs in the expression for C_p

D_5, D_6, D_7 and D_8 - coefficients that appear in the function g(x) that occurs in the expression for C_p.

$$E_1 = D_1 x^3 + D_2 x^2 + D_3 x + D_4$$

$$E_2 = 3D_1x^2 + 2D_2x + D_3$$

$$E_3 = D_5x^3 + D_6x^2 + D_7x + D_8$$

$$E_4 = 3D_5x^2 + 2D_6x + D_7$$

$$M_1 = (U_e)(U_e - U_1)[\text{Exp}(-kG_0^2) - 1] - (U_e - U_1)^2[\text{Exp}(-2kG_0^2) - 1]$$
$$- (U_e)(U_0 - U_1)[1 - \text{Exp}(-kG_1^2)] + U_1(U_0 - U_1)[1 - \text{Exp}(-kG_1^2)]$$
$$- [U_eG_0L_0 + 2(U_e - U_1)L_0A_3 - U_eL_0A_4 - 2(U_e - U_1)L_0A_4](\frac{E_1}{2U_e})$$
$$- [U_eL_1B_4 - U_eG_1L_1 + U_1G_1L_1 - U_1L_1B_4](\frac{E_1}{2U_0})$$

$$M_2 = (U_eL_0A_4) - 2(U_e - U_1)L_0A_3 - (U_eL_1B_4) + (U_1L_1B_4)$$

$$M_3 = [4k(U_e - U_1)^2A_1] - [2kU_e(U_e - U_1)A_2]$$
$$- [U_eG_0L_0 + 2(U_e - U_1)L_0A_3 - U_eL_0A_4 - 2(U_e - U_1)L_0A_4](\frac{G_0E_1}{2U_e})$$

$$M_4 = [2kU_e(U_0 - U_1)B_2] - [2kU_1(U_0 - U_1)B_2]$$
$$+ [U_eL_1B_4 - U_eG_1L_1 + U_1G_1L_1 - U_1L_1B_4](\frac{G_1E_1}{2U_0})$$

$$M_5 = (U_1 - U_e)[\frac{A}{L}(\delta - L_3) + \frac{AC_1}{L} + B(\delta - L_3) + 2PC_6]$$

$$M_6 = (U_1 - U_e)[2U_\tau C_6]$$

$$M_7 = (U_e - U_1)[\frac{2PU_\tau \pi C_5}{\delta^2}]$$

$$M_8 = (2U_e)(U_e - U_1)[\text{Exp}(-k) - 1] - (U_e - U_1)^2[\text{Exp}(-2k) - 1]$$
$$-(\frac{1}{2})(U_e + U_1)(U_e - U_1)[\text{Exp}(-k) - 1]$$
$$-(\frac{1}{2})(U_e + U_1)(U_0 - U_1)[1 - \text{Exp}(-kG_1^2)] + U_1(U_0 - U_1)[1 - \text{Exp}(-kG_1^2)]$$
$$-[2U_eL_0 + 2(U_e - U_1)L_0A_7 - 2U_eL_0A_8 - 2(U_e - U_1)L_0A_8$$
$$- (U_e + U_1)(\frac{L_0}{2})(1 - A_8)](\frac{E_1}{2U_e})$$
$$- [(U_e + U_1)(\frac{L_1}{2})B_4 - (U_e + U_1)(\frac{L_1}{2})G_1 + U_1G_1L_1 - U_1L_1B_4](\frac{E_1}{2U_0})$$

$$M_9 = (2U_eL_0A_8) - [2(U_e - U_1)L_0A_7] - (U_e + U_1)\left(\frac{L_0}{2}\right)(A_8)$$
$$- [(U_e + U_1)\left(\frac{L_1}{2}\right)B_4] + (U_1L_1B_4)$$

$$M_{10} = 4k(U_e - U_1)^2A_5 - 4kU_e(U_e - U_1)A_6 + k(U_e + U_1)(U_e - U_1)A_6$$
$$- [2U_eL_0 + 2(U_e - U_1)L_0A_7 - 2U_eL_0A_8$$
$$- 2(U_e - U_1)L_0A_8 - (U_e + U_1)\left(\frac{L_0}{2}\right)(1 - A_8)]\left(\frac{G_0E_1}{2U_e}\right)$$

$$M_{11} = [k(U_e + U_1)(U_0 - U_1)B_2] - [2kU_1(U_0 - U_1)B_2]$$
$$+ [(U_e + U_1)\left(\frac{L_1}{2}\right)B_4 - (U_e + U_1)\left(\frac{L_1}{2}\right)G_1 + U_1G_1L_1 - U_1L_1B_4]\left(\frac{G_1E_1}{2U_0}\right)$$

$$M_{12} = \left(\frac{1}{2}\right)(U_1 - U_e)\left[\frac{A}{L}(\delta - L_3) + \frac{AC_1}{L} + B(\delta - L_3) + 2PC_6\right]$$

$$M_{13} = (U_1 - U_e)[U_\tau C_6]$$

$$M_{14} = (U_e - U_1)\left(\frac{\pi}{\delta^2}\right)[PU_\tau C_5]$$

$$M_{15} = (2U_0)(U_0 - U_1)[1 - \mathrm{Exp}(-kG_1^2)] - (U_0 - U_1)^2[1 - \mathrm{Exp}(-2kG_1^2)]$$
$$- (U_1)(U_0 - U_1)[1 - \mathrm{Exp}(-kG_1^2)]$$
$$- [2U_0G_1L_1 + 2(U_0 - U_1)L_1B_3 - 2U_0L_1B_4$$
$$- 2(U_0 - U_1)L_1B_4 - U_1G_1L_1 + U_1L_1B_4]\left(\frac{E_1}{2U_0}\right)$$

$$M_{16} = (2U_0L_1B_4) - [2(U_0 - U_1)L_1B_3] - (U_1L_1B_4)$$

$$M_{17} = [4k(U_0 - U_1)^2B_1] - [4kU_0(U_0 - U_1)B_2] + [2kU_1(U_0 - U_1)B_2]$$
$$+ [2U_0G_1L_1 + 2(U_0 - U_1)L_1B_3 - 2U_0L_1B_4$$
$$- 2(U_0 - U_1)L_1B_4 - U_1G_1L_1 + U_1L_1B_4]\left(\frac{G_1E_1}{2U_0}\right)$$

$$M_{18} = (U_0 - U_1)\left[\frac{A}{L}(\delta - L_3) + \frac{AC_1}{L} + B(\delta - L_3) + 2PC_6\right]$$

$$M_{19} = [2(U_0 - U_1)U_\tau C_6]$$

$$M_{20} = [2(U_1 - U_0)\left(\frac{\pi}{\delta^2}\right)(PU_\tau C_5)]$$

$$M_{21} = [2(\frac{A^2}{L^2})U_\tau + 4(\frac{A}{L})BU_\tau - U_i(\frac{A}{L})](C_1)$$
$$+ [2(\frac{A^2}{L^2})U_\tau C_2] + [8U_\tau P^2 C_4]$$
$$+ [8BU_\tau P + 4(\frac{A}{L})U_\tau P - 2U_i P](C_6)$$
$$+ [8(\frac{A}{L})PU_\tau C_7]$$
$$+ [2B^2U_\tau(\delta - L_3) + 2(\frac{A}{L})BU_\tau(\delta - L_3) - U_i(\frac{A}{L})(\delta - L_3) - U_iB(\delta - L_3)]$$

$$M_{22} = (8PU_\tau^2 C_4) + (4BU_\tau^2 - 2U_iU_\tau)(C_6) + [4(\frac{A}{L})U_\tau^2 C_7]$$

$$M_{23} = [-8(\frac{\pi}{\delta^2})P^2U_\tau^2 C_3] + [2(\frac{\pi}{\delta^2})U_iPU_\tau - 4(\frac{\pi}{\delta^2})BPU_\tau^2](C_5)$$
$$+ [-4(\frac{A}{L})(\frac{\pi}{\delta^2})PU_\tau^2 C_8]$$

$$M_{24} = [-U_i(\frac{A}{L})C_1] + [2(\frac{A^2}{L^2})U_\tau + 4(\frac{A}{L})BU_\tau](C_9) + [2(\frac{A^2}{L^2})U_\tau C_{10}]$$
$$+ [8U_\tau P^2 C_{12}] + [8BU_\tau P + 4(\frac{A}{L})PU_\tau](C_{14})$$
$$+ [8(\frac{A}{L})PU_\tau C_{15}] + [-2U_iPC_6] + [(U_{\delta/2})(\frac{A}{L})C_{17}]$$
$$+ [2(U_{\delta/2})PC_{19}]$$
$$+ [B^2U_\tau\delta + (\frac{A}{L})BU_\tau\delta - U_i(\frac{A}{L})(\delta - L_3) - U_iB(\delta - L_3)]$$
$$+ (U_{\delta/2})[(\frac{A}{L})(\frac{\delta}{2} - L_3) + B(\frac{\delta}{2} - L_3)]$$

$$M_{25} = [8PU_\tau^2 C_{12} + 4BU_\tau^2 C_{14} + 4(\frac{A}{L})U_\tau^2 C_{15}$$
$$- 2U_iU_\tau C_6 + 2(U_{\delta/2})U_\tau C_{19}]$$

$$M_{26} = [-8(\frac{\pi}{\delta^2})P^2U_\tau^2 C_{11}] + [-4(\frac{\pi}{\delta^2})BPU_\tau^2 C_{13}]$$
$$+ [-4(\frac{A}{L})(\frac{\pi}{\delta^2})PU_\tau^2 C_{16}] + [2(\frac{\pi}{\delta^2})U_iPU_\tau C_5]$$
$$+ [-2(U_{\delta/2})(\frac{\pi}{\delta^2})PU_\tau C_{18}]$$

$$M_{27} = [U_0 - (G_1L_1 - B_4L_1)(\frac{E_1}{2U_0})]$$

$$M_{28} = [B_4 L_1]$$

$$M_{29} = [(\frac{G_1 E_1}{2U_0})(G_1 L_1 - B_4 L_1) - B_4(U_0 - U_1)]$$

$$M_{30} = [(\frac{A}{L})\delta \ln(\frac{\delta U_\tau}{\nu}) + B\delta + P\delta - (\frac{A}{L})L_3 \ln(\frac{L_3 U_\tau}{\nu}) - BL_3 - PL_3] + [\sin(\frac{\pi L_3}{\delta})](\frac{P\delta}{\pi})$$

$$M_{31} = [U_\tau \delta - U_\tau L_3] + [\sin(\frac{\pi L_3}{\delta})](\frac{U_\tau \delta}{\pi})$$

$$M_{32} = [(\frac{A}{L})U_\tau \ln(\frac{\delta U_\tau}{\nu}) + BU_\tau + PU_\tau - U_i] + [\sin(\frac{\pi L_3}{\delta})](\frac{PU_\tau}{\pi}) - [\cos(\frac{\pi L_3}{\delta})](\frac{L_3}{\delta})(PU_\tau)$$

$$M_{33} = [\frac{U_i}{U_\tau} + \frac{A}{L}]$$

$$M_{34} = [2U_\tau]$$

$$M_{35} = [(\frac{AU_\tau}{L\delta}) + (\frac{E_1}{2U_i})]$$

$$N_1 = [\tau(\delta_2 + G_0 L_0) - \tau\delta_2 - H_1] + [U_e L_1 B_4 - U_e G_1 L_1 + U_1 G_1 L_1 - U_1 L_1 B_4][(\delta_2 - G_1 L_1)E_2 + E_4](\frac{1}{2U_0}) + [U_e G_0 L_0 + 2(U_e - U_1)L_0 A_3 - U_e L_0 A_4 - 2(U_e - U_1) L_0 A_4][(\delta_2 + G_0 L_0)E_2 + E_4](\frac{1}{2U_e})$$

$$N_2 = [\tau(\delta_2 + L_0) - \tau\delta_2 - H_2] + [2U_e L_0 + 2(U_e - U_1)L_0 A_7 - 2U_e L_0 A_8 - 2(U_e - U_1)L_0 A_8 - (U_e + U_1)(\frac{L_0}{2})(1 - A_8)][(\delta_2 + G_0 L_0)E_2 + E_4](\frac{1}{2U_e}) + [(U_e + U_1)(\frac{L_1}{2})B_4 - (U_e + U_1)G_1(\frac{L_1}{2}) + U_1 G_1 L_1 - U_1 L_1 B_4][(\delta_2 - G_1 L_1)E_2 + E_4](\frac{1}{2U_0})$$

$$N_3 = [\tau\delta_2 - \tau(\delta_2 - G_1 L_1) - H_3] + [2U_0 G_1 L_1 + 2(U_0 - U_1)L_1 B_3 - 2U_0 L_1 B_4 - 2(U_0 - U_1)L_1 B_4 - U_1 G_1 L_1 + U_1 L_1 B_4][(\delta_2 - G_1 L_1)E_2 + E_4](\frac{1}{2U_0})$$

$$N_4 = [\tau_\delta - U_\tau^2 - H_4]$$

$$N_5 = [\tau_\delta - \tau_{\delta/2} - H_5]$$

$$N_6 = (F) + \left(\frac{2E_2}{3E_1^2}\right)(U_i^3 - U_0^3) + \left(\frac{U_i}{E_1}\right)[\delta E_2 + E_4]$$

$$-\left(\frac{U_0}{E_1}\right)[(\delta_2 - G_1L_1)E_2 + E_4]$$

$$+ (G_1L_1 - B_4L_1)[(\delta_2 - G_1L_1)E_2 + E_4]\left(\frac{1}{2U_0}\right)$$

$$N_7 = [-(\delta E_2 + E_4)\left(\frac{1}{2U_i}\right)]$$

$$R_1 = (2U_e)(U_e - U_1)[\text{Exp}(-kG_0^2) - 1] - (U_e - U_1)^2[\text{Exp}(-2kG_0^2) - 1]$$

$$- U_e(U_e - U_1)[\text{Exp}(-kG_0^2) - 1] - U_e(U_3 - U_1)[1 - \text{Exp}(-kG_1^2)]$$

$$+ U_1(U_3 - U_1)[1 - \text{Exp}(-kG_1^2)]$$

$$- [U_eG_0L_0 + 2(U_e - U_1)L_0A_3 - U_eL_0A_4 - 2(U_e - U_1)L_0A_4]\left(\frac{E_1}{2U_e}\right)$$

$$R_2 = [U_eL_0A_4 - 2(U_e - U_1)L_0A_3 - U_eL_1B_4 + U_1L_1B_4]$$

$$R_3 = [4k(U_e - U_1)^2A_1] - [2kU_e(U_e - U_1)A_2]$$

$$- [U_eG_0L_0 + 2(U_e - U_1)L_0A_3 - U_eL_0A_4 - 2(U_e - U_1)L_0A_4]\left(\frac{G_0E_1}{2U_e}\right)$$

$$R_4 = [2kU_e(U_3 - U_1)B_2 - 2kU_1(U_3 - U_1)B_2]$$

$$R_5 = (U_1 - U_e)[\left(\frac{A}{L}\right)(\delta_3 - L_3) + B(\delta_3 - L_3) + \frac{AC_1}{L} + 2PC_6]$$

$$R_6 = [2(U_1 - U_e)U_\tau C_6]$$

$$R_7 = [2(U_e - U_1)\left(\frac{\pi}{\delta_3^2}\right) PU_\tau C_5]$$

$$R_8 = [(U_1 - U_e)(G_1L_1 - B_4L_1)]$$

$$R_9 = (2U_e)(U_e - U_1)\,[\mathrm{Exp}(-k) - 1] - (U_e - U_1)^2\,[\mathrm{Exp}(-2k) - 1]$$
$$- (\tfrac{1}{2})\,(U_e + U_1)\,(U_e - U_1)\,[\mathrm{Exp}(-k) - 1]$$
$$- (\tfrac{1}{2})\,(U_e + U_1)(U_3 - U_1)\,[1 - \mathrm{Exp}(-kG_1^2)] + U_1(U_3 - U_1)\,[1 - \mathrm{Exp}(-kG_1^2)]$$
$$- [2U_eL_0 + 2(U_e - U_1)L_0A_7 - 2U_eL_0A_8 - 2(U_e - U_1)L_0A_8$$
$$- (U_e + U_1)(\tfrac{L_0}{2})(1 - A_8)](\tfrac{E_1}{2U_e})$$

$$R_{10} = (2U_eL_0A_8) - [2(U_e - U_1)L_0A_7] - [(\tfrac{1}{2})(U_e + U_1)(L_0A_8 + L_1B_4)] + (U_1L_1B_4)$$

$$R_{11} = [4k(U_e - U_1)^2A_5] - [4kU_e(U_e - U_1)A_6] + [k(U_e + U_1)(U_e - U_1)A_6]$$
$$-[2U_eL_0 + 2(U_e - U_1)L_0A_7 - 2U_eL_0A_8 - 2(U_e - U_1)L_0A_8$$
$$- (U_e + U_1)(\tfrac{L_0}{2})(1 - A_8)](\tfrac{G_0E_1}{2U_e})$$

$$R_{12} = [k(U_e + U_1)(U_3 - U_1)B_2 - 2kU_1(U_3 - U_1)B_2]$$

$$R_{13} = (\tfrac{1}{2})(U_1 - U_e)[(\tfrac{A}{L})(\delta_3 - L_3) + B(\delta_3 - L_3) + (\tfrac{A}{L})C_1 + 2PC_6]$$

$$R_{14} = [(U_1 - U_e)\,U_\tau\,C_6]$$

$$R_{15} = [(U_e - U_1)(\tfrac{\pi}{2\delta_3^2})(PU_\tau\,C_5)]$$

$$R_{16} = (U_1G_1L_1) - (U_1L_1B_4) - [(\tfrac{1}{2})(U_e + U_1)(G_1L_1 - L_1B_4)]$$

$$R_{17} = (2U_3)(U_3 - U_1)\,[1 - \mathrm{Exp}(-kG_1^2)] - (U_3 - U_1)^2\,[1 - \mathrm{Exp}(-2kG_1^2)]$$
$$-(U_1)(U_3 - U_1)\,[1 - \mathrm{Exp}(-kG_1^2)]$$

$$R_{18} = (2U_3L_1B_4) - [2(U_3 - U_1)L_1B_3] - (U_1L_1B_4)$$

$$R_{19} = [4k(U_3 - U_1)^2B_1] - [4kU_3(U_3 - U_1)B_2] + [2kU_1(U_3 - U_1)B_2]$$

$$R_{20} = (U_3 - U_1)[(\tfrac{A}{L})(\delta_3 - L_3) + (\tfrac{A}{L})C_1 + B(\delta_3 - L_3) + 2PC_6]$$

$$R_{21} = [2(U_3 - U_1)U_\tau\,C_6]$$

$$R_{22} = [2(U_1 - U_3)(\tfrac{\pi}{2\delta_3^2})\,PU_\tau\,C_5]$$

$$R_{23} = [2U_3G_1L_1 + 2(U_3 - U_1)L_1B_3 - 2U_3L_1B_4$$

$$- 2(U_3 - U_1)L_1B_4 + U_1L_1B_4 - U_1G_1L_1]$$

$$R_{24} = [2(\frac{A^2}{L^2})U_\tau + 4(\frac{A}{L})BU_\tau - U_3(\frac{A}{L})] (C_1) + [2(\frac{A^2}{L^2})U_\tau C_2]$$

$$+ [8U_\tau P^2C_4] + [8BU_\tau P + 4(\frac{A}{L}) U_\tau P - 2U_3P](C_6)$$

$$+ [8(\frac{A}{L})U_\tau PC_7]$$

$$+ [2B^2U_\tau (\delta_3 - L_3) + 2(\frac{A}{L})BU_\tau (\delta_3 - L_3) - U_3(\frac{A}{L})(\delta_3 - L_3) - U_3B(\delta_3 - L_3)]$$

$$R_{25} = (8PU_\tau^2C_4) + (4BU_\tau^2C_6) - (2U_3U_\tau C_6) + [4(\frac{A}{L})U_\tau^2 C_7]$$

$$R_{26} = [-8(\frac{\pi}{\delta_3^2})P^2U_\tau^2 C_3] - [4(\frac{\pi}{\delta_3^2})BPU_\tau^2 C_5]$$

$$+[2(\frac{\pi}{\delta_3^2})U_3PU_\tau C_5] - [4(\frac{A}{L})(\frac{\pi}{\delta_3^2})PU_\tau^2 C_8]$$

$$R_{27} = [2(\frac{A^2}{L^2})U_\tau + 4(\frac{A}{L})BU_\tau] (C_9) + [2(\frac{A^2}{L^2})U_\tau C_{10}]$$

$$+ [8U_\tau P^2C_{12}] + [8BPU_\tau + 4(\frac{A}{L})PU_\tau] (C_{14})$$

$$+ [8(\frac{A}{L})PU_\tau](C_{15}) + [-(\frac{A}{L})U_3 C_1]$$

$$+ [-2U_3PC_6] + [(U_{\delta_3/2})(\frac{A}{L})C_{17}] + [2(U_{\delta_3/2})PC_{19}]$$

$$+ [B^2U_\tau \delta_3 + (\frac{A}{L})BU_\tau \delta_3 - U_3(\frac{A}{L})(\delta_3 - L_3) - U_3B(\delta_3 - L_3)]$$

$$+ [(U_{\delta_3/2})(\frac{A}{L})(\frac{\delta_3}{2} - L_3) + (U_{\delta_3/2}) B (\frac{\delta_3}{2} - L_3)]$$

$$R_{28} = (8PU_\tau^2 C_{12}) + (4BU_\tau^2 C_{14}) + [4(\frac{A}{L})U_\tau^2 C_{15}]$$

$$- (2U_3U_\tau C_6) + [2 U_{\delta_3/2} U_\tau C_{19}]$$

$$R_{29} = [-8(\frac{\pi}{\delta_3^2})P^2U_\tau^2 C_{11}] + [-4(\frac{\pi}{\delta_3^2})BPU_\tau^2 C_{13}]$$

$$+ [-4(\frac{A}{L})(\frac{\pi}{\delta_3^2})PU_\tau^2 C_{16}] + [2(\frac{\pi}{\delta_3^2})U_3PU_\tau C_5]$$

$$+ [-2(U_{\delta_3/2})(\frac{\pi}{\delta_3^2})PU_\tau C_{18}]$$

$$R_{30} = (B_4 L_1)$$

$$R_{31} = [G_1 U_3 - B_4(U_3 - U_1)]$$

$$R_{32} = [(\frac{A}{L})\delta_3 \ln(\frac{\delta_3 U_\tau}{\nu}) + B\delta_3 + P\delta_3 - (\frac{A}{L})L_3 \ln(\frac{L_3 U_\tau}{\nu}) - BL_3 - PL_3] + [\sin(\frac{\pi L_3}{\delta_3})](\frac{P\delta_3}{\pi})$$

$$R_{33} = [U_\tau \delta_3 - U_\tau L_3] + [\sin(\frac{\pi L_3}{\delta_3})](\frac{U_\tau \delta_3}{\pi})$$

$$R_{34} = [(\frac{A}{L})U_\tau \ln(\frac{\delta_3 U_\tau}{\nu}) + BU_\tau + PU_\tau] + [\sin(\frac{\pi L_3}{\delta_3})](\frac{PU_\tau}{\pi}) - (\cos(\frac{\pi L_3}{\delta_3})](\frac{L_3}{\delta_3})(PU_\tau)$$

$$R_{35} = [G_1 L_1 - B_4 L_1]$$

$$R_{36} = [\frac{U_3}{U_\tau} + \frac{A}{L}]$$

$$R_{37} = [2U_\tau]$$

$$R_{38} = [(\frac{A}{L})(\frac{U_\tau}{\delta_3})]$$

$$R_{39} = -1.0$$

$$R_{40} = 1.0$$

$$R_{41} = -G_1$$

$$R_{42} = -1.0$$

$$T_1 = [\tau(\delta_2 + G_0 L_0) - \tau\delta_2 - H_1] + [U_e G_0 L_0 + 2(U_e - U_1)L_0 A_3 - U_e L_0 A_4 - 2(U_e - U_1)L_0 A_4][(\delta_2 + G_0 L_0)E_2 + E_4](\frac{1}{2U_e})$$

$$T_2 = [\tau_{(\delta_2 + L_0)} - \tau_{\delta_2} - H_2]$$

$$+ [2U_eL_0 + 2(U_e - U_1)L_0A_7 - 2U_eL_0A_8 - 2(U_e - U_1)L_0A_8$$

$$- (U_e+U_1)(\frac{L_0}{2})(1 - A_8)] [(\delta_2 + G_0L_0)E_2 + E_4](\frac{1}{2U_e})$$

$$T_3 = [\tau_{\delta_2} - \tau_{(\delta_2 - G_1L_1)} - H_3]$$

$$T_4 = [\tau_{\delta_3} - \tau_W - H_4]$$

$$T_5 = [\tau_{\delta_3} - \tau_{\delta_3/2} - H_5]$$

$$T_6 = (F)$$

APPENDIX - B

Derivation of the Integral Parameters:

(1) Integral Parameters of the Separate Shear Layers

Boundary Layer

The displacement thickness and the momentum thickness in this region are given by the following equations

$$\delta_B^* = \int_0^{\delta} (1 - \frac{U}{U_i}) dy \qquad \text{(B-1)}$$

$$\theta_B = \int_0^{\delta} (\frac{U}{U_i})(1 - \frac{U}{U_i}) dy \qquad \text{(B-2)}$$

The velocity U is given by

$$U = (\frac{AU_\tau}{L}) \ln(\frac{yU_\tau}{\nu}) + BU_\tau + 2PU_\tau \sin^2(\frac{\pi y}{2\delta}) \qquad \text{(B-3)}$$

Using the trignometric relation,

$$\sin^2(\frac{\pi y}{2\delta}) = (\frac{1}{2})[1 - \cos(\frac{\pi y}{\delta})] \qquad \text{(B-4)}$$

equation (B-1) can be evaluated as

$$\delta_B^* = \int_0^{\delta} [1 - (\frac{AU_\tau}{LU_i}) \ln(\frac{yU_\tau}{\nu}) - (\frac{BU_\tau}{U_i}) - (\frac{PU_\tau}{U_i}) + (\frac{PU_\tau}{U_i}) \cos(\frac{\pi y}{\delta})] dy$$

$$= [y]_0^{\delta} - (\frac{AU_\tau}{LU_i})[y\ln(\frac{yU_\tau}{\nu}) - y]_0^{\delta} - (\frac{BU_\tau}{U_i})[y]_0^{\delta}$$

$$- \frac{PU_\tau}{U_i}[y]_0^{\delta} + \frac{PU_\tau}{U_i}[(\frac{\delta}{\pi}) \sin(\frac{\pi y}{\delta})]_0^{\delta} \qquad \text{(B-5)}$$

Since $[y\ln(\frac{yU_\tau}{\nu})]$ tends to zero as y tends to zero, equation (B-5) leads to

$$\delta_B^* = (\delta)\left(\frac{U_\tau}{U_i}\right)\left[\frac{A}{L} + P\right] \tag{B-6}$$

A slightly different approach has been adopted in evaluating the momentum thickness. The momentum thickness θ_B be written as

$$\theta_B = \int_0^\delta \left[\left(1-\frac{U}{U_i}\right)^2 + 2\left(\frac{U}{U_i}\right)\left(1 - \frac{U}{U_i}\right) - \left(1 - \frac{U}{U_i}\right)\right]dy$$

$$= \int_0^\delta \left(1 - \frac{U}{U_i}\right)^2 dy + 2\theta_B - \delta_B^*$$

$$= \delta \int_0^1 \left(1 - \frac{U}{U_i}\right)^2 d\eta + 2\theta_B - \delta_B^* \tag{B-7}$$

The relation for the velocity at the outer edge of the boundary layer is given by

$$\left(\frac{U_i}{U_\tau}\right) = \frac{A}{L} \ln\left(\frac{\delta U_\tau}{\nu}\right) + B + 2P \tag{B-8}$$

Using equations (B-3) and (B-8), the following relation is obtained

$$\left(\frac{U_i - U}{U_\tau}\right) = -\frac{A}{L} \ln(y/\delta) + 2P\left[1 - \sin^2\left(\frac{\pi y}{2\delta}\right)\right]$$

$$= \left[-\frac{A}{L} \ln\eta + 2P \cos^2\left(\frac{\pi\eta}{2}\right)\right] \tag{B-9}$$

So,

$$\left(1 - \frac{U}{U_i}\right) = \left[-\left(\frac{AU_\tau}{LU_i}\right) \ln\eta + 2\left(\frac{PU_\tau}{U_i}\right)\cos^2\left(\frac{\pi\eta}{2}\right)\right] \tag{B-10}$$

Thus the first term in equation (B-7) can be evaluated as

$$\delta\int_0^1 \left(1-\frac{U}{U_i}\right)^2 d\eta = \delta\int_0^1 \left[\left(\frac{AU_\tau}{LU_i}\right)^2 \ln^2\eta + 4\left(\frac{PU_\tau}{U_i}\right)^2 \cos^4\left(\frac{\pi\eta}{2}\right) - 4\frac{AP}{L}\left(\frac{U_\tau}{U_i}\right)^2 \ln\eta \cos^2\left(\frac{\pi\eta}{2}\right)\right] d\eta$$

$$= \delta\left(\frac{AU_\tau}{LU_i}\right)^2 \left[\eta\ln^2\eta - 2\eta\ln\eta + 2\eta\right]_0^1$$

$$+ \delta\left(\frac{PU_\tau}{U_i}\right)^2 \int_0^1 \left[1 + \cos^2\pi\eta + 2\cos\pi\eta\right] d\eta$$

$$- 4\,\frac{\delta AP}{L}\left(\frac{U_\tau}{U_i}\right)^2 \int_0^1 \ln\eta\left[1 - \sin^2\frac{\pi\eta}{2}\right] d\eta$$

$$= \left[\delta\left(\frac{AU_\tau}{LU_i}\right)^2 (2)\right] + \left[\delta\left(\frac{PU_\tau}{U_i}\right)^2 + \frac{\delta}{2}\left(\frac{PU_\tau}{U_i}\right)^2\right]$$

$$+ \left[\frac{4\delta AP}{L}\left(\frac{U_\tau}{U_i}\right)^2 + \frac{2\delta AP}{L}\left(\frac{U_\tau}{U_i}\right)^2 \int_0^1 2(\ln\eta)\sin^2\left(\frac{\pi\eta}{2}\right) d\eta\right]$$

$$= \delta\left(\frac{U_\tau}{U_i}\right)^2 \left[1.5P^2 + \frac{2AP}{L}(2 - 0.41) + 2\frac{A^2}{L^2}\right]$$

Hence the momentum thickness is given by

$$\theta_B = \delta_B^* - \delta\left(\frac{U_\tau}{U_i}\right)^2 \left[1.5P^2 + 3.18\frac{AP}{L} + 2\,\frac{A^2}{L^2}\right] \qquad \text{(B-11)}$$

The shape parameter H_B is given by

$$\frac{1}{H_B} = 1 - \frac{U_\tau\left[1.5P^2 + (3.18)(AP/L) + 2(A^2/L^2)\right]}{U_i\left(\frac{A}{L} + P\right)} \qquad \text{(B-12)}$$

Inner Wake

The displacement thickness and momentum thickness in this region are given by the following equations.

$$\delta^*_{IW} = \int_{(\delta_2 - G_1 L_1)}^{\delta_2} (1 - \frac{U}{U_0}) dy \qquad \text{(B-13)}$$

$$\theta_{IW} = \int_{(\delta_2 - G_1 L_1)}^{\delta_2} (\frac{U}{U_0})(1 - \frac{U}{U_0}) dy \qquad \text{(B-14)}$$

The velocity U is given by,

$$\frac{U}{U_0} = 1 - (\frac{U_0 - U_1}{U_0}) \; Exp[-k(\frac{y - \delta_2}{L_1})^2] \qquad \text{(B-15)}$$

Hence δ^*_{IW} can be evaluated as

$$\delta^*_{IW} = \int_{(\delta_2 - G_1 L_1)}^{\delta_2} (\frac{U_0 - U_1}{U_0}) Exp[-k(\frac{y - \delta_2}{L_1})^2] dy$$

$$= L_1 \int_{-G_1}^{0} (\frac{U_0 - U_1}{U_0}) \; Exp(-k\eta^2) d\eta$$

$$= (1 - \frac{U_1}{U_0}) \; L_1 B_4 \qquad \text{(B-16)}$$

Where B_4 is the integral given in section (ii), Appendix - A.

The momentum thickness θ_{IW} can be evaluated as ,

$$\theta_{IW} = \int_{(\delta_2 - G_1 L_1)}^{\delta_2} (\frac{U}{U_0}) \; (1 - \frac{U}{U_0}) dy$$

$$= \int_{(\delta_2 - G_1 L_1)}^{\delta_2} (\frac{U_0 - U_1}{U_0}) \; Exp[-k(\frac{y - \delta_2}{L_1})^2] dy$$

$$- \int_{(\delta_2 - G_1 L_1)}^{\delta_2} (\frac{U_0 - U_1}{U_0})^2 Exp[-2k(\frac{y - \delta_2}{L_1})^2] dy$$

$$\theta_{IW} = \left(\frac{U_0 - U_1}{U_0}\right) L_1 B_4 - \left(\frac{U_0 - U_1}{U_0}\right)^2 L_1 B_3$$

$$= \left(1 - \frac{U_1}{U_0}\right)\left[L_1 B_4 - \left(1 - \frac{U_1}{U_0}\right) L_1 B_3\right]$$

where B_3 is the integral given in section (ii) of Appendix A. The shape parameter H_{IW} is given by

$$H_{IW} = \frac{1}{\left[1 - \left(1 - \frac{U_1}{U_0}\right)\left(\frac{B_3}{B_4}\right)\right]} \qquad \text{(B-17)}$$

In the merged case δ is replaced by δ_3 and U_i , U_0 by U_3 in the above equations.

Outer Wake

The displacement thickness and momentum thickness in this region are given by

$$\delta^*_{OW} = \int_{\delta_2}^{(\delta_2 + G_0 L_0)} \left(1 - \frac{U}{U_e}\right) dy \qquad \text{(B-18)}$$

$$\theta_{OW} = \int_{\delta_2}^{(\delta_2 + G_0 L_0)} \left(\frac{U}{U_e}\right)\left(1 - \frac{U}{U_e}\right) dy \qquad \text{(B-19)}$$

The velocity U is given by

$$\frac{U}{U_e} = 1 - \left(\frac{U_e - U_1}{U_e}\right) \mathrm{Exp}\left[-k\left(\frac{y - \delta_2}{L_0}\right)^2\right] \qquad \text{(B-20)}$$

Hence δ^*_{OW} can be evaluated as

$$\delta^*_{OW} = \int_{\delta_2}^{(\delta_2 + G_0 L_0)} \left(\frac{U_e - U_1}{U_e}\right) \mathrm{Exp}\left[-k\left(\frac{y - \delta_2}{L_0}\right)^2\right] dy$$

$$\delta^*_{OW} = L_0 \int_0^{G_0} \left(\frac{U_e - U_1}{U_e}\right) \mathrm{Exp}(-k\eta^2)\,d\eta$$

$$= \left(1 - \frac{U_1}{U_e}\right) L_0 A_4 \qquad \text{(B-21)}$$

where A_4 is the integral given in section (ii) of Appendix-A. The momentum thickness θ_{OW} can be evaluated as

$$\theta_{OW} = \int_{\delta_2}^{(\delta_2 + G_0 L_0)} \left(\frac{U}{U_e}\right)\left(1 - \frac{U}{U_e}\right) dy$$

$$= \int_{\delta_2}^{(\delta_2 + G_0 L_0} \left(\frac{U_e - U_1}{U_e}\right) \mathrm{Exp}\left[-k\left(\frac{y - \delta_2}{L_0}\right)^2\right] dy$$

$$- \int_{\delta_2}^{(\delta_2 + G_0 L_0)} \left(\frac{U_e - U_1}{U_e}\right)^2 \mathrm{Exp}\left[-2k\left(\frac{y - \delta_2}{L_0}\right)^2\right] dy$$

$$= \left(\frac{U_e - U_1}{U_e}\right) L_0 A_4 - \left(\frac{U_e - U_1}{U_e}\right)^2 L_0 A_3$$

$$= \left(1 - \frac{U_1}{U_e}\right)\left[L_0 A_4 - \left(1 - \frac{U_1}{U_e}\right) L_0 A_3\right] \qquad \text{(B-22)}$$

where A_3 is the integral given in section (ii) of Appendix-A. The shape parameter H_{OW} is given by

$$H_{OW} = \frac{1}{\left[1 - \left(1 - \frac{U_1}{U_e}\right)\left(\frac{A_3}{A_4}\right)\right]} \qquad \text{(B-23)}$$

Considering the whole layer as one single shear layer, the total displacement thickness is defined by

$$\delta_T^* = \int_0^{(\delta_2 + G_0 L_0)} (1 - \frac{U}{U_e})dy$$

$$= \int_0^{\delta_3} (1 - \frac{U}{U_e})dy + \int_{\delta_3}^{\delta_2} (1 - \frac{U}{U_e})dy + \int_{\delta_2}^{(\delta_2 + G_0 L_0)} (\frac{U}{U_e})dy \qquad \text{(B-24)}$$

The first term in equation (B-24) is given by

$$\int_0^{\delta_3} (1 - \frac{U}{U_e})dy = (1 - \frac{U_3}{U_e})\delta_3 + (\frac{U_3}{U_e})\delta_B^* \qquad \text{(B-25)}$$

The second term is given by

$$\int_{\delta_3}^{\delta_2} (1 - \frac{U}{U_e})dy = \int_{(\delta_2 - G_1 L_1)}^{\delta_2} (1 - \frac{U}{U_e})dy$$

$$= (1 - \frac{U_3}{U_e})G_1 L_1 + (\frac{U_3}{U_e})\delta_{IW}^* \qquad \text{(B-26)}$$

The third term is the same as equation (B-21).

Hence the total displacement thickness is given by

$$\delta_T^* = (1 - \frac{U_3}{U_e})\delta_3 + (\frac{U_3}{U_e})\delta_B^*$$

$$+ (1 - \frac{U_3}{U_e})G_1 L_1 + (\frac{U_3}{U_e})\delta_{IW}^* + (1 - \frac{U_1}{U_e})L_0 A_4 \qquad \text{(B-27)}$$

Similarly the total momentum thickness is defined by

$$\theta_T = \int_0^{(\delta_2 + G_0 L_0)} (\frac{U}{U_e})(1 - \frac{U}{U_e})dy$$

$$\theta_T = \int_0^{\delta_3} (\frac{U}{U_e})(1 - \frac{U}{U_e})dy + \int_{(\delta_2 - G_1L_1)}^{\delta_2} (\frac{U}{U_e})(1 - \frac{U}{U_e})dy$$

$$+ \int_{\delta_2}^{(\delta_2 + G_0L_0)} (\frac{U}{U_e})(1 - \frac{U}{U_e})dy \qquad \text{(B-28)}$$

The first term is given by

$$\int_0^{\delta_3} (\frac{U}{U_e})(1 - \frac{U}{U_e})dy = (\frac{U_3}{U_e})(1 - \frac{U_3}{U_e})\delta_3 - (1 - \frac{U_3}{U_e})(\frac{U_3}{U_e})\delta_B^* + (\frac{U_3}{U_e})^2 \theta_B \qquad \text{(B-29)}$$

The second term is given by

$$\int_{(\delta_2 - G_1L_1)}^{\delta_2} (\frac{U}{U_e})(1 - \frac{U}{U_e})dy = (1 - \frac{U_3}{U_e})(\frac{U_3}{U_e})G_1L_1 - (1 - \frac{U_3}{U_e})(\frac{U_3}{U_e})\delta_{IW}^*$$

$$+ (\frac{U_3}{U_e})^2 \theta_{IW} \qquad \text{(B-30)}$$

The third term is the same as equation (B-22). Hence the total momentum thickness is given by,

$$\theta_T = (\frac{U_3}{U_e})(1 - \frac{U_3}{U_e})\delta_3 - (1 - \frac{U_3}{U_e})(\frac{U_3}{U_e})\delta_B^* + (\frac{U_3}{U_e})^2 \theta_B$$

$$+ (\frac{U_3}{U_e})(1 - \frac{U_3}{U_e})G_1L_1 - (1 - \frac{U_3}{U_e})(\frac{U_3}{U_e})\delta_{IW}^* + (\frac{U_3}{U_e})^2 \theta_{IW} + \theta_{OW} \qquad \text{(B-31)}$$

APPENDIX - C

Flow Chart

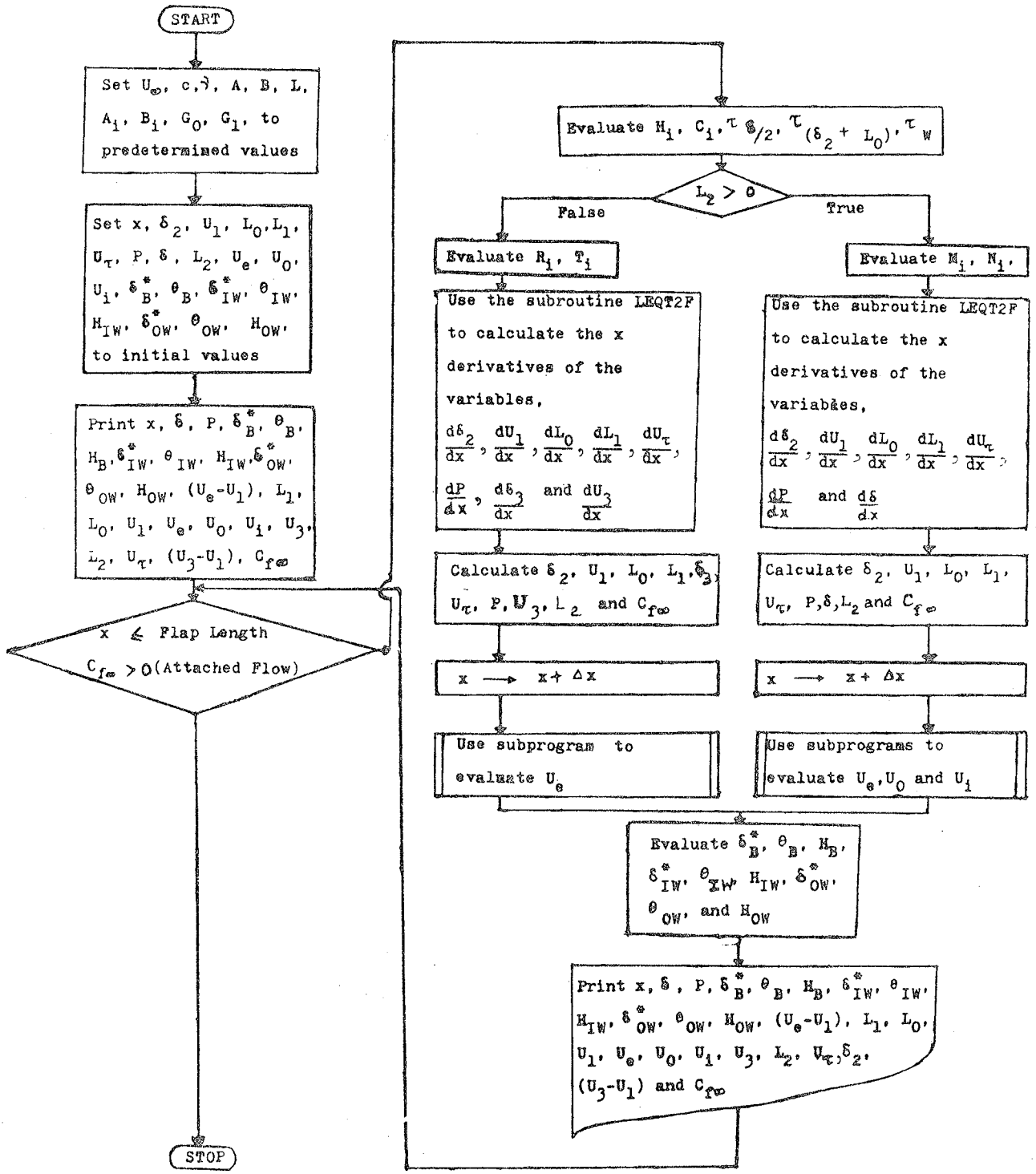

APPENDIX - D

```
C CALCULATIONS FOR THE SLOTTED FLAP MEASUREMENTS REPORTED BY IRWIN
C FLAP DEFLECTION = 30 DEG ; SLOT HEIGHT = 0.020C ANGLE OF ATTACK = 8 DG
C VARIABLE DIRECTORY
C NU  -  DIMENSIONAL KINEMATIC VISCOSITY
C DLOG,DSIN,DCOS  -  BUILT-IN FUNCTIONS
C LMT1,LMT2  -  LOWER AND UPPER LIMIT OF INTEGRALS
C DCPDX,CP  -  FUNCTION SUBPROGRAMS USED TO EVALUATE PRESSURE INTEGRALS
C AND POTENTIAL FLOW VELOCITIES.
C B11,B22  -  FUNCTION SUBPROGRAMS USED TO EVALUATE NUMERICAL INTEGRALS
C C7,C8,C15 AND C16
C LT1,LT2  -  VARIABLES CORRESPONDING TO LMT1,LMT2 USED IN THE SUBPROGRA
C -MS
C DY1  -  LENGTH OF THE INTERVAL USED IN THE EVALUATION OF THE NUMERICAL
C  INTEGRALS BY SIMPSON'S METHOD
C DY  -  STEP DISTANCE USED IN THE EVALUATION OF EACH INTERVAL
C D,F,G  -  ABSCISSAE USED IN THE EVALUATION OF EACH INTERVAL
C N  -  NUMBER OF INTERVALS
C MTRX,COL,ROW,IA,MTRXIN,IDGT,WKAREA,IER,SQ,RO,IA1,SQIN  -  PARAMETERS O
C -F THE BUILT-IN SUBROUTINE LEQT2F USED IN SOLVING THE SYSTEM OF EQUATI
C -ONS
      DOUBLE PRECISION X,Y,GO,G1,LO,L1,L2,US2,U1,UE,UO,U3,UI,P,S,S2,S3,C
     *FIF,UT,THETB,S1B,HB,THETIW,S1IW,HIW,THETOW,S1OW,HOW,F
      DOUBLE PRECISION A,B,C,E,K,L,D1,D2,D3,D4,D5,D6,D7,D8,E1,E2,E3,E4,P
     *I,UIF
      DOUBLE PRECISION A1,A2,A3,A4,A5,A6,A7,A8,B1,B2,B3,B4,C1,C2,C3,C4,C
     *5,C6,C7,C8,C9,C10,C11,C12,C13,C14,C15,C16,C17,C18,C19,H1,H2,H3,H4,
     *H5
      DOUBLE PRECISION M1,M2,M3,M4,M5,M6,M7,M8,M9,M10,M11,M12,M13,M14,M1
     *5,M16,M17,M18,M19,M20,M21,M22,M23,M24,M25,M26,M27,M28,M29,M30,M31,
     *M32,M33,M34,M35,N1,N2,N3,N4,N5,N6,N7,R1,R2,R3,R4,R5,R6,R7,R8,R9,R1
     *0,R11,R12,R13,R14,R15,R16,R17,R18,R19,R20,R21,R22,R23,R24,R25,R26,
     *R27,R28,R29,R30,R31,R32,R33,R34,R35,R36,R37,R38,R39,R40,R41,R42,T1
     *,T2,T3,T4,T5,T6
      DOUBLE PRECISION LT1,LT2,LMT1,LMT2,B11,B22,DCPDX,CP
      DOUBLE PRECISION DLOG,DSIN,DCOS
      DOUBLE PRECISION NU,NUND,RTW
      DOUBLE PRECISION TOUW,TOUS,TOU2,TOUS2,TOUGL1,TOULO,TOUGLO,TOUS3
      DOUBLE PRECISION DS2DX,DU1DX,DLODX,DL1DX,DUTDX,DPDX,DSDX,DS3DX,DU3
     *DX,DX
      REAL MTRX(7,7),MTRXIN(7,1),WKAREA(200),SQ(8,8),SQIN(8,1)
      INTEGER COL,ROW,IA,IDGT,IER,RO,IA1
      COL = 1
      ROW = 7
      X = 0.114
      C = 0.915
      UIF = 61.0
      F = 0.0
      IDGT = 4
      IA = 7
      RO = 8
      IA1 = 8
      E = 2.718289
      DX = 0.001
      NU = 0.0000155
      NUND = (NU/(C*UIF))
      RTW = 40.0
      A = 5.616
      B = 4.8
      L = 2.3026
      K = 0.6931472
      D1 = -51.7
      D2 =  66.1
      D3 = -44.1
      D4 =  08.80
```

```
D5 = -06.2
D6 = -00.77
D7 =  06.61
D8 = -01.98
CFIF = 0.00644
GO = 2.77
G1 = 2.5
PI = 3.141593
LO = 0.0088272
L1 = 0.0075283
S2 = 0.025
S1B = 0.0005444
THETB = 0.0003478
HB = 1.5652174
UT = 0.0567644
P = 3.1873793
U1 = 1.0447774
UE = 1.4220698
UO = 1.4897411
UI = 1.4951318
U3 = UI
THETIW = 0.0018478
HIW = 1.2608696
THETOW = 0.0020652
HOW = 1.2391304
S1IW = 0.0023298
S1OW = 0.0025591
S = 0.00265
E1 = ((D1*X*X*X)+(D2*X*X)+(D3*X)+D4)
E3 = ((D5*X*X*X)+(D6*X*X)+(D7*X)+D8)
E2 = ((3.0*D1*X*X)+(2.0*D2*X)+D3)
E4 = ((3.0*D5*X*X)+(2.0*D6*X)+D7)
L2 = S2-(G1*L1)-S
LMT1 = 0.0
LMT2 = GO
A1 = ((E**((-2.0)*K*LMT1*LMT1))*LMT1/(4.0*K)) - ((E**((-2.0)*K*LMT
*2*LMT2))*LMT2/(4.0*K)) + (0.7527/(4.0*K))
A2 = ((E**((-K)*LMT1*LMT1))*LMT1/(2.0*K)) - ((E**((-K)*LMT2*LMT2))
**LMT2/(2.0*K)) + (1.0633/(2.0*K))
A3 = 0.7527
A4 = 1.0633
LMT2 = 1.0
A5 = ((E**((-2.0)*K*LMT1*LMT1))*LMT1/(4.0*K)) - ((E**((-2.0)*K*LMT
*2*LMT2))*LMT2/(4.0*K)) + (0.6805/(4.0*K))
A6 = ((E**((-K)*LMT1*LMT1))*LMT1/(2.0*K)) - ((E**((-K)*LMT2*LMT2))
**LMT2/(2.0*K)) + (0.8101/(2.0*K))
A7 = 0.6805
A8 = 0.8101
LMT1 = -G1
LMT2 = 0.0
B1 = ((E**((-2.0)*K*LMT1*LMT1))*LMT1/(4.0*K)) - ((E**((-2.0)*K*LMT
*2*LMT2))*LMT2/(4.0*K)) + (0.7526/(4.0*K))
B2 = ((E**((-K)*LMT1*LMT1))*LMT1/(2.0*K)) - ((E**((-K)*LMT2*LMT2))
**LMT2/(2.0*K)) + (1.0610/(2.0*K))
B3 = 0.7526
B4 = 1.0610
TOUS = TOUGL1 = TOUGLO = TOUS2 = TOUS3 = 0.0
PRINT 200
PRINT 210
PRINT 220,X,S,P,S1B,THETB,HB,S1IW,THETIW,HIW,S1OW,THETOW,HOW,UE-U1
PRINT 240
PRINT 250,L1,LO,U1,UE,UO,UI,U3,L2,S2,UT,U3-U1,CFIF
PRINT 230
WHILE   (  X  .LE.  0.4  .AND.  CFIF  .GT.  0.0  )  DO
```

```
      LMT1 = S2
      LMT2 = (S2+(GO*LO))
      H1 = (0.5*(DCPDX(X,LMT1,LMT2,D1,D2,D3,D5,D6,D7)))
      LMT2 = (S2+LO)
      H2 = (0.5*(DCPDX(X,LMT1,LMT2,D1,D2,D3,D5,D6,D7)))
      LMT1 = (S2-(G1*L1))
      LMT2 = S2
      H3 = (0.5*(DCPDX(X,LMT1,LMT2,D1,D2,D3,D5,D6,D7)))
      LMT1 = (2.0*NUND/UT)
      LMT2 = S
      H4 = (0.5*(DCPDX(X,LMT1,LMT2,D1,D2,D3,D5,D6,D7)))
      LMT1 = S/2.0
      H5 = (0.5*(DCPDX(X,LMT1,LMT2,D1,D2,D3,D5,D6,D7)))
      LMT1 = (2.0*NUND/UT)
      LMT2 = S
      C1 = ((DLOG(LMT2*UT/NUND))*LMT2) - ((DLOG(LMT1*UT/NUND))*LMT1)
      C1 = C1 - (LMT2-LMT1)
      C2 = (((DLOG(LMT2*UT/NUND))**2)*LMT2) - (((DLOG(LMT1*UT/NUND)
*)**2)*LMT1) - (2.0*LMT2*(DLOG(LMT2*UT/NUND))) + (2.0*LMT1*(DLOG(
*LMT1*UT/NUND))) + (2.0*(LMT2-LMT1))
      C3 = (((DSIN(PI*LMT2/(2.0*S)))**4)*S*LMT2/(2.0*PI)) - (((DSIN
*(PI*LMT1/(2.0*S)))**4)*S*LMT1/(2.0*PI)) - (S*LMT2/(8.0*PI)) + (S
**LMT1/(8.0*PI)) - (S*LMT2/(16.0*PI)) + (S*LMT1/(16.0*PI)) - ((DSIN
*(2.0*PI*LMT2/S))*S*S/(32.0*PI*PI)) + ((DSIN(2.0*PI*LMT1/S))*S*S/(3
*2.0*PI*PI)) + ((DSIN(PI*LMT2/S))*S*S/(4.0*PI*PI)) - ((DSIN(PI*LMT1
*/S))*S*S/(4.0*PI*PI))
      C4 = ((LMT2-LMT1)/4.0) + ((LMT2-LMT1)/8.0) + ((DSIN(2.0*PI*LMT2
*/S))*S/(16.0*PI)) - ((DSIN(2.0*PI*LMT1/S))*S/(16.0*PI))
      C4 = C4 - ((DSIN(PI*LMT2/S))*S/(2.0*PI)) + ((DSIN(PI*LMT1/S))*S
*/(2.0*PI))
      C5 = ((DCOS(PI*LMT1/S))*LMT1*S/(2.0*PI)) - ((DCOS(PI*LMT2/S))*L
*MT2*S/(2.0*PI)) + ((DSIN(PI*LMT2/S))*S*S/(2.0*PI*PI)) - ((DSIN(PI*
*LMT1/S))*S*S/(2.0*PI*PI))
      C6 = ((LMT2-LMT1)/2.0) - ((DSIN(PI*LMT2/S))*S/(2.0*PI)) + ((DSI
*N(PI*LMT1/S))*S/(2.0*PI))
      C7 = B11(UT,NUND,LMT1,LMT2,S)
      C8 = B22(UT,NUND,LMT1,LMT2,S)
      LMT1 = 0.5*S
      C9 = ((DLOG(LMT2*UT/NUND))*LMT2) - ((DLOG(LMT1*UT/NUND))*LMT1)
      C9 = C9 - (LMT2-LMT1)
      C10 = (((DLOG(LMT2*UT/NUND))**2)*LMT2) - (((DLOG(LMT1*UT/NUND)
*)**2)*LMT1) - (2.0*LMT2*(DLOG(LMT2*UT/NUND))) + (2.0*LMT1*(DLOG(
*LMT1*UT/NUND))) + (2.0*(LMT2-LMT1))
      C11 = (((DSIN(PI*LMT2/(2.0*S)))**4)*S*LMT2/(2.0*PI)) - (((DSIN
*(PI*LMT1/(2.0*S)))**4)*S*LMT1/(2.0*PI)) - (S*LMT2/(8.0*PI)) + (S
**LMT1/(8.0*PI)) - (S*LMT2/(16.0*PI)) + (S*LMT1/(16.0*PI)) - ((DSIN
*(2.0*PI*LMT2/S))*S*S/(32.0*PI*PI)) + ((DSIN(2.0*PI*LMT1/S))*S*S/(3
*2.0*PI*PI)) + ((DSIN(PI*LMT2/S))*S*S/(4.0*PI*PI)) - ((DSIN(PI*LMT1
*/S))*S*S/(4.0*PI*PI))
      C12 = ((LMT2-LMT1)/4.0) + ((LMT2-LMT1)/8.0) + ((DSIN(2.0*PI*LMT
*2/S))*S/(16.0*PI)) - ((DSIN(2.0*PI*LMT1/S))*S/(16.0*PI))
      C12 = C12 - ((DSIN(PI*LMT2/S))*S/(2.0*PI)) + ((DSIN(PI*LMT1/S))
**S/(2.0*PI))
      C13 = ((DCOS(PI*LMT1/S))*LMT1*S/(2.0*PI)) - ((DCOS(PI*LMT2/S))*
*LMT2*S/(2.0*PI)) + ((DSIN(PI*LMT2/S))*S*S/(2.0*PI*PI)) - ((DSIN(PI
**LMT1/S))*S*S/(2.0*PI*PI))
      C14 = ((LMT2-LMT1)/2.0) - ((DSIN(PI*LMT2/S))*S/(2.0*PI)) + ((DS
*IN(PI*LMT1/S))*S/(2.0*PI))
      C15 = B11(UT,NUND,LMT1,LMT2,S)
      C16 = B22(UT,NUND,LMT1,LMT2,S)
      LMT1 = (2.0*NUND/UT)
      LMT2 = 0.5*S
      C17 = ((DLOG(LMT2*UT/NUND))*LMT2) - ((DLOG(LMT1*UT/NUND))*LMT1)
      C17 = C17 - (LMT2-LMT1)
```

```
      C18 = ((DCOS(PI*LMT1/S))*LMT1*S/(2.0*PI)) - ((DCOS(PI*LMT2/S))*
     *LMT2*S/(2.0*PI)) + ((DSIN(PI*LMT2/S))*S*S/(2.0*PI*PI)) - ((DSIN(PI
     **LMT1/S))*S*S/(2.0*PI*PI))
      C19 = ((LMT2-LMT1)/2.0) - ((DSIN(PI*LMT2/S))*S/(2.0*PI)) + ((DS
     *IN(PI*LMT1/S))*S/(2.0*PI))
      US2 = (((DLOG(S*UT/(2.0*NUND))))*A*UT/L) + (B*UT) + (P*UT)
      TOUW = UT*UT
      TOU2 = (0.01547)*S*UT*((A/L) + P)
      TOU2 = TOU2*((2.0*A*UT/(L*S))+(PI*P*UT/S))
      TOULO = (2.0*K*(UE-U1)*(UE-U1)*(E**(-K))/RTW)
      M21 = (2.0*A*A*UT*C1/(L*L)) + (4.0*A*B*UT*C1/L)
      M21 = M21 - (UI*A*C1/L) + (2.0*A*A*UT*C2/(L*L))
      M21 = M21 + (8.0*P*P*UT*C4) + (8.0*B*UT*P*C6)
      M21 = M21 + (4.0*A*UT*P*C6/L) - (2.0*UI*P*C6)
      M21 = M21 + (8.0*A*P*UT*C7/L) + (2.0*B*B*UT*(S-LMT1))
      M21 = M21 + (2.0*A*B*UT*(S-LMT1)/L) - (UI*A*(S-LMT1)/L)
      M21 = M21 - (UI*B*(S-LMT1))
      M22 = (8.0*P*UT*UT*C4) + (4.0*B*UT*UT*C6) - (2.0*UI*UT*C6)
      M22 = M22 + (4.0*A*UT*UT*C7/L)
      M23 = (2.0*PI*UI*P*UT*C5/(S*S)) - (4.0*PI*B*P*UT*UT*C5/(S*S))
      M23 = M23 - (8.0*PI*P*P*UT*UT*C3/(S*S))
      M23 = M23 - (4.0*A*PI*P*UT*UT*C8/(L*S*S))
      M24 = (2.0*A*A*UT*C9/(L*L)) + (4.0*A*B*UT*C9/L) -(UI*A*C1/L)
      M24 = M24 + (2.0*A*A*UT*C10/(L*L)) + (8.0*P*P*UT*C12)
      M24 = M24 + (8.0*B*UT*P*C14) + (4.0*A*UT*P*C14/L)
      M24 = M24 + (8.0*A*P*UT*C15/L) - (2.0*UI*P*C6) + (US2*A*C17/L)
      M24 = M24 + (2.0*US2*P*C19) + (B*B*UT*S) + (A*B*UT*S/L)
      M24 = M24 - (UI*A*(S-LMT1)/L) - (UI*B*(S-LMT1))
      M24 = M24 + ((A*((S/2.0)-LMT1)/L)+(B*((S/2.0)-LMT1)))*US2
      M25 = (8.0*P*UT*UT*C12) + (4.0*B*UT*UT*C14)
      M25 = M25 + (4.0*A*UT*UT*C15/L) - (2.0*UI*UT*C6)
      M25 = M25 + (2.0*US2*UT*C19)
      M26 = (2.0*PI*UT*P*UI*C5/(S*S)) - (2.0*US2*PI*P*UT*C18/(S*S))
      M26 = M26 - (8.0*PI*P*P*UT*UT*C11/(S*S))
      M26 = M26 - (4.0*PI*B*P*UT*UT*C13/(S*S))
      M26 = M26 - (4.0*A*PI*P*UT*UT*C16/(L*S*S))
      IF   (  L2  .GT.  0.0  )   THEN   DO
         M1 = (UE*(UE-U1)*((E**((-K)*GO*GO))-1.0))
         M1 = M1 + ((U1-UE)*(UE-U1)*((E**((-2.0)*K*GO*GO))-1.0))
         M1 = M1 - (UE*(UO-U1)*(1.0-(E**((-K)*G1*G1))))
         M1 = M1 + (U1*(UO-U1)*(1.0-(E**((-K)*G1*G1))))
         M1 = M1 - ((UE*GO*LO)+(2.0*(UE-U1)*LO*A3)-(UE*LO*A4)-(2.0*(U
     *E-U1)*LO*A4))*(E1/(2.0*UE))
         M1 = M1 - ((UE*L1*B4)-(UE*G1*L1)+(U1*G1*L1)-(U1*L1*B4))*(E1/
     *(2.0*UO))
         M2 = (UE*LO*A4) - (2.0*(UE-U1)*LO*A3)
         M2 = M2 - (UE*L1*B4) + (U1*L1*B4)
         M3 = (4.0*K*A1*(UE-U1)*(UE-U1)) - (2.0*K*A2*UE*(UE-U1))
         M3 = M3 - ((UE*GO*LO)+(2.0*(UE-U1)*LO*A3)- (UE*LO*A4)-(2.0*(
     *UE-U1)*LO*A4))*(E1*GO/(2.0*UE))
         M4 = (2.0*K*UE*(UO-U1)*B2) - (2.0*K*U1*(UO-U1)*B2)
         M4 = M4 + ((UE*L1*B4)-(UE*G1*L1)+(U1*G1*L1)-(U1*L1*B4))*(G1*
     *E1/(2.0*UO))
         M5 = ((A*(S-LMT1)/L)+(A*C1/L)+(B*(S-LMT1))+(2.0*P*C6))
         M5 = (M5*(U1-UE))
         M6 = ((U1-UE)*2.0*UT*C6)
         M7 = ((UE-U1)*2.0*P*UT*PI*C5/(S*S))
         M8 = (2.0*UE*(UE-U1)*((E**(-K))-1.0))
         M8 = M8 + ((U1-UE)*(UE-U1)*((E**((-2.0)*K))-1.0))
         M8 = M8 - (((UE+U1)/2.0)*(UE-U1)*((E**(-K))-1.0))
         M8 = M8 - (((UE+U1)/2.0)*(UO-U1)*(1.0-(E**((-K)*G1*G1))))
         M8 = M8 + (U1*(UO-U1)*(1.0-(E**((-K)*G1*G1))))
         M8 = M8 - ((2.0*UE*LO)+(2.0*(UE-U1)*LO*A7)-(2.0*UE*LO*A8)-(2
     *.0*(UE-U1)*LO*A8)-((UE+U1)*(LO/2.0)*(1.0-A8)))*(E1/(2.0*UE))
```

```
      M8 = M8 - (((UE+U1)*(L1/2.0)*B4)-((UE+U1)*(L1/2.0)*G1)+(U1*G
*1*L1)-(U1*L1*B4))*(E1/(2.0*UO))
      M9 = (2.0*UE*LO*A8) - (2.0*(UE-U1)*LO*A7)
      M9 = M9 - (((UE+U1)/2.0)*LO*A8) - (((UE+U1)/2.0)*L1*B4)
      M9 = M9 + (U1*L1*B4)
      M10 = (4.0*K*(UE-U1)*(UE-U1)*A5) - (4.0*K*UE*(UE-U1)*A6)
      M10 = M10 + (2.0*K*((UE+U1)/2.0)*(UE-U1)*A6)
      M10 = M10 - ((2.0*UE*LO)+(2.0*(UE-U1)*LO*A7)-(2.0*UE*LO*A8)-
*(2.0*(UE-U1)*LO*A8)-((UE+U1)*(LO/2.0)*(1.0-A8)))*(GO*E1/(2.0*UE))
      M11 = (2.0*K*((UE+U1)/2.0)*(UO-U1)*B2) - (2.0*K*U1*(UO-U1)*B
*2) + (((UE+U1)*(L1/2.0)*B4)-((UE+U1)*(L1/2.0)*G1)+(U1*G1*L1)-(U1*L
*1*B4))*(G1*E1/(2.0*UO))
      M12 = ((A*(S-LMT1)/L)+(A*C1/L)+(B*(S-LMT1))+(2.0*P*C6))
      M12 = (M12*((U1-UE)/2.0))
      M13 = ((U1-UE)*UT*C6)
      M14 = ((UE-U1)*P*UT*PI*C5/(S*S))
      M15 = (2.0*UO*(UO-U1)*(1.0-(E**((-K)*G1*G1))))
      M15 = M15 + ((U1-UO)*(UO-U1)*(1.0-(E**((-2.0)*K*G1*G1))))
      M15 = M15 - (U1*(UO-U1)*(1.0-(E**((-K)*G1*G1))))
      M15 = M15 - ((2.0*UO*G1*L1)+(2.0*(UO-U1)*L1*B3)-(2.0*UO*L1*B
*4)-(2.0*(UO-U1)*L1*B4)-(U1*G1*L1)+(U1*L1*B4))*(E1/(2.0*UO))
      M16 = (2.0*UO*L1*B4) - (2.0*(UO-U1)*L1*B3) - (U1*L1*B4)
      M17 = (4.0*K*(UO-U1)*(UO-U1)*B1) - (4.0*K*UO*(UO-U1)*B2)
      M17 = M17 + (2.0*K*U1*(UO-U1)*B2)
      M17 = M17 + ((2.0*UO*G1*L1)+(2.0*(UO-U1)*L1*B3)-(2.0*UO*L1*B
*4)-(2.0*(UO-U1)*L1*B4)-(U1*G1*L1)+(U1*L1*B4))*(G1*E1/(2.0*UO))
      M18 = ((A*(S-LMT1)/L)+(A*C1/L)+(B*(S-LMT1))+(2.0*P*C6))
      M18 = (M18*(UO-U1))
      M19 = ((UO-U1)*2.0*UT*C6)
      M20 = ((U1-UO)*2.0*P*UT*PI*C5/(S*S))
      M27 = (UO-(((G1*L1)-(B4*L1))*(E1/(2.0*UO))))
      M28 = (B4*L1)
      M29 = ((((G1*L1)-(B4*L1))*(G1*E1/(2.0*UO)))-(B4*(UO-U1)))
      M30 = (((DLOG(S*UT/NUND))*A*S/L)+(B*S)+(P*S)-(LMT1*A*(DLOG(L
*MT1*UT/NUND))/L)-(B*LMT1)-(P*LMT1)+((P*S/PI)*(DSIN(PI*LMT1/S))))
      M31 = (UT*S)-(LMT1*UT)+((UT*S/PI)*(DSIN(PI*LMT1/S)))
      M32 = (((DLOG(S*UT/NUND))*A*UT/L)+(B*UT)+(P*UT)-(UI)+((P*UT/
*PI)*(DSIN(PI*LMT1/S)))-((P*UT*LMT1/S)*(DCOS(PI*LMT1/S))))
      M33 = ((UI/UT)+(A/L))
      M34 = (2.0*UT)
      M35 = ((A*UT/(L*S))+(E1/(2.0*UI)))
      N1 = TOUGLO - TOUS2 - H1 + ((UE*L1*B4)-(UE*G1*L1)+(U1*G1*L1
*)-(U1*L1*B4))*((S2-(G1*L1))*E2+E4)*(1.0/(2.0*UO)) + ((UE*GO*LO)+(2
*.0*(UE-U1)*LO*A3)-(UE*LO*A4)-(2.0*(UE-U1)*LO*A4))*((S2+(GO*LO))*E2
*+E4)*(1.0/(2.0*UE))
      N2 = TOULO - TOUS2 - H2 + ((2.0*UE*LO)+(2.0*(UE-U1)*LO*A7)-(
*2.0*UE*LO*A8)-(2.0*(UE-U1)*LO*A8)-((UE+U1)*(LO/2.0)*(1.0-A8)))*((S
*2+(GO*LO))*E2+E4)*(1.0/(2.0*UE))+(((UE+U1)*(L1/2.0)*B4)-((UE+U1)*G
*1*(L1/2.0))+(U1*G1*L1)-(U1*L1*B4))*((S2-(G1*L1))*E2+E4)*(1.0/(2.0*
*UO))
      N3 = TOUS2 - TOUGL1 - H3 + ((2.0*UO*G1*L1)+(2.0*(UO-U1)*L1*B
*3)-(2.0*UO*L1*B4)-(2.0*(UO-U1)*L1*B4)-(U1*G1*L1)+(U1*L1*B4))*((S2-
*(G1*L1))*E2+E4)*(1.0/(2.0*UO))
      N4 = TOUS - TOUW - H4
      N5 = TOUS - TOU2 - H5
      N6 = F + (2.0*E2/(3.0*E1*E1))*((UI*UI*UI)-(UO*UO*UO)) + (UI/
*E1)*((S*E2)+E4) - (UO/E1)*((S2-(G1*L1))*E2+E4) + (G1*L1-B4*L1)*((S
*2-(G1*L1))*E2+E4)*(1.0/(2.0*UO))
      N7 = (S*E2+E4)*((-1.0)/(2.0*UI))
      MTRX(1,1) = M1
      MTRX(1,2) = M2
      MTRX(1,3) = M3
      MTRX(1,4) = M4
      MTRX(1,5) = M5
```

```
MTRX(1,6) = M6
MTRX(1,7) = M7
MTRX(2,1) = M8
MTRX(2,2) = M9
MTRX(2,3) = M10
MTRX(2,4) = M11
MTRX(2,5) = M12
MTRX(2,6) = M13
MTRX(2,7) = M14
MTRX(3,1) = M15
MTRX(3,2) = M16
MTRX(3,3) = 0.0
MTRX(3,4) = M17
MTRX(3,5) = M18
MTRX(3,6) = M19
MTRX(3,7) = M20
MTRX(4,1) = MTRX(4,2) = MTRX(4,3) = MTRX(4,4) = 0.0
MTRX(4,5) = M21
MTRX(4,6) = M22
MTRX(4,7) = M23
MTRX(5,1) = MTRX(5,2) = MTRX(5,3) = MTRX(5,4) = 0.0
MTRX(5,5) = M24
MTRX(5,6) = M25
MTRX(5,7) = M26
MTRX(6,1) = M27
MTRX(6,2) = M28
MTRX(6,3) = 0.0
MTRX(6,4) = M29
MTRX(6,5) = M30
MTRX(6,6) = M31
MTRX(6,7) = M32
MTRX(7,1) = MTRX(7,2) = MTRX(7,3) = MTRX(7,4) = 0.0
MTRX(7,5) = M33
MTRX(7,6) = M34
MTRX(7,7) = M35
MTRXIN(1,1) = N1
MTRXIN(2,1) = N2
MTRXIN(3,1) = N3
MTRXIN(4,1) = N4
MTRXIN(5,1) = N5
MTRXIN(6,1) = N6
MTRXIN(7,1) = N7
CALL LEQT2F(MTRX,COL,ROW,IA,MTRXIN,IDGT,WKAREA,IER)
DS2DX = MTRXIN(1,1)
DU1DX = MTRXIN(2,1)
DLODX = MTRXIN(3,1)
DL1DX = MTRXIN(4,1)
DUTDX = MTRXIN(5,1)
DPDX = MTRXIN(6,1)
DSDX = MTRXIN(7,1)
S2 = S2 + (DS2DX*DX)
U1 = U1 + (DU1DX*DX)
LO = LO + (DLODX*DX)
L1 = L1 + (DL1DX*DX)
UT = UT + (DUTDX*DX)
P = P + (DPDX*DX)
S = S3 = S + (DSDX*DX)
CFIF = (2.0*UT*UT)
L2 = (S2-(G1*L1)-S)
X = X + DX
Y = (S2+(GO*LO))
UF = CP(X,Y,D1,D2,D3,D4,D5,D6,D7,D8)
Y = (S2-(G1*L1))
UO = CP(X,Y,D1,D2,D3,D4,D5,D6,D7,D8)
```

```
      Y = S
      UI = CP(X,Y,D1,D2,D3,D4,D5,D6,D7,D8)
      U3 = UI
   ELSE   DO
      R1 = (UE*(UE-U1)*((E**((-K)*GO*GO))-1.0))
      R1 = R1 + ((UE-U1)*(U1-UE)*((E**((-2.0)*K*GO*GO))-1.0))
      R1 = R1 - (UE*(U3-U1)*(1.0-(E**((-K)*G1*G1))))
      R1 = R1 + (U1*(U3-U1)*(1.0-(E**((-K)*G1*G1))))
      R1 = R1 - ((UE*GO*LO)+(2.0*(UE-U1)*LO*A3)-(UE*LO*A4)-(2.0*(U
*E-U1)*LO*A4))*(E1/(2.0*UE))
      R2 = (UE*LO*A4) - (2.0*(UE-U1)*LO*A3) + (U1*L1*B4)
      R2 = R2 - (UE*L1*B4)
      R3 = (4.0*K*(UE-U1)*(UE-U1)*A1) - (2.0*K*UE*(UE-U1)*A2)
      R3 = R3 - ((UE*GO*LO)+(2.0*(UE-U1)*LO*A3)-(UE*LO*A4)-(2.0*(U
*E-U1)*LO*A4))*(GO*E1/(2.0*UE))
      R4 = (2.0*K*(UE-U1)*(U3-U1)*B2)
      R5 = ((A*(S3-LMT1)/L)+(B*(S3-LMT1))+(A*C1/L)+(2.0*P*C6))
      R5 = (R5*(U1-UE))
      R6 = (2.0*(U1-UE)*UT*C6)
      R7 = ((UE-U1)*2.0*P*UT*PI*C5/(S3*S3))
      R8 = ((U1-UE)*(G1*L1-B4*L1))
      R9 = (2.0*UE*(UE-U1)*((E**(-K))-1.0))
      R9 = R9 - ((UE-U1)*(UE-U1)*((E**((-2.0)*K))-1.0))
      R9 = R9 - (((UE+U1)/2.0)*(UE-U1)*((E**(-K))-1.0))
      R9 = R9 - (((UE+U1)/2.0)*(U3-U1)*(1.0-(E**((-K)*G1*G1))))
      R9 = R9 + (U1*(U3-U1)*(1.0-(E**((-K)*G1*G1))))
      R9 = R9 - ((2.0*UE*LO)+(2.0*(UE-U1)*LO*A7)-(2.0*UE*LO*A8)-((
*UE+U1)*(LO/2.0)*(1.0-A8))-(2.0*(UE-U1)*LO*A8))*(E1/(2.0*UE))
      R10 = (2.0*UE*LO*A8) - (2.0*(UE-U1)*LO*A7)
      R10 = R10 - (((UE+U1)/2.0)*(LO*A8+L1*B4)) + (U1*L1*B4)
      R11 = (4.0*K*A5*(UE-U1)*(UE-U1)) - (4.0*K*UE*(UE-U1)*A6)
      R11 = R11 + (((UE+U1)/2.0)*2.0*K*(UE-U1)*A6)
      R11 = R11 - ((2.0*UE*LO)+(2.0*(UE-U1)*LO*A7)-(2.0*UE*LO*A8)-
*(2.0*(UE-U1)*LO*A8)-((UE+U1)*(LO/2.0)*(1.0-A8)))*(GO*E1/(2.0*UE))
      R12 = (K*(UE+U1)*(U3-U1)*B2) - (2.0*K*U1*(U3-U1)*B2)
      R13 = ((A*(S3-LMT1)/L)+(B*(S3-LMT1))+(A*C1/L)+(2.0*P*C6))
      R13 = R13*((U1-UE)/2.0)
      R14 = ((U1-UE)*UT*C6)
      R15 = ((UE-U1)*PI*P*UT*C5/(S3*S3))
      R16 = (U1*G1*L1) - (U1*L1*B4) - (((UE+U1)/2.0)*(G1*L1-B4*L1)
*)
      R17 = (2.0*U3*(U3-U1)*(1.0-(E**((-K)*G1*G1))))
      R17 = R17 - ((U3-U1)*(U3-U1)*(1.0-(E**((-2.0)*K*G1*G1))))
      R17 = R17 - (U1*(U3-U1)*(1.0-(E**((-K)*G1*G1))))
      R18  = (2.0*U3*L1*B4) - (2.0*(U3-U1)*L1*B3) - (U1*L1*B4)
      R19 = (4.0*K*B1*(U3-U1)*(U3-U1)) - (4.0*K*U3*(U3-U1)*B2)
      R19 = R19 + (2.0*K*U1*(U3-U1)*B2)
      R20 = ((U3-U1)*((A*(S3-LMT1)/L)+(A*C1/L)+(B*(S3-LMT1))+(2.0*
*P*C6)))
      R21 = ((U3-U1)*2.0*UT*C6)
      R22 = ((U1-U3)*2.0*P*UT*PI*C5/(S3*S3))
      R23 = (2.0*U3*G1*L1) + (2.0*(U3-U1)*L1*B3) - (2.0*U3*L1*B4)
      R23 = R23 - (2.0*(U3-U1)*L1*B4) + (U1*L1*B4) - (U1*G1*L1)
      R24 = M21
      R25 = M22
      R26 = M23
      R27 = M24
      R28 = M25
      R29 = M26
      R30 = (B4*L1)
      R31 = ((G1*U3)-(B4*(U3-U1)))
      R32 = (A*S3*(DLOG(S3*UT/NUND))/L) + (B*S3) + (P*S3)
      R32 = R32 - (A*LMT1*(DLOG(LMT1*UT/NUND))/L) - (B*LMT1)
      R32 = R32 - (P*LMT1) + ((P*S3/PI)*(DSIN(PI*LMT1/S3)))
```

```
      R33 = (UT*S3) - (LMT1*UT) + ((UT*S3/PI)*(DSIN(PI*LMT1/S3)))
      R34 = (((DLOG(S3*UT/NUND))*A*UT/L)+(B*UT)+(P*UT))
      R34 = R34 + ((P*UT/PI)*(DSIN(PI*LMT1/S3)))
      R34 = R34 - ((DCOS(PI*LMT1/S3))*P*UT*LMT1/S3)
      R35 = ((G1*L1)-(B4*L1))
      R36 = ((U3/UT)+(A/L))
      R37 = (2.0*UT)
      R38 = (A*UT/(L*S3))
      R39 = -1.0
      R40 = 1.0
      R41 = -G1
      R42 = -1.0
      T1 = TOUGLO - TOUS2 - H1 + ((UE*GO*LO)+(2.0*(UE-U1)*LO*A3)-(
*UE*LO*A4)-(2.0*(UE-U1)*LO*A4))*((S2+(GO*LO))*E2+E4)*(1.0/(2.0*UE))
      T2 = TOULO - TOUS2 - H2 + ((2.0*UE*LO)+(2.0*(UE-U1)*LO*A7)-(
*2.0*UE*LO*A8)-(2.0*(UE-U1)*LO*A8)-((UE+U1)*(LO/2.0)*(1.0-A8)))*((S
*2+(GO*LO))*E2+E4)*(1.0/(2.0*UE))
      T3 = TOUS2 - TOUGL1 - H3
      T4 = TOUS3 - TOUW - H4
      T5 = TOUS3 - TOU2 - H5
      T6 = F
      SQ(1,1) = R1
      SQ(1,2) = R2
      SQ(1,3) = R3
      SQ(1,4) = R4
      SQ(1,5) = R5
      SQ(1,6) = R6
      SQ(1,7) = R7
      SQ(1,8) = R8
      SQ(2,1) = R9
      SQ(2,2) = R10
      SQ(2,3) = R11
      SQ(2,4) = R12
      SQ(2,5) = R13
      SQ(2,6) = R14
      SQ(2,7) = R15
      SQ(2,8) = R16
      SQ(3,1) = R17
      SQ(3,2) = R18
      SQ(3,3) = 0.0
      SQ(3,4) = R19
      SQ(3,5) = R20
      SQ(3,6) = R21
      SQ(3,7) = R22
      SQ(3,8) = R23
      SQ(4,1) = SQ(4,2) = SQ(4,3) = SQ(4,4) = SQ(4,8) = 0.0
      SQ(4,5) = R24
      SQ(4,6) = R25
      SQ(4,7) = R26
      SQ(5,1) = SQ(5,2) = SQ(5,3) = SQ(5,4) = SQ(5,8) = 0.0
      SQ(5,5) = R27
      SQ(5,6) = R28
      SQ(5,7) = R29
      SQ(6,1) = SQ(6,3) = 0.0
      SQ(6,2) = R30
      SQ(6,4) = R31
      SQ(6,5) = R32
      SQ(6,6) = R33
      SQ(6,7) = R34
      SQ(6,8) = R35
      SQ(7,1) = SQ(7,2) = SQ(7,3) = SQ(7,4) = 0.0
      SQ(7,5) = R36
      SQ(7,6) = R37
      SQ(7,7) = R38
```

```
            SQ(7,8) = R39
            SQ(8,2) = SQ(8,3) = SQ(8,5) = SQ(8,6) = SQ(8,8) = 0.0
            SQ(8,1) = R40
            SQ(8,4) = R41
            SQ(8,7) = R42
            SQIN(1,1) = T1
            SQIN(2,1) = T2
            SQIN(3,1) = T3
            SQIN(4,1) = T4
            SQIN(5,1) = T5
            SQIN(6,1) = T6
            SQIN(7,1) = SQIN(8,1) = 0.0
            CALL LEQT2F(SQ,COL,RO,IA1,SQIN,IDGT,WKAREA,IER)
            DS2DX = SQIN(1,1)
            DU1DX = SQIN(2,1)
            DLODX = SQIN(3,1)
            DL1DX = SQIN(4,1)
            DUTDX = SQIN(5,1)
            DPDX = SQIN(6,1)
            DS3DX = SQIN(7,1)
            DU3DX = SQIN(8,1)
            S2 = S2 + (DS2DX*DX)
            U1 = U1 + (DU1DX*DX)
            LO = LO + (DLODX*DX)
            L1 = L1 + (DL1DX*DX)
            UT = UT + (DUTDX*DX)
            P = P + (DPDX*DX)
            S = S3 = S3 + (DS3DX*DX)
            U3 = U3 + (DU3DX*DX)
            CFIF = (2.0*UT*UT)
            L2 = (S2-(G1*L1)-S3)
            UO = UI = U3
            X = X + DX
            Y = (S2+(GO*LO))
            UE = CP(X,Y,D1,D2,D3,D4,D5,D6,D7,D8)
         END   IF
         E1 = ((D1*X*X*X)+(D2*X*X)+(D3*X)+D4)
         E3 = ((D5*X*X*X)+(D6*X*X)+(D7*X)+D8)
         E2 = ((3.0*D1*X*X)+(2.0*D2*X)+D3)
         E4 = ((3.0*D5*X*X)+(2.0*D6*X)+D7)
         S1B = S*(UT/UI)*((A/L)+P)
         THETB = ((2.0*(A/L)*(A/L))+(3.18*A*P/L)+(1.5*P*P))*S*(UT/UI)
         THETB = (THETB)*(UT/UI)
         THETB = S1B - THETB
         HB = S1B/THETB
         S1IW = (1.0-(U1/UO))*(L1)*(1.0610)
         HIW = (1.0/(1.0-((0.7526/1.0610)*(1.0-(U1/UO)))))
         THETIW = S1IW/HIW
         S1OW = (1.0-(U1/UE))*LO*1.0633
         HOW = (1.0/(1.0-((0.7527/1.0633)*(1.0-(U1/UE)))))
         THETOW = S1OW/HOW
         PRINT 210
         PRINT 220,X,S,P,S1B,THETB,HB,S1IW,THETIW,HIW,S1OW,THETOW,HOW,UE
     *-U1
         PRINT 240
         PRINT 250,L1,LO,U1,UE,UO,UI,U3,L2,S2,UT,U3-U1,CFIF
         PRINT 260
      END   WHILE
      STOP
200   FORMAT ('1','**********************************************************
     ************************************************************************
     *************',/,' ','*************************************************
     ************************',/,' ',58X,'STARTING   VALUES')
```

```
 230  FORMAT ('0','**********************************************************
     ************************************************************************
     **************','/',' ','**********************************************
     ************************************************************************
     ************************')
 210  FORMAT ('0','FLAPDIS',3X,'SOFBL',3X,'POFBL',2X,'S*OFBL',3X,'THTOFB
     *L',2X,'HOFBL',3X,'S* OF IW',5X,'THT OF IW',4X,'H OF IW',4X,'S* OF
     *OW',4X,'THT OF OW',4X,'H OF OW',3X,'(UE-U1)')
 240  FORMAT ('0',3X,'L1',9X,'LO',9X,'U1',9X,'UE',9X,'UO',9X,'UI',9X,'U3
     *',10X,'L2',10X,'S2',11X,'UT',6X,'(U3-U1)',4X,'CFIF')
 220  FORMAT ('0',1X,F5.3,3X,F7.5,1X,F7.3,1X,F8.5,1X,F8.5,1X,F6.3,3X,F9
     *.7,3X,F10.7,3X,F6.3,5X,F9.7,3X,F10.7,4X,F6.3,4X,F7.5)
 250  FORMAT ('0',F8.6,6(3X,F8.6),3X,F9.6,3X,F9.7,3X,F9.6,3X,F8.5,3X,F8.
     *6)
 260  FORMAT (' ','**********************************************************
     ************************************************************************
     **************')
      END
C     ******************************************************************
C     ******************************************************************
      DOUBLE PRECISION FUNCTION B11(UT,NUND,LMT1,LMT2,S)
      DOUBLE PRECISION UT,NUND,LT1,LT2,DY,PI,DLOG,DSIN,S,D,F,G,LMT1,LMT2
     *,DY1
      INTEGER N
      LT1 = LMT1
      LT2 = LMT2
      PI = 3.141593
      DY1 = ((LT2-LT1)/400.0)
      DY = (DY1/2.0)
      B11 = 0.0
      DO 10 N = 1,400
         D = (DSIN(PI*LT1/(2.0*S)))*(DSIN(PI*LT1/(2.0*S)))*(DLOG(LT1*UT/
     *NUND))
         F = (DSIN(PI*(LT1+DY1)/(2.0*S)))*(DSIN(PI*(LT1+DY1)/(2.0*S)))*(
     *DLOG((LT1+DY1)*UT/NUND))
         G = (DSIN(PI*((LT1+LT1+DY1)/2.0)/(2.0*S)))*(DSIN(PI*((LT1+LT1+D
     *Y1)/2.0)/(2.0*S)))*(DLOG(((LT1+LT1+DY1)/2.0)*UT/NUND))
         B11 = B11 + ((DY/3.0)*(D+(4.0*G)+F))
         LT1 = LT1 + DY1
10    CONTINUE
      RETURN
      END
C     ******************************************************************
C     ******************************************************************
      DOUBLE PRECISION FUNCTION B22(UT,NUND,LMT1,LMT2,S)
      DOUBLE PRECISION UT,NUND,LT1,LT2,PI,DY,DLOG,DSIN,DCOS,S,D,F,G,LMT1
     *,LMT2,DY1
      INTEGER N
      LT1 = LMT1
      LT2 = LMT2
      PI = 3.141593
      DY1 = ((LT2-LT1)/400.0)
      DY = (DY1/2.0)
      B22 = 0.0
      DO 10 N = 1,400
         D = (LT1)*(DSIN(PI*LT1/(2.0*S)))*(DCOS(PI*LT1/(2.0*S)))*(DLOG(L
     *T1*UT/NUND))
         F = (LT1+DY1)*(DSIN(PI*(LT1+DY1)/(2.0*S)))*(DCOS(PI*(LT1+DY1)/(
     *2.0*S)))*(DLOG((LT1+DY1)*UT/NUND))
         G = ((LT1+LT1+DY1)/2.0)*(DSIN(PI*((LT1+LT1+DY1)/2.0)/(2.0*S)))*
     *(DCOS(PI*((LT1+LT1+DY1)/2.0)/(2.0*S)))*(DLOG(((LT1+LT1+DY1)/2.0)*U
     *T/NUND))
         B22 = B22 + ((DY/3.0)*(D+(4.0*G)+F))
         LT1 = LT1 + DY1
```

```
10    CONTINUE
      RETURN
      END
C     ***********************************************************************
C     ***********************************************************************
      DOUBLE PRECISION FUNCTION DCPDX(X,LMT1,LMT2,D1,D2,D3,D5,D6,D7)
      DOUBLE PRECISION X,LT1,LT2,D1,D2,D3,D5,D6,D7,LMT1,LMT2
      LT1 = LMT1
      LT2 = LMT2
      DCPDX = ((3.0*D1*X*X)+(2.0*D2*X)+(D3))*((LT2*LT2/2.0)-(LT1*LT1/2.0
     *))
      DCPDX = DCPDX + ((3.0*D5*X*X)+(2.0*D6*X)+(D7))*(LT2-LT1)
      RETURN
      END
C     ***********************************************************************
C     ***********************************************************************
      DOUBLE PRECISION FUNCTION CP(X,Y,D1,D2,D3,D4,D5,D6,D7,D8)
      DOUBLE PRECISION X,Y,D1,D2,D3,D4,D5,D6,D7,D8
      CP = ((D1*X*X*X)+(D2*X*X)+(D3*X)+(D4))*Y
      CP = CP + ((D5*X*X*X)+(D6*X*X)+(D7*X)+(D8))
      CP = ((1.0-CP)**0.5)
      RETURN
      END
C     ***********************************************************************
C     ***********************************************************************
$ENTRY
```

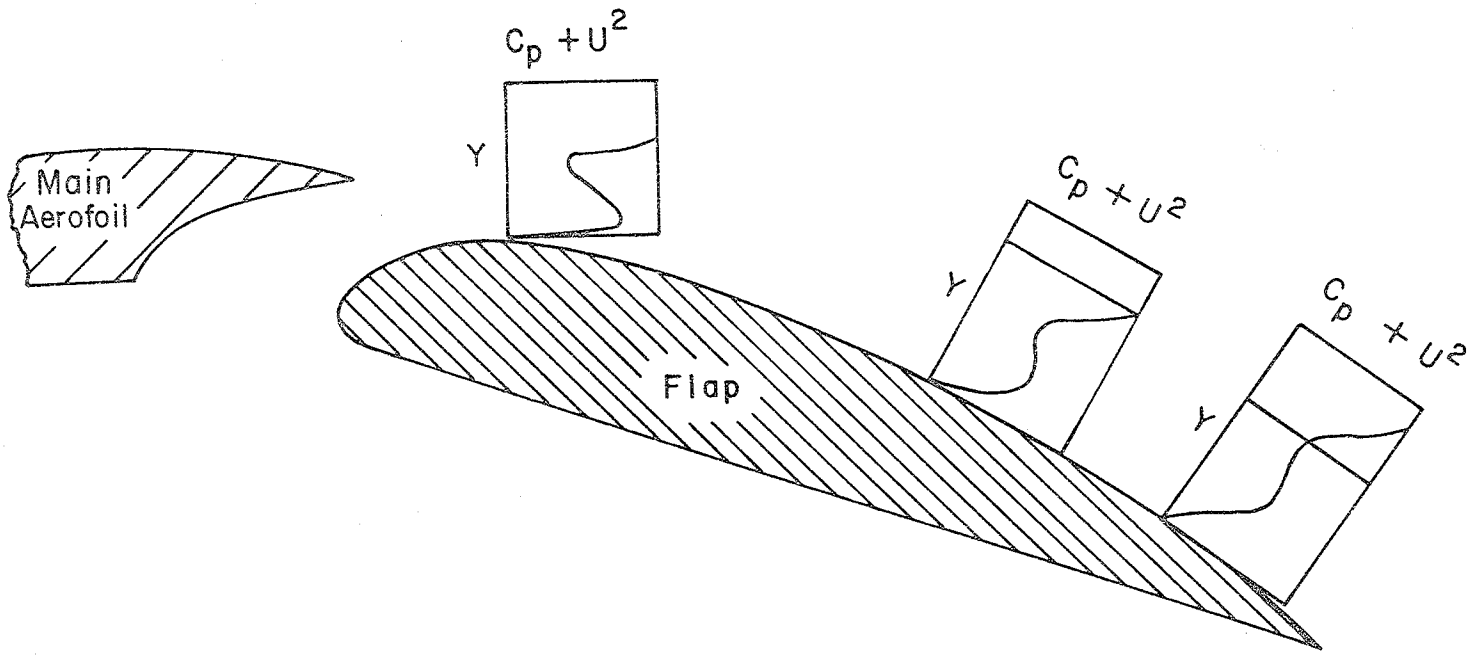

Fig. 1 Typical Measured Total Head Profiles on a slotted Flap.

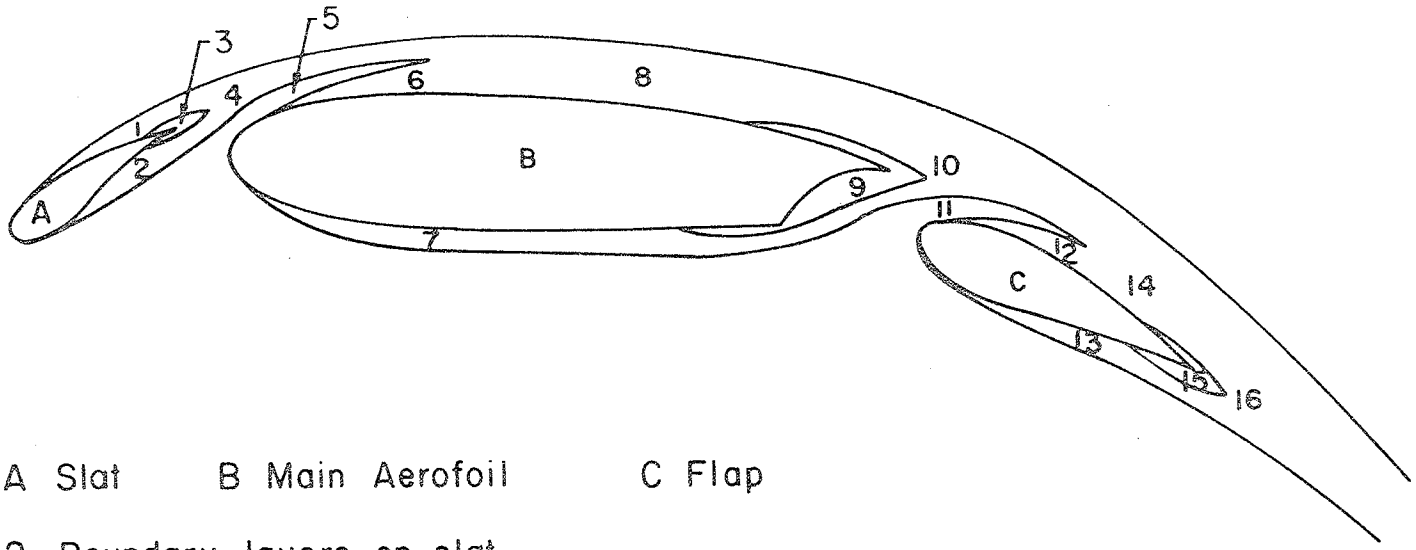

A Slat B Main Aerofoil C Flap

1,2 Boundary layers on slat
3 Separated region of slat
4 Near wake region of slat
5 Potential core
6,7 Boundary layers on main aerofoil
8 Shear layer on main aerofoil
9 Separated region of main aerofoil
10 Near wake region of main aerofoil
11 Potential core
12,13 Boundary layers on flap
14 Shear layer on flap
15 Separated region of flap
16 Near wake region of flap

Fig. 2 Typical Flow Development on Three Element Aerofoil

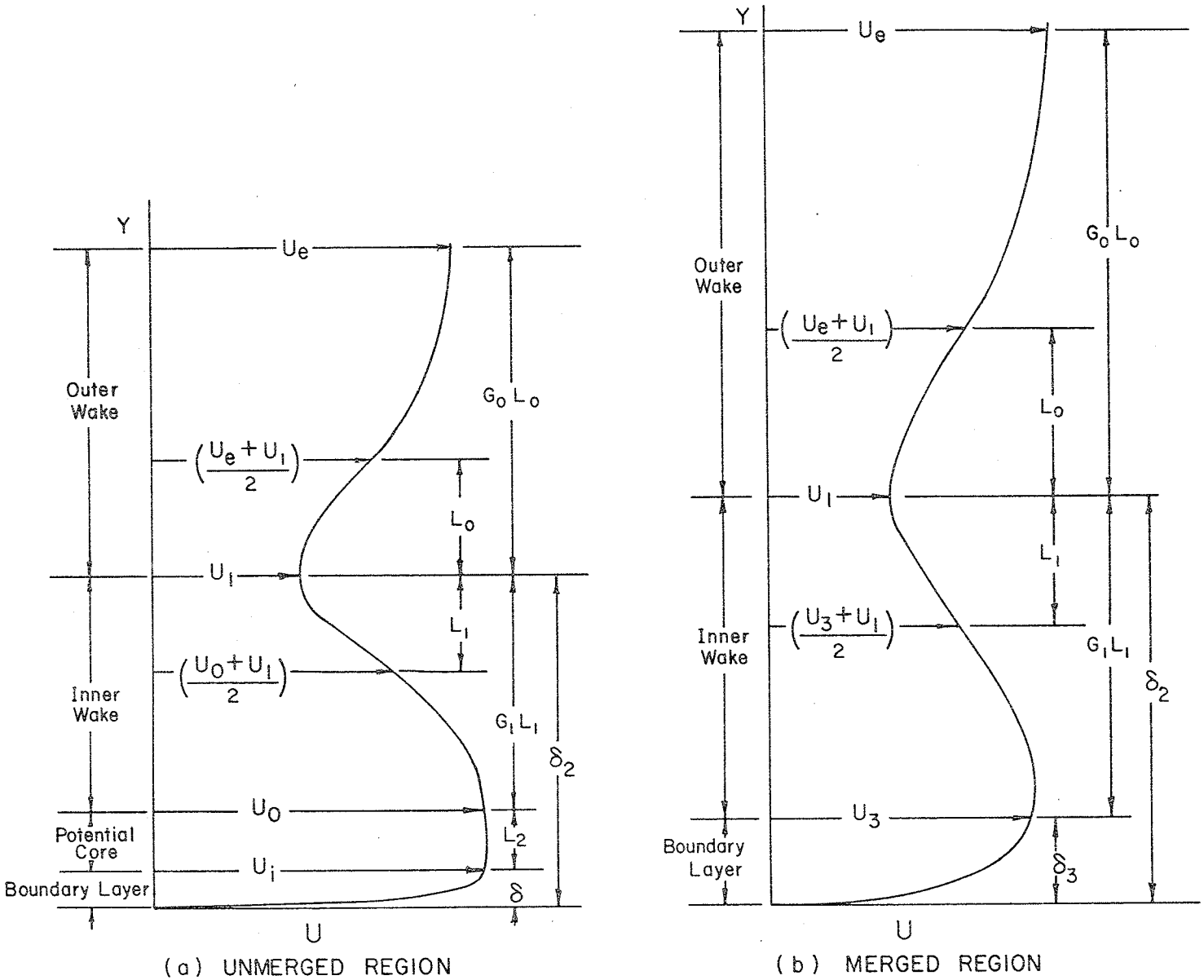

Fig. 3 Typical Velocity Profiles on a slotted Flap , with Notation .

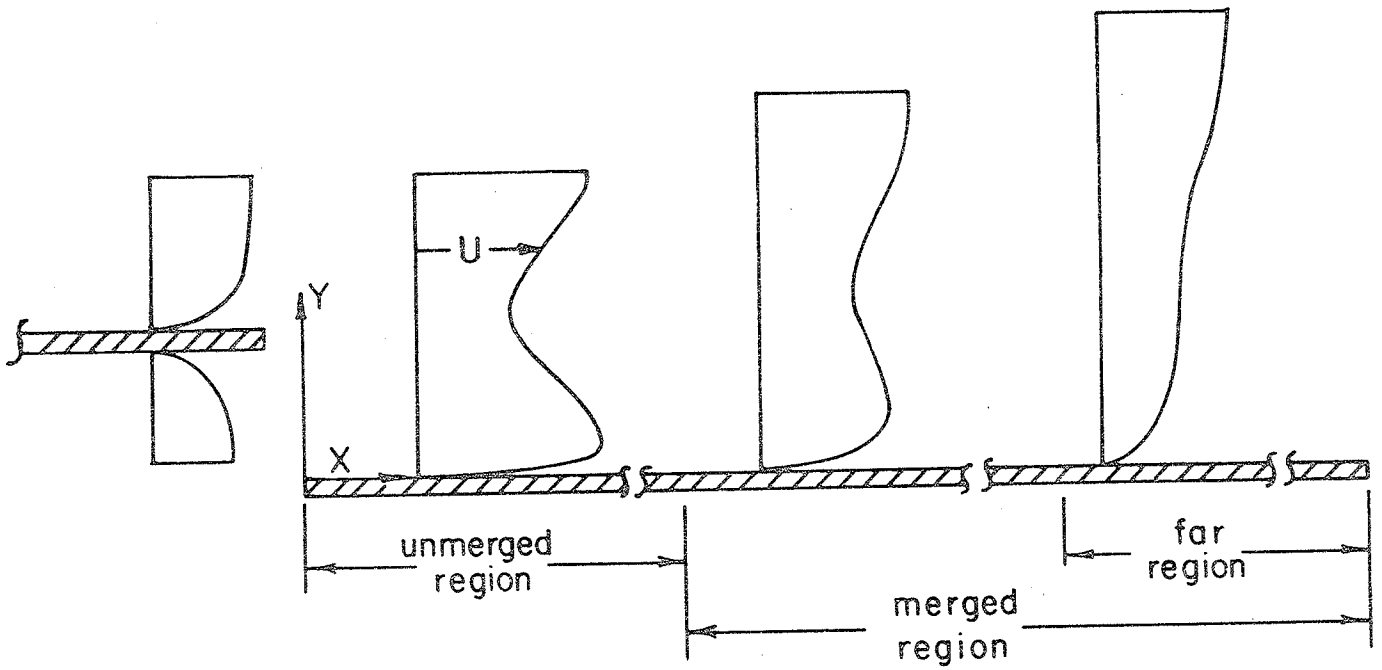

Fig. 4 Simplified Model of the Merging of a Wake with a Boundary Layer .

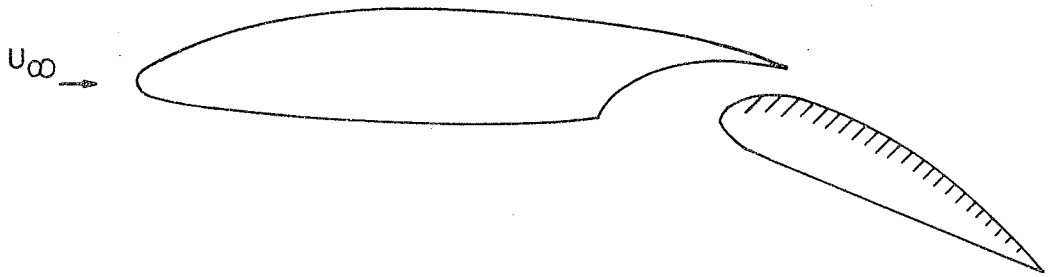

Test Case 1. : Foster , Irwin and Williams (4) Slot Gap 0.025C

Test Case 2. : Foster , Irwin and Williams (4) Slot Gap 0.020 C

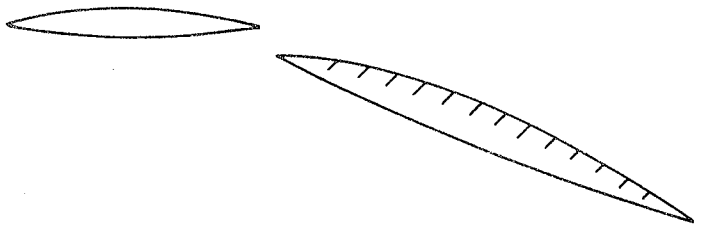

Test Case 3 . : Bario Et Al (6)

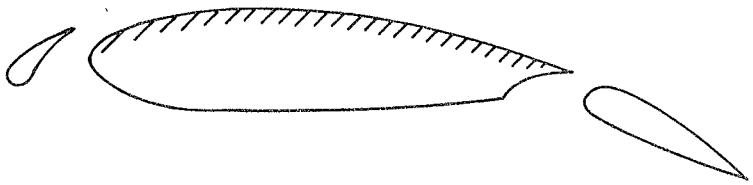

Test Case 4 . : Ljungstrom (5)

Fig. 5. Aerofoil Configurations used for the Test Cases.
(Interaction over the hatched element has been analyzed)

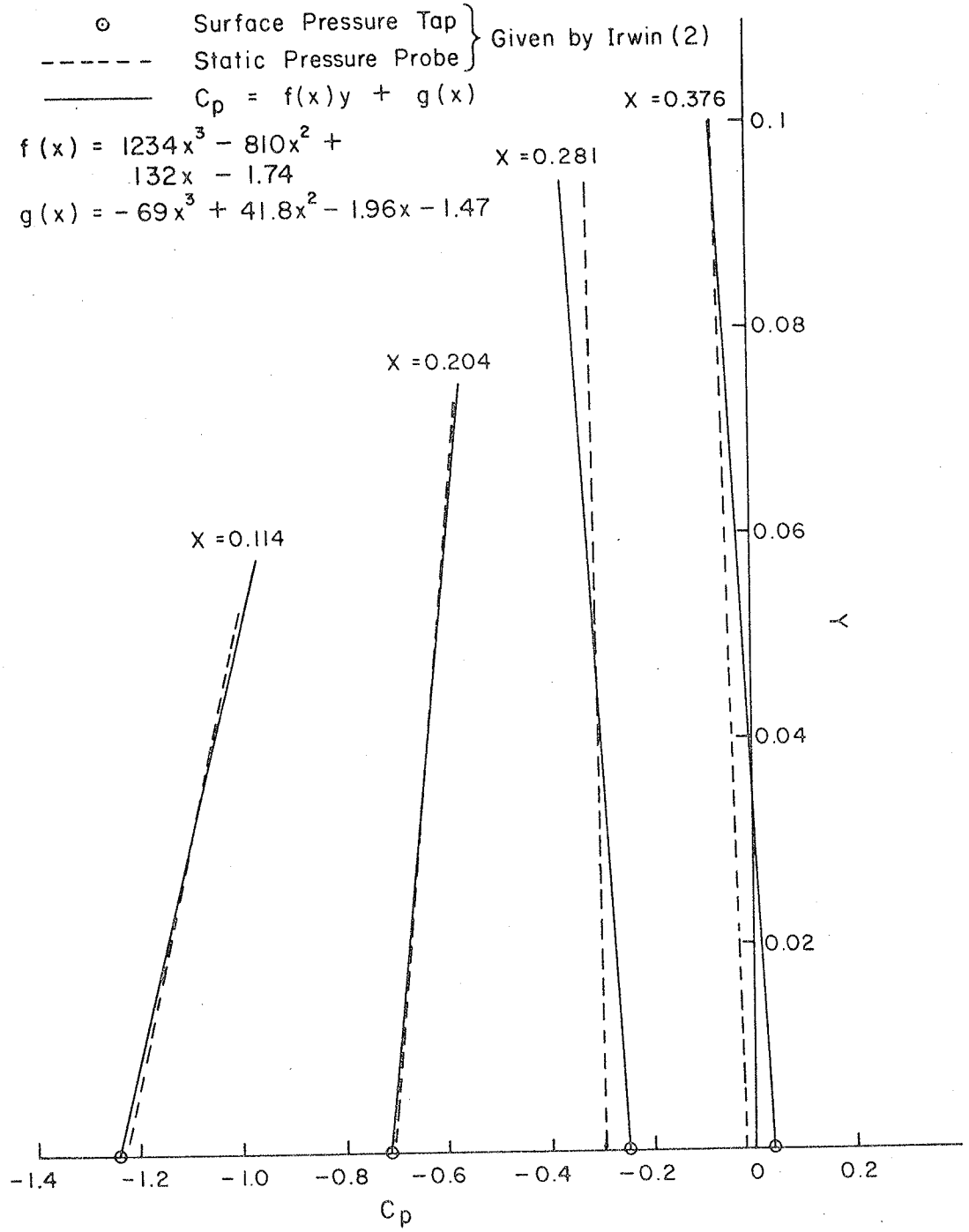

Fig. 6 Pressure Field over the Flap.
Test Case I : Experimental Measurements reported by Foster , Irwin and Williams.
Flap Deflections 30° , Slot Gap 0.025C , α = 8°

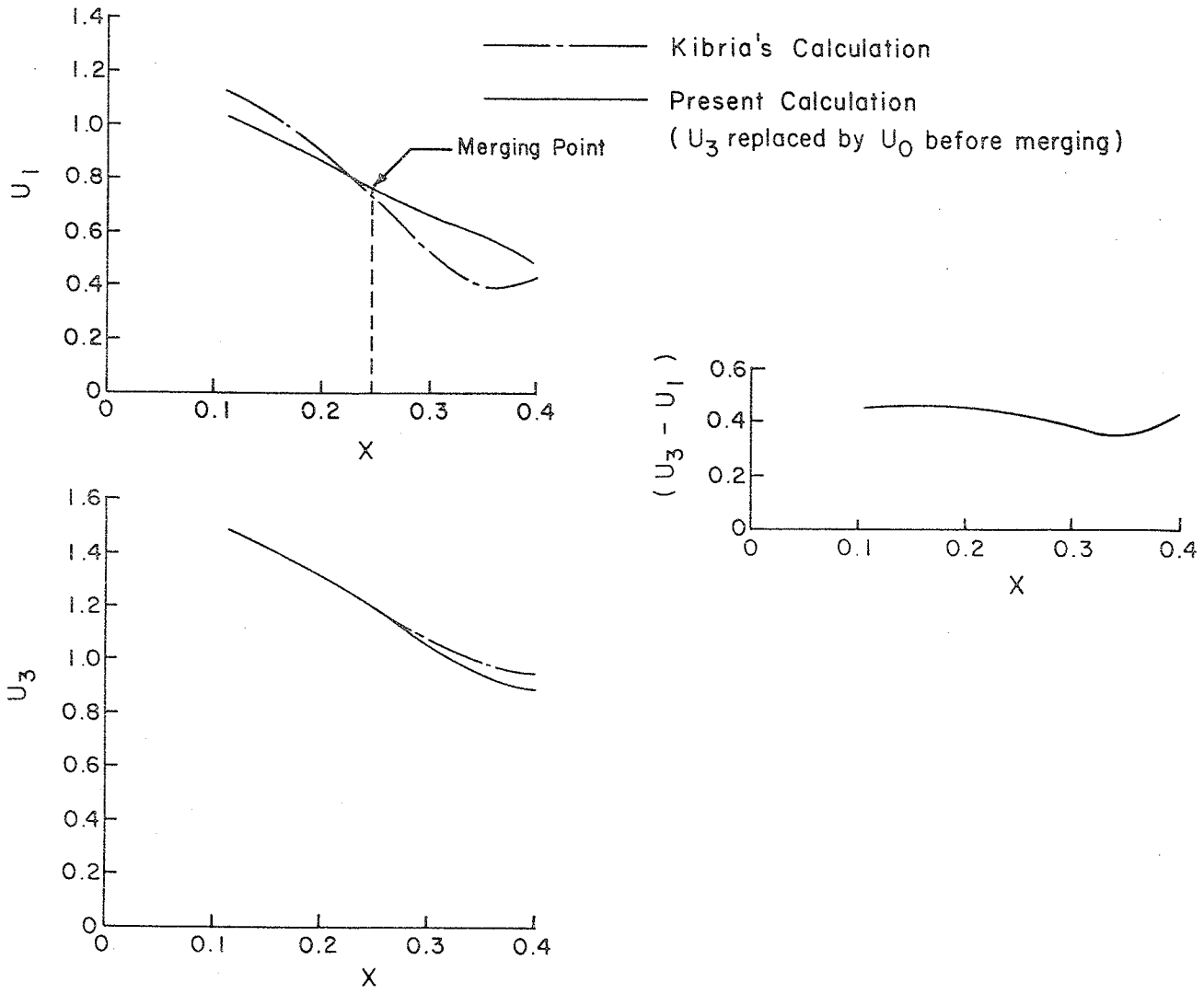

Fig. 7 Development of U_1, U_3 and $(U_3 - U_1)$ along the Flap. (Test Case I.)

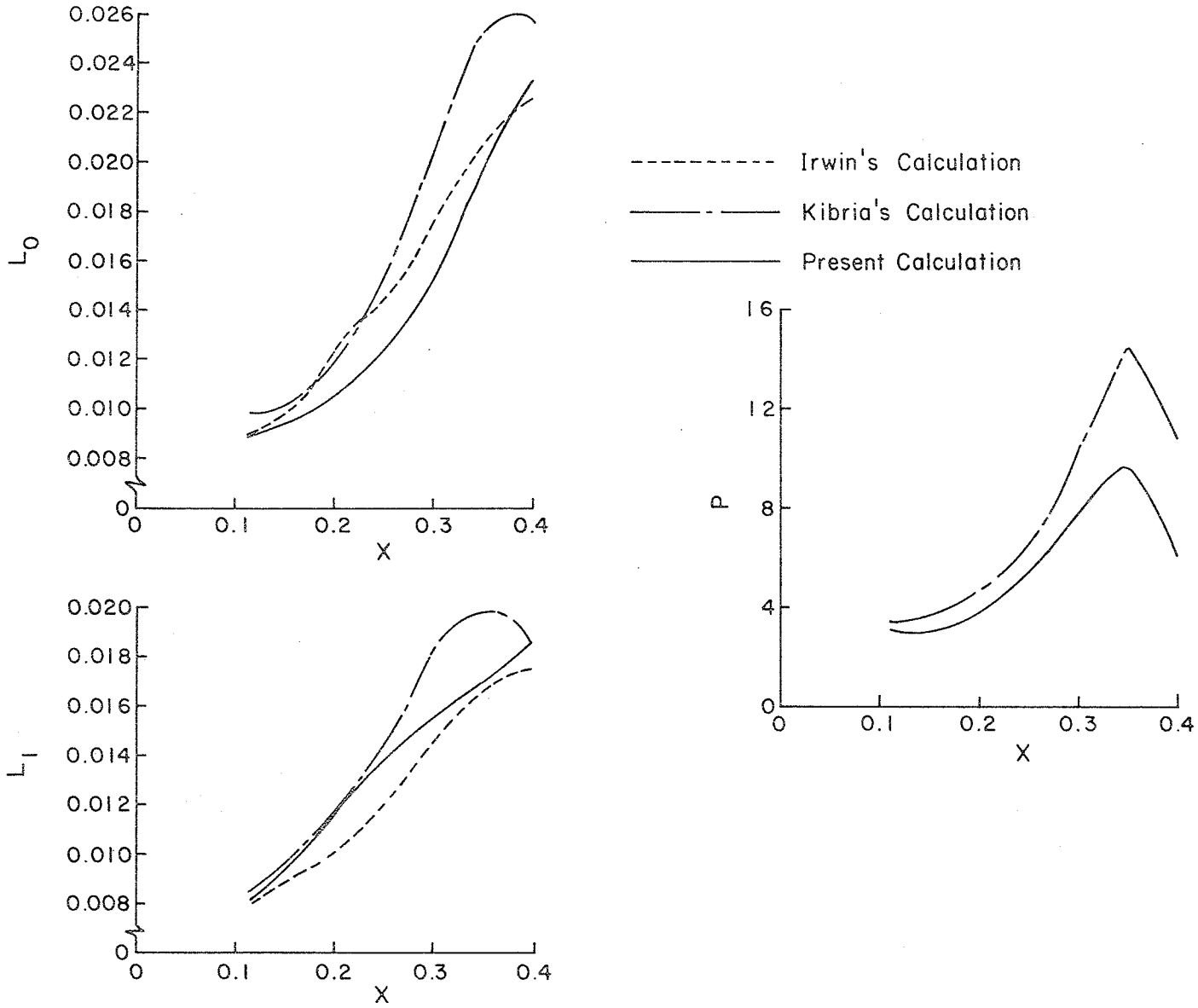

Fig. 8 Development of L_1 , L_o and P along the Flap. (Test Case I.)

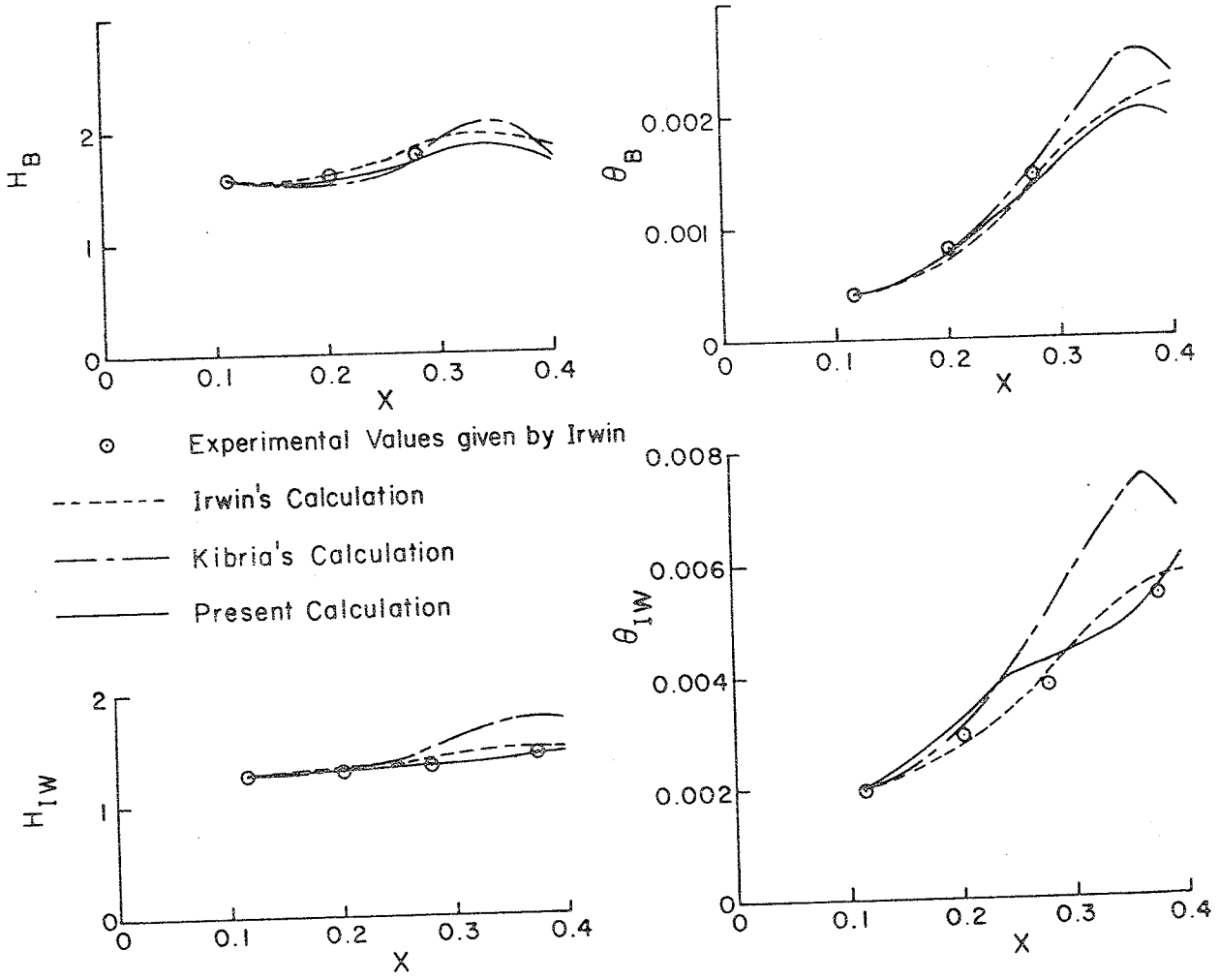

Fig. 9 Development of H_B, θ_B, H_{IW} and θ_{IW} along the Flap. (Test Case I.)

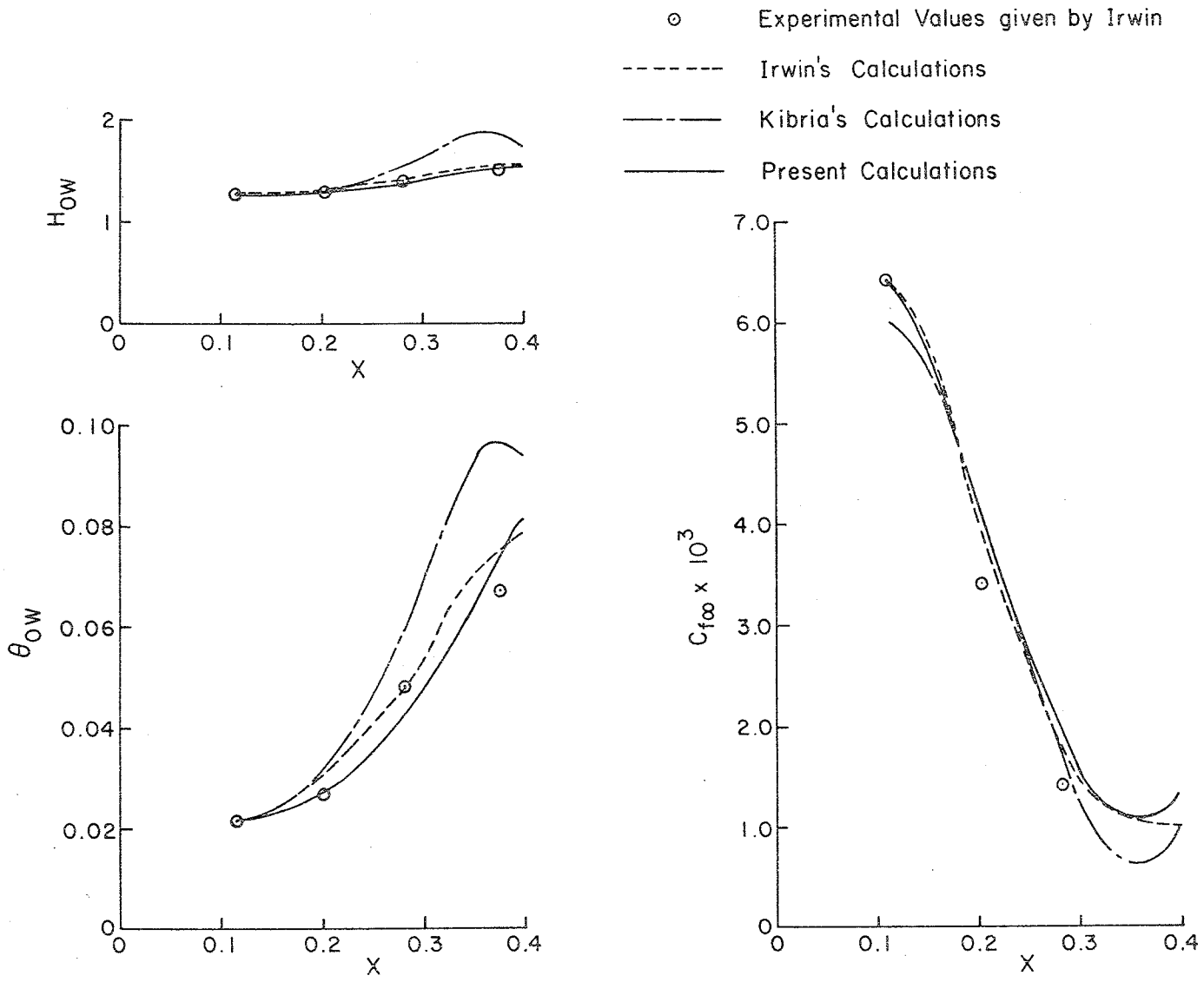

Fig. 10 Development of H_{OW}, θ_{OW} and $C_{f\infty}$ along the Flap. (Test Case I.)

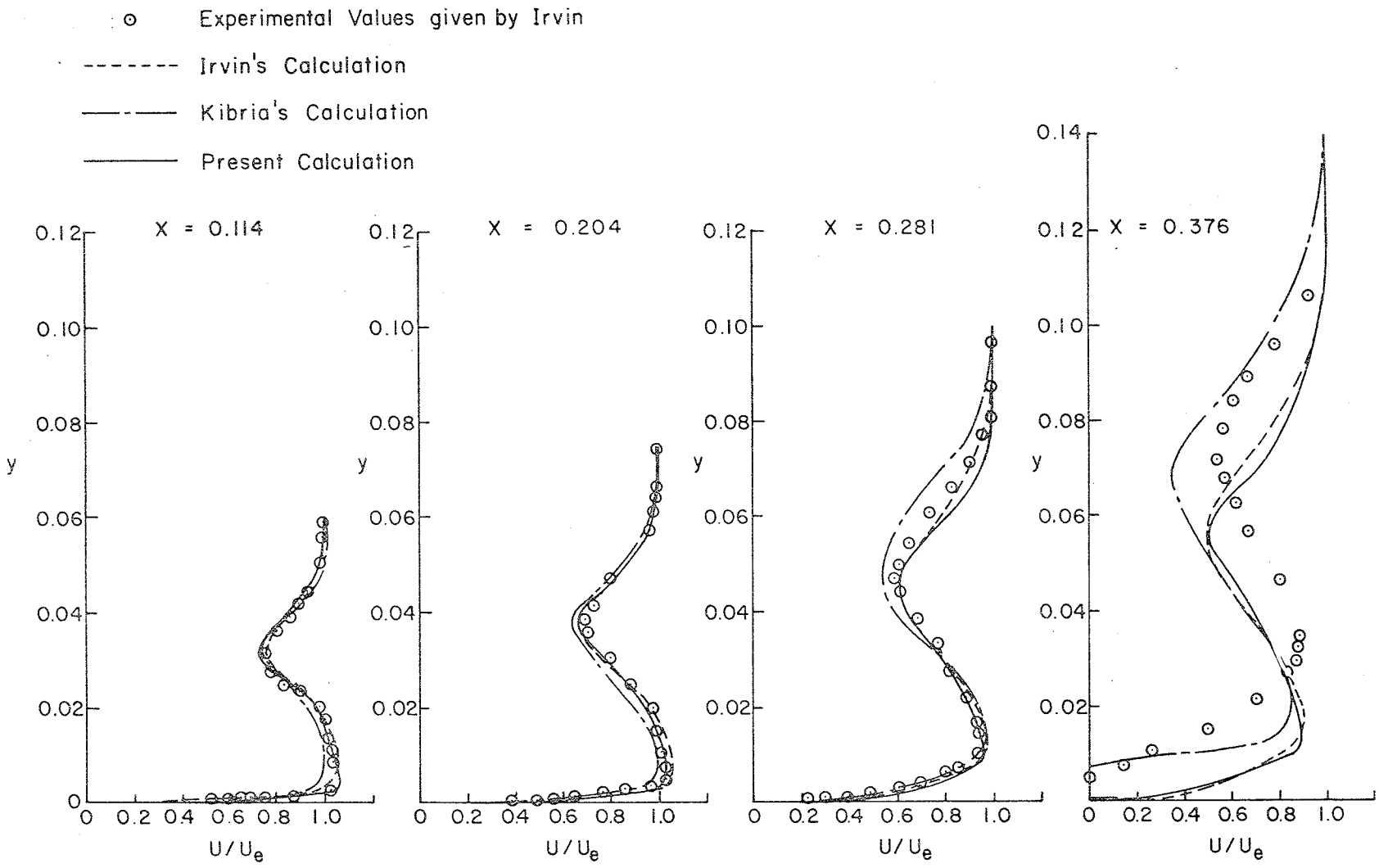

Fig. 11 Development of the Velocity Profiles along the Flap. (Test Case I.)

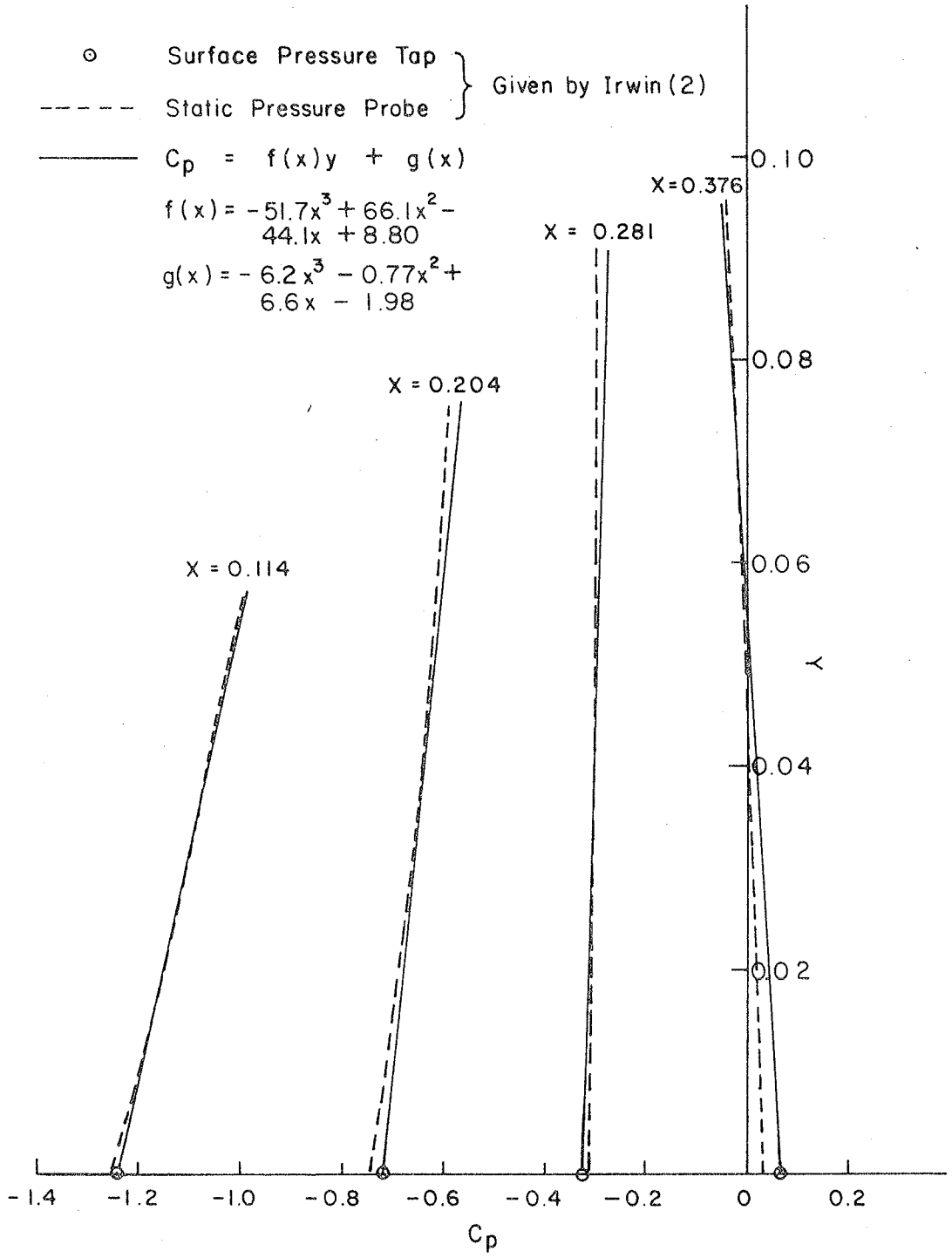

Fig. 12 Pressure Field over the Flap.
Test Case 2 : Experimental Measurements reported by Foster, Irwin and Williams.
Flap Deflection 30°, Slot Gap 0.020C, α = 8°

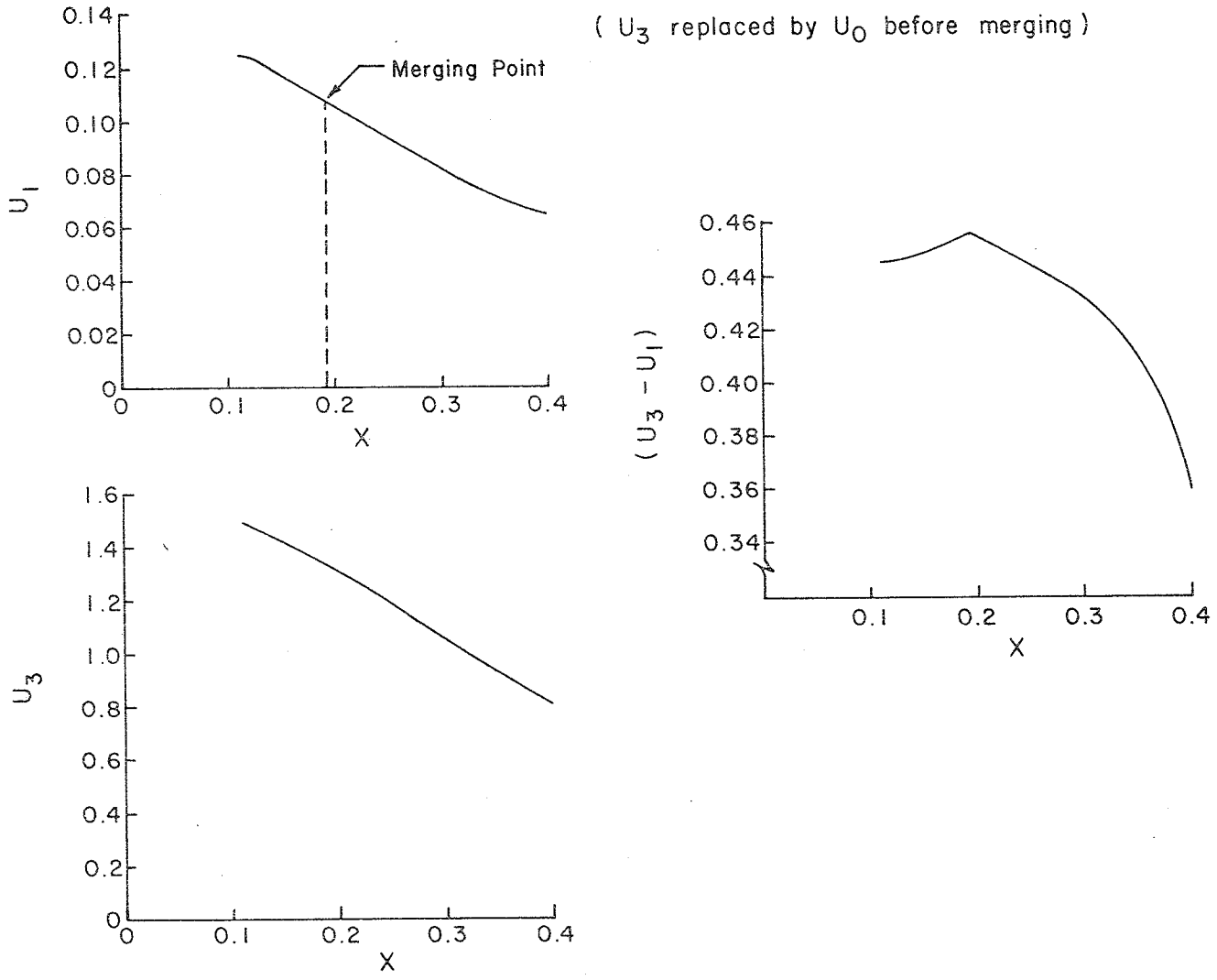

Fig. 13 Development of U_1, U_3 and $(U_3 - U_1)$ along the Flap. (Test Case 2.)

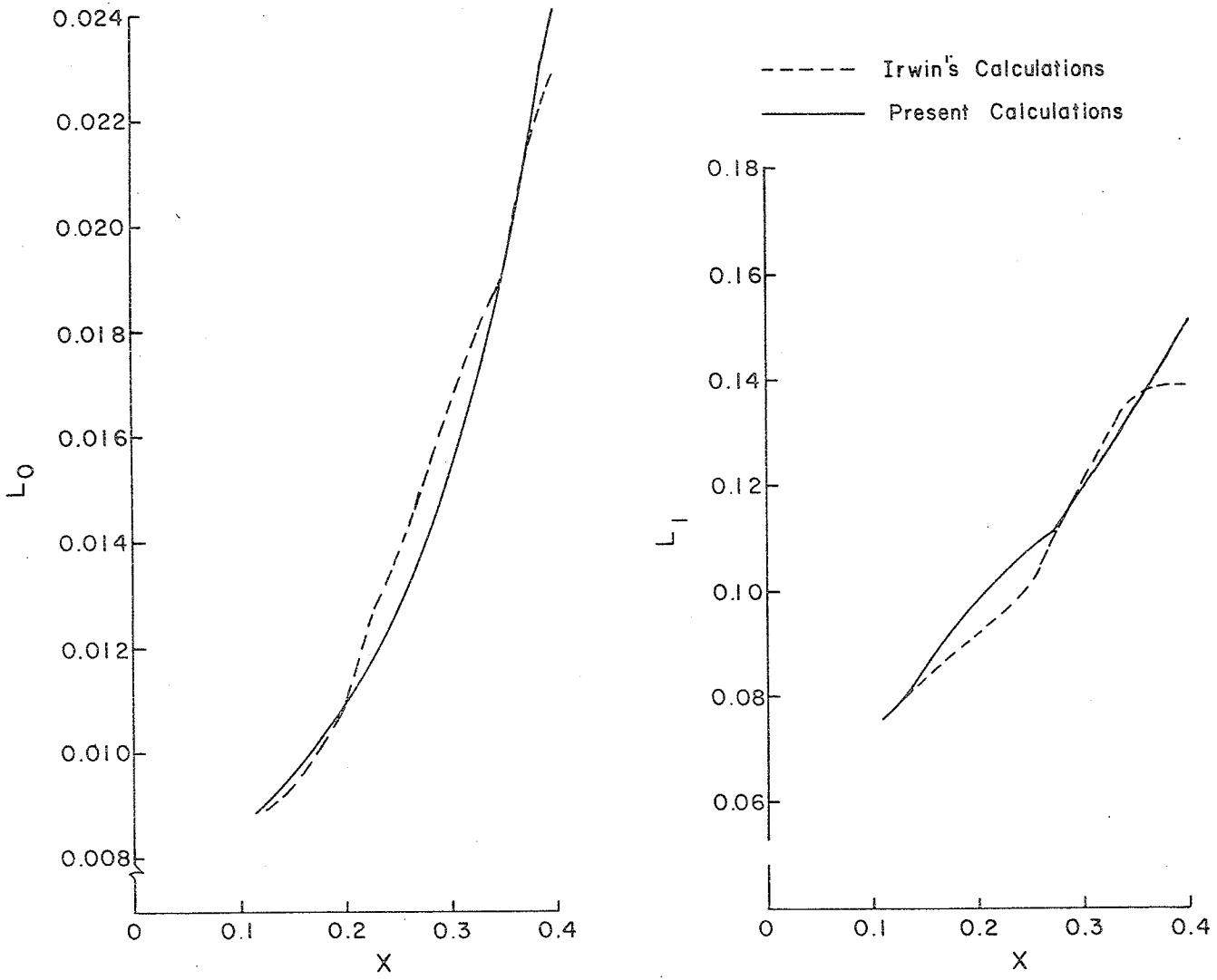

Fig. 14 Development of L_1 and L_0 along the Flap. (Test Case 2.)

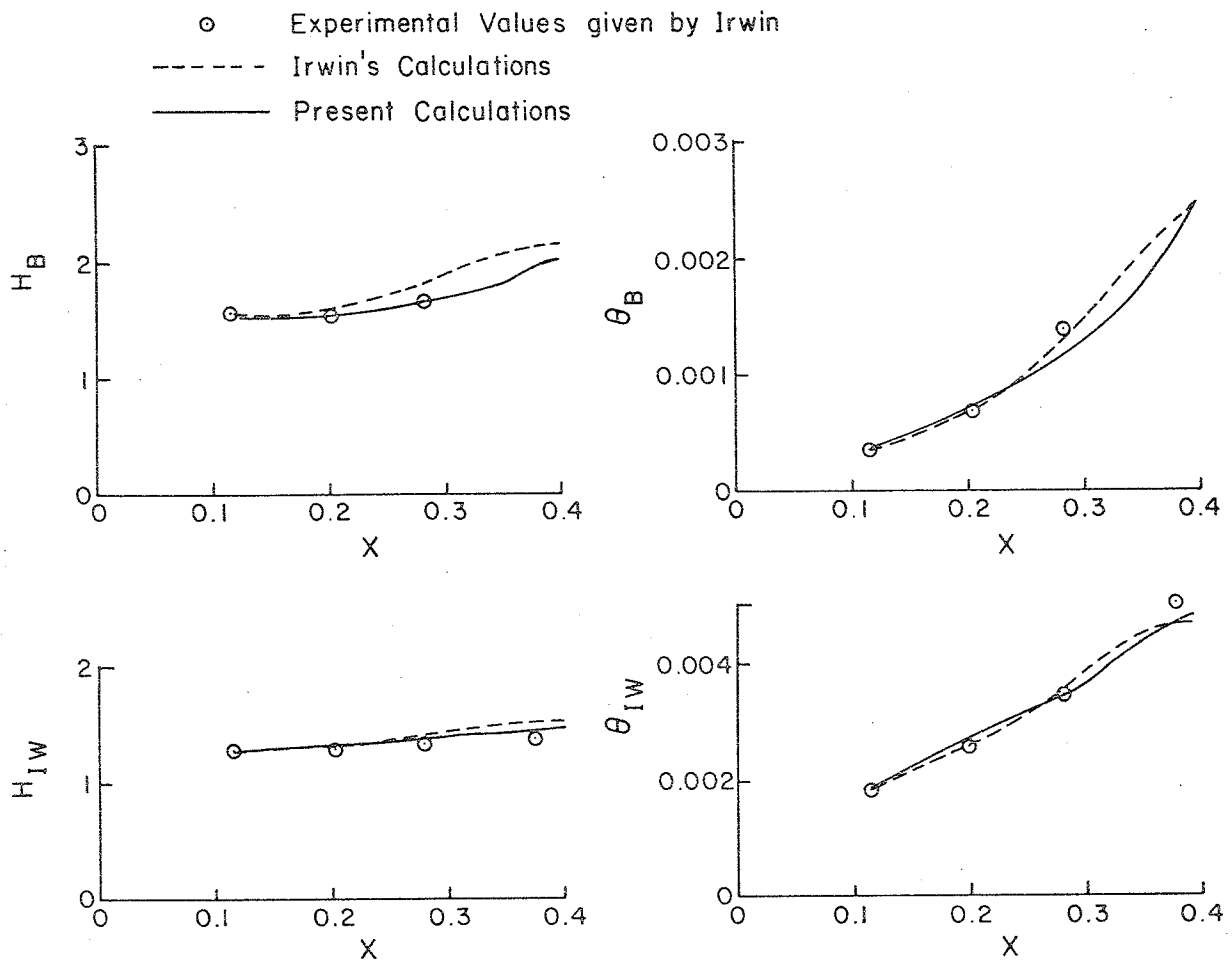

Fig. 15 Development of H_B, θ_B, H_{IW} and θ_{IW} along the Flap. (Test Case 2.)

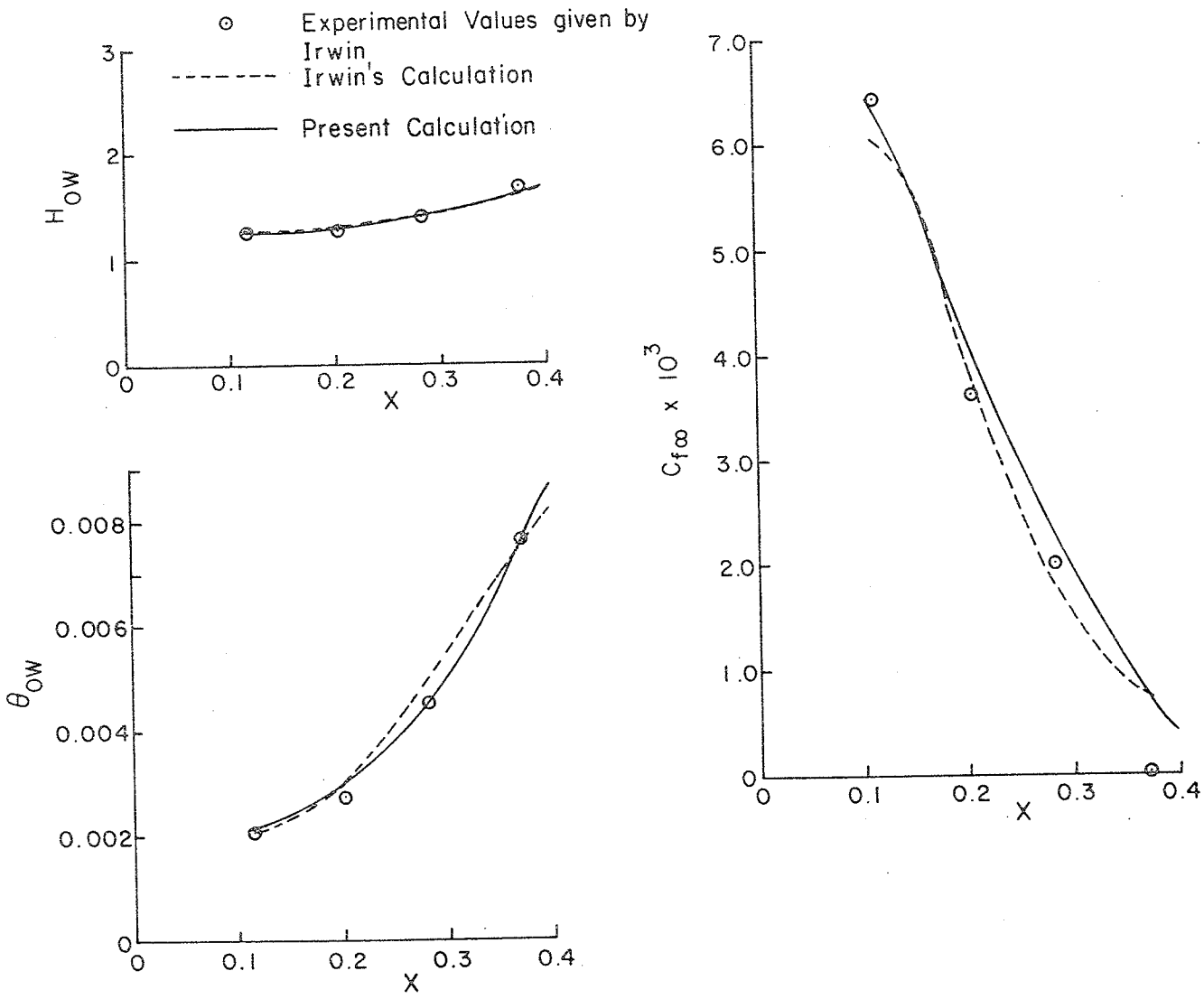

Fig. 16 Development of H_{OW}, θ_{OW} and $C_{f\infty}$ along the Flap. (Test Case 2 .)

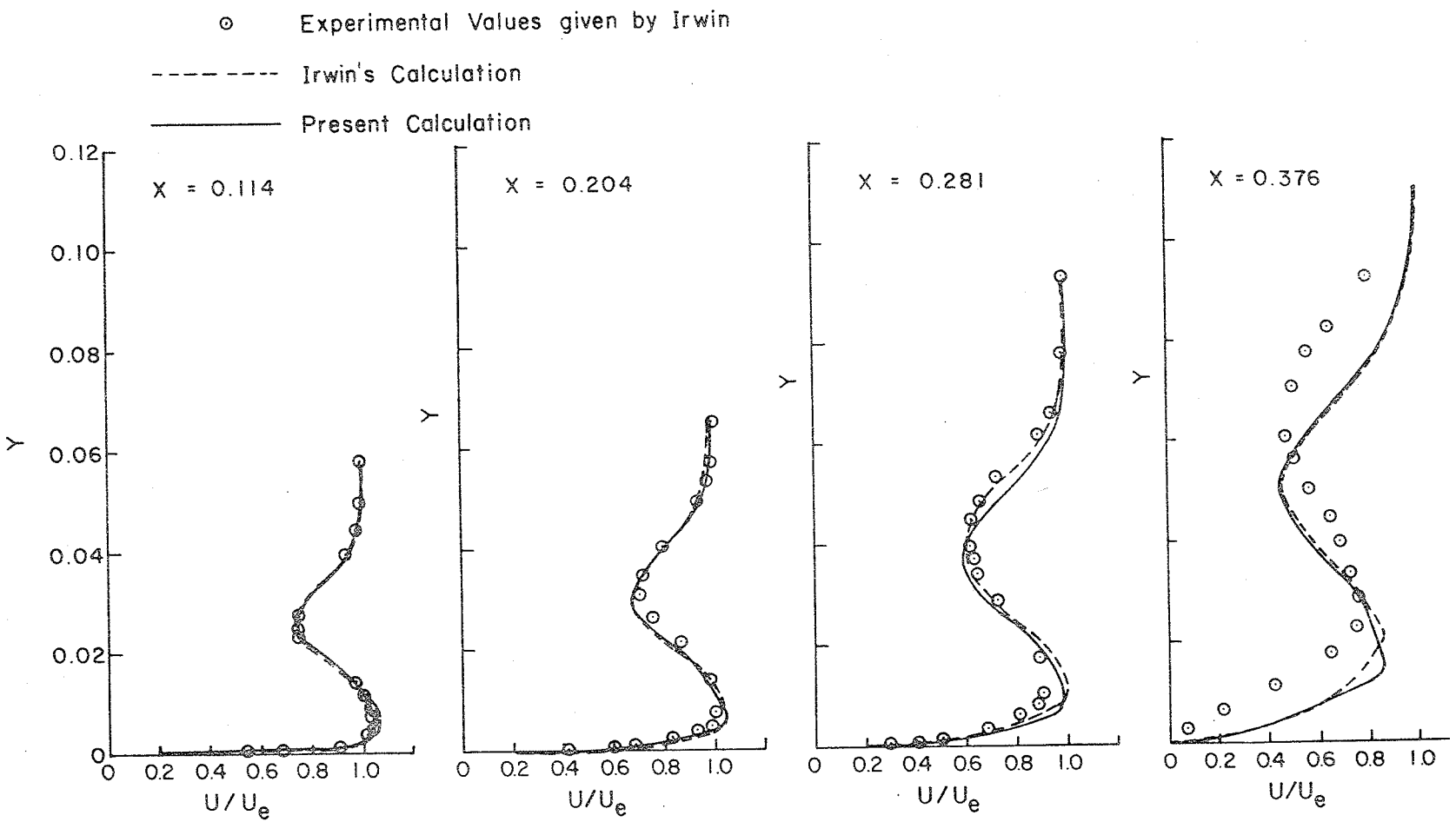

Fig. 17 Development of the Velocity Profiles along the Flap. (Test Case 2 .)

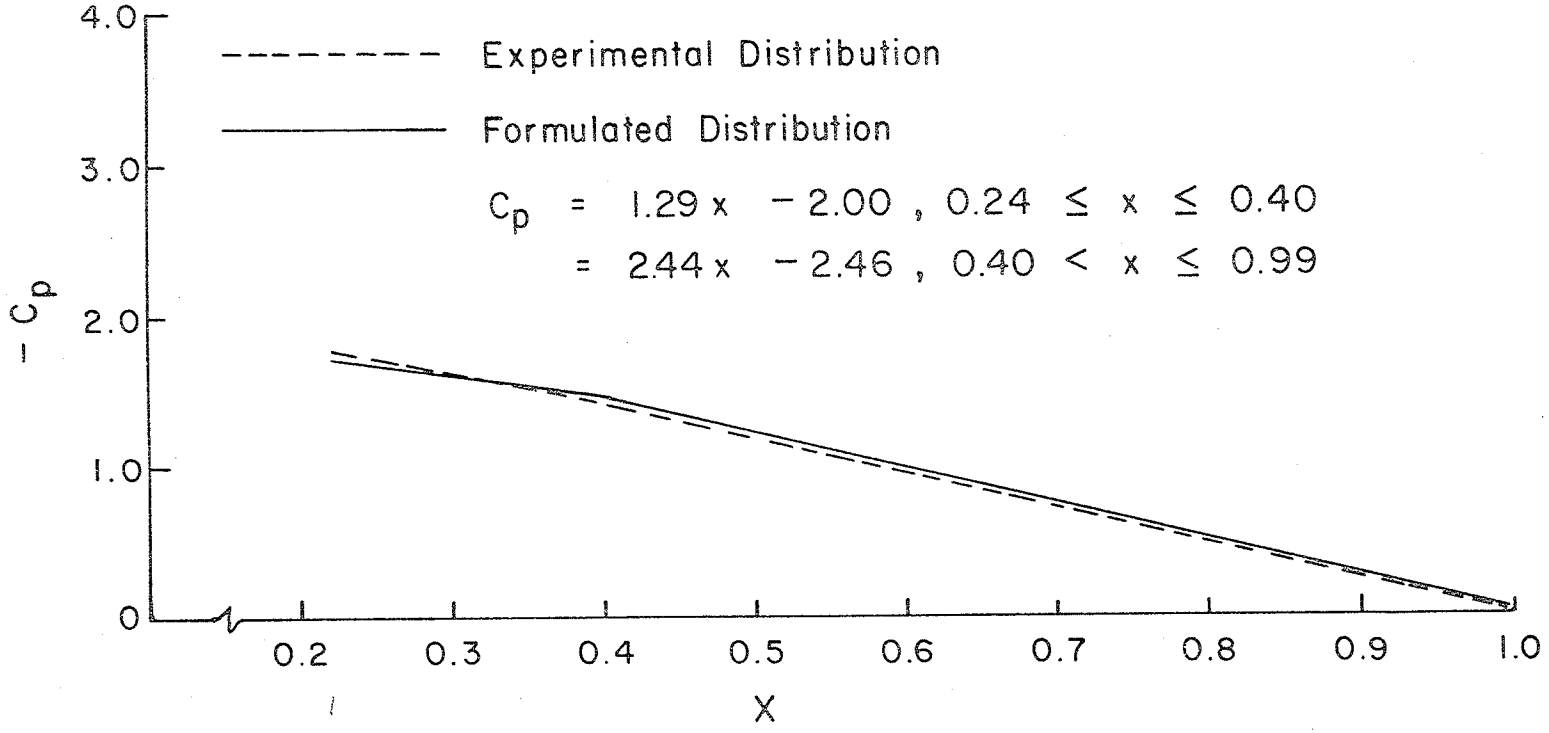

Fig. 18 Pressure Field over the Aerofoil
Test Case 3 : Experimental Measurements reported by Bario Et Al
Aerofoil Deflection 7°

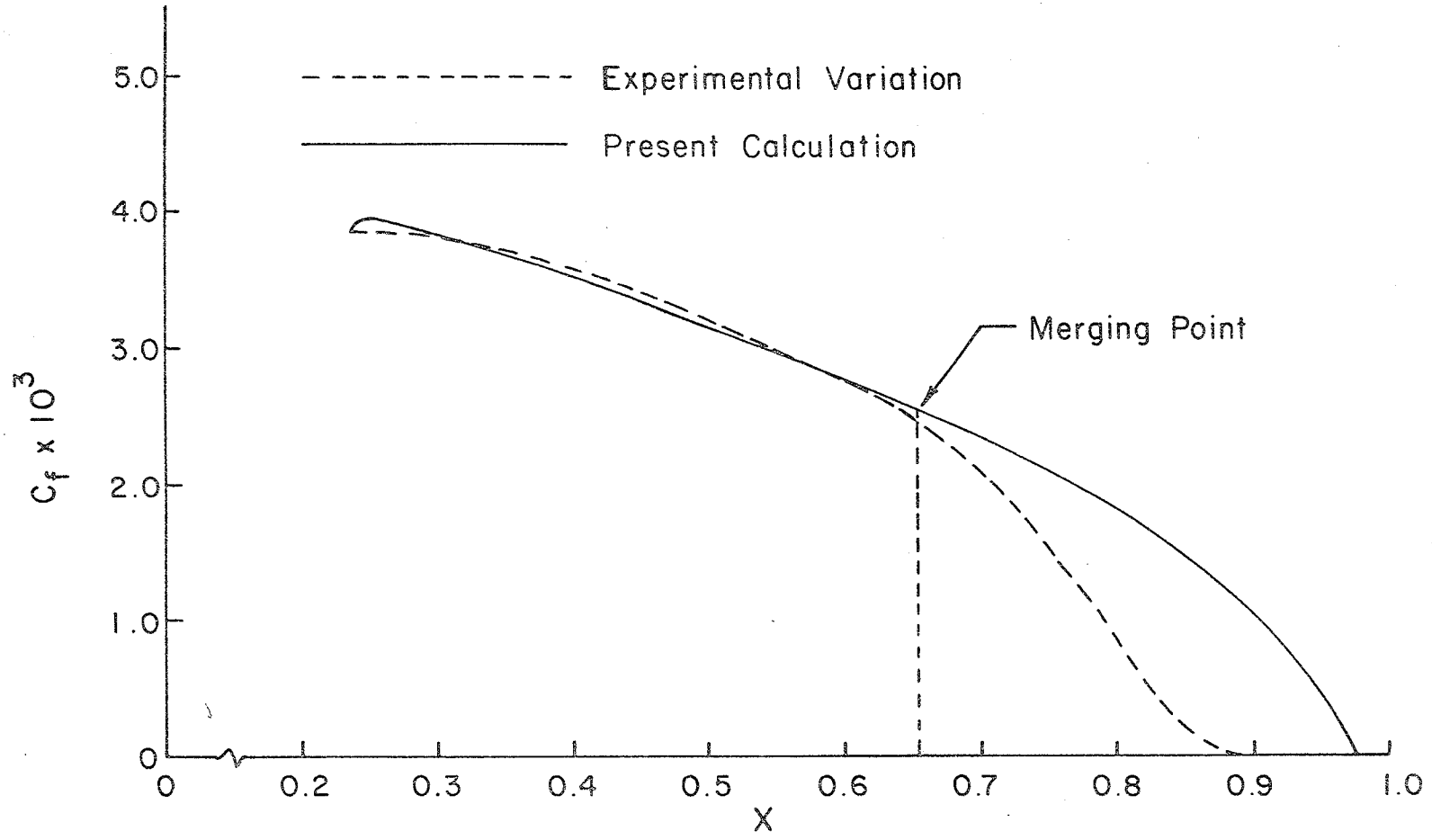

Fig. 19 Development of C_f along the Aerofoil (Test Case 3.)

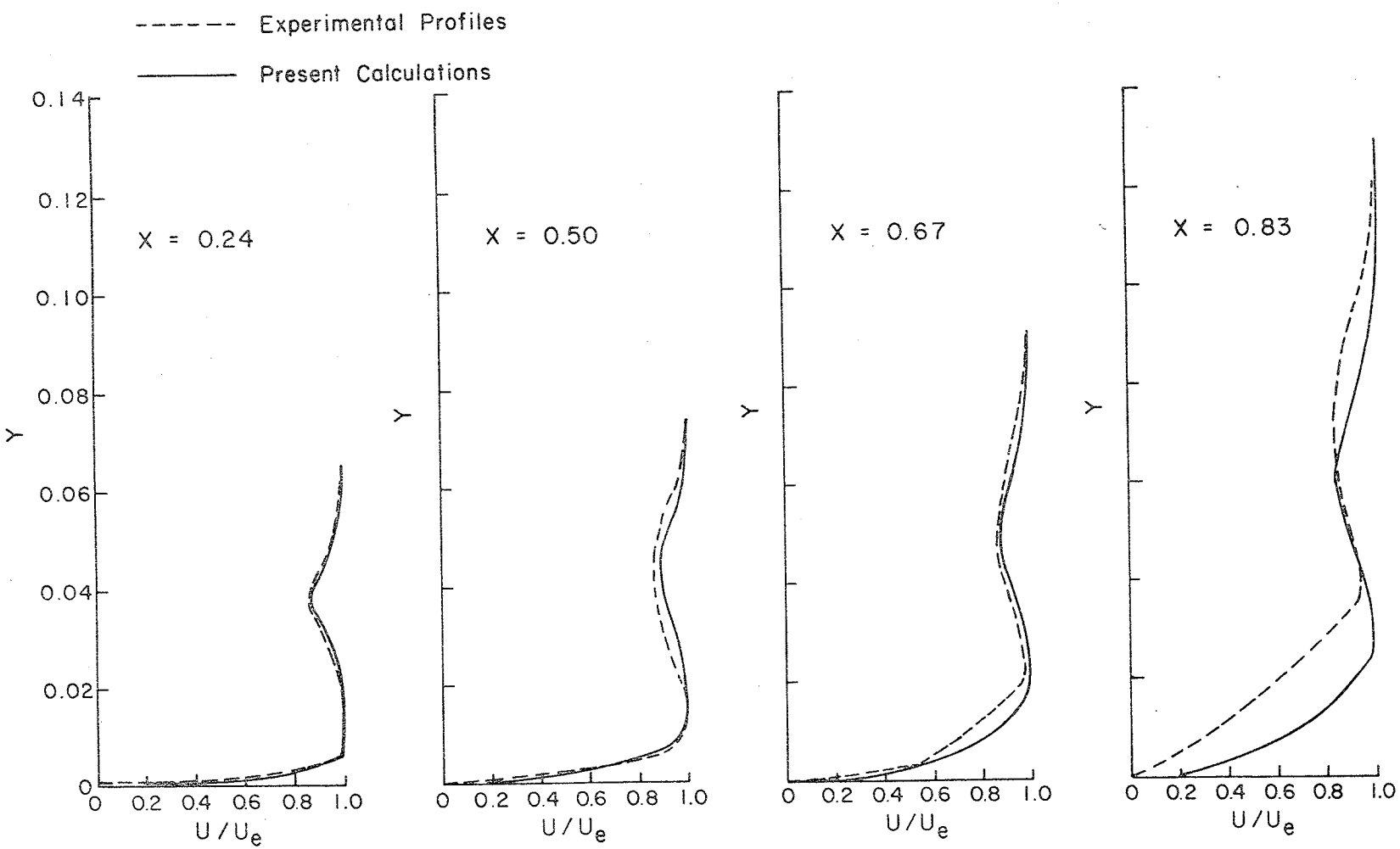

Fig. 20 Development of the Velocity Profiles along the Aerofoil. (Test Case 3.)

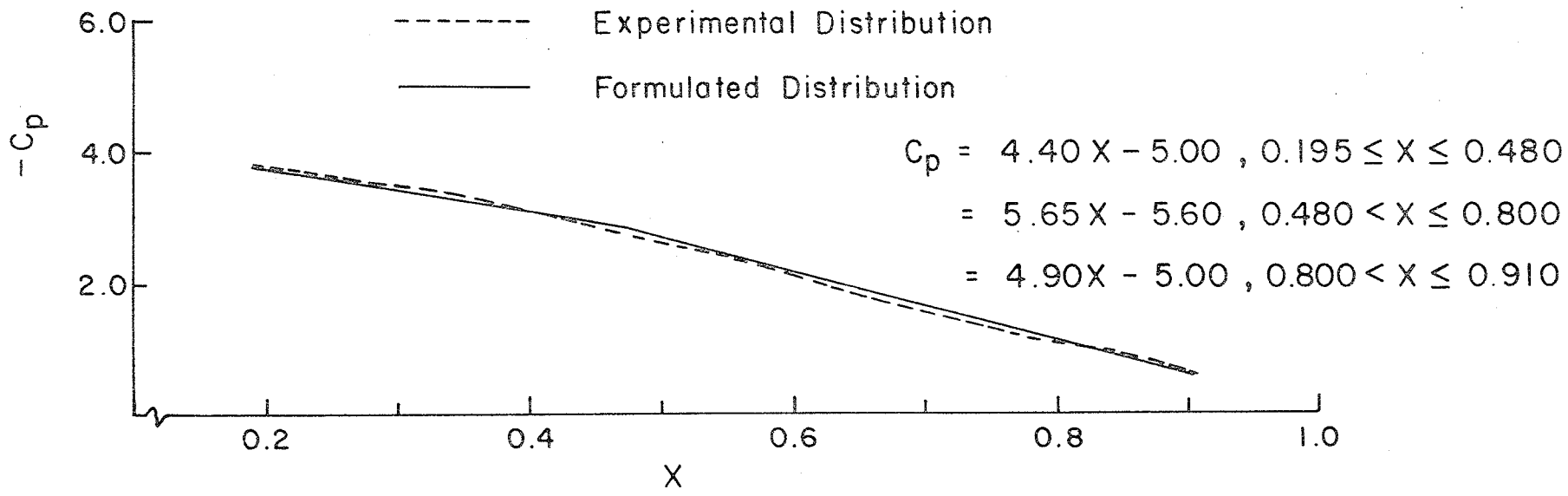

Fig. 21 Pressure Field over the Main Aerofoil
Test Case 4 : Experimental Measurements reported by Ljungstrom
Slat Deflection 25°, Slat Gap 0.0085C

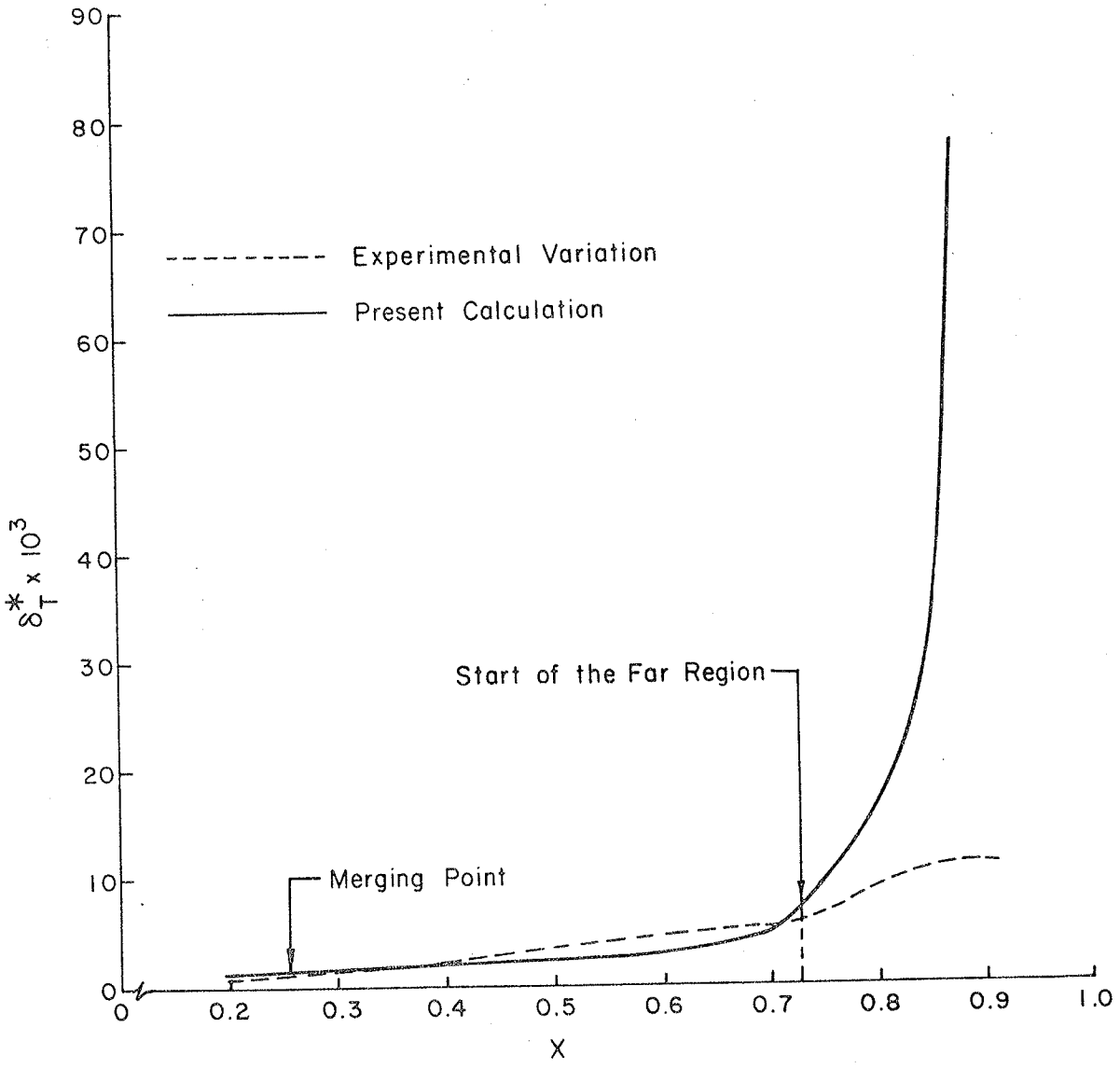

Fig.22 Development of δ_T^* along the main Aerofoil. (Test Case 4.)

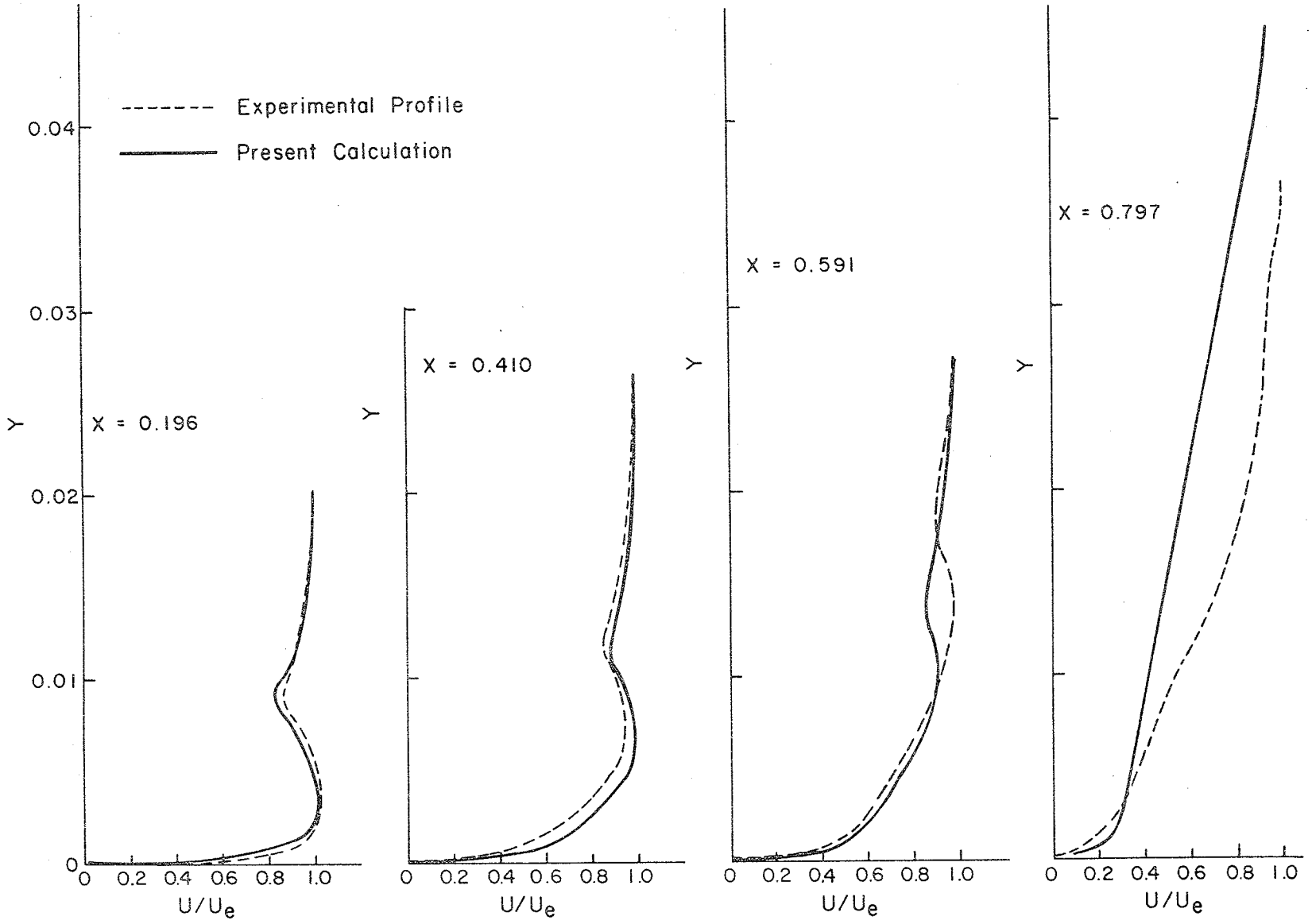

Fig. 23 Development of the Velocity Profiles along the main Aerofoil. (Test Case 4.)